A Live Cell Reporter of Human Adenovirus Chromatin

Dissertation

zur

Erlangung der naturwissenschaftlichen Doktorwürde

(Dr. sc. nat.)

vorgelegt der

Mathematisch-naturwissenschaftlichen Fakultät

der Universität Zürich

von

Daniel Püntener

von

Erstfeld UR

Promotionskomitee:

Prof. Dr. Urs F. Greber (Vorsitz, Leitung der Dissertation)

Prof. Dr. Michael O. Hottiger

Prof. Dr. Ulrike Kutay

Zürich, 2010

TABLE OF CONTENTS

SUMMARY

Virology has contributed substantially to the biological revolution in the last century. Studying virus-host-interactions has revealed many of the fundamental molecular mechanisms such as the nature of genes and splicing. Adenoviruses have received intense attention in this regard as they are of low pathogenicity, easy to grow and rather well characterized. Still, biological mechanisms enabling adenovirus infections are not completely understood. In particular, processes that lead to disassembly of viral particles during entry as well as release of newly synthesized particles upon cell lysis at the end of the viral replication cycle have been difficult to address.

Here we generated a novel human adenovirus with fluorescently tagged chromatin by replacing protein V by GFP-pV while keeping all the other viral genes intact. This virus, named Ad2-GFP-pV, completed the full replication cycle and therefore allowed us to study transport of incoming viral cores as well as viral egress from infected cells. We showed that the viral core component GFP-pV is released from Ad2-GFP-pV during entry and disassembly in two distinct steps. A fast one within 30 min where about 65% of GFP-pV is released and a slower up to 90 min pi leading to full dissociation of GFP-pV from viral particles. The full dissociation is dependent on an interaction of the incoming virus with the nucleus. Using this virus we were also able for the first time to visualize dynamics of viral egress upon cell lysis. We observed that this process is nonisotropic and occurs in two morphologically distinct steps, nuclear disintegration preceding lysis of the plasma membrane.

Taken together we showed that this new virus is suitable to study the whole viral replication cycle and thus might prove useful for live analyses of viral infection and spreading in organisms, as well as for applications in gene therapy.

ZUSAMMENFASSUNG

Die Untersuchung von Viren hat substanziell zur biologischen Revolution im letzten Jahrhundert beigetragen. Die Analyse von Virus-Wirt Interaktionen hat viele zelluläre Prinzipien offenbart wie zum Beispiel die Gesetzmässigkeiten von Genen und deren Spleissung. Ein oft benutztes Modelsystem sind Adenoviren. Dies, weil sie nur beschränkt krankmachend, einfach zu vermehren und gut charakterisiert sind. Trotzdem sind die zugrundeliegenden zellulären Mechanismen, welche eine Infektion ermöglichen, immer noch nicht gut verstanden. Insbesondere Prozesse die zum Abbau viraler Kapside während des Imports führen und wie Viren die Zelle verlassen, war bisher schwierig zu untersuchen.

In dieser Arbeit haben wir das Chromatin eines humanen Adenovirus fluoreszent markiert, indem wir das Protein V gegen das fluoreszierende Fusionsprotein GFP-pV ausgetauscht haben, ohne dabei andere virale Gene zu zerstören. Dieses Virus, genannt Ad2-GFP-pV, durchlief den vollen Replikationszyklus und erlaubte es uns daher, viralen Transport und Freisetzung von Viren am Ende des Zyklus zu untersuchen. Wir konnten zeigen, dass während des Eintritts des Kapsids in die Zellen das GFP-pV in zwei Schritten dissoziiert. Innerhalb von 30 Minuten wurden 65% vom GFP-pV ins Zytosol abgegeben und nach 90 Minuten das restliche Protein. Der zweite Schritt war dabei abhängig von einer Interaktion der Viren mit dem Zellkern. Im Weiteren ist es uns gelungen, zum ersten Mal die Dynamik der Virenfreisetzung am Ende des viralen Replikationszykluses zu bestimmen. Wir konnten zeigen, dass dieser Prozess anisotrop ist und in zwei Schritten geschieht. Einem Zerfall der Kernmembran folgt die Lyse der Plasmamembran.

Zusammenfassend konnten wir zeigen, dass dieses neue Virus ermöglicht, den vollständigen Replikationszyklus von Adenoviren zu untersuchen. Es hat das Potential, Echtzeituntersuchungen von Infektionen und deren Ausbreitung in Organismen zu machen oder als diagnostisches Virus in der Gentherapie eingesetzt zu werden.

INTRODUCTION

1. Why we do virology

1.1 Insights into cellular mechanisms through viral studies

The field of virology contributed substantially to the biological revolution in the last century. This is not by chance. The reason lies in the intrinsic properties of viruses and the way they interact with their hosts. As obligatory parasites viruses depend heavily on the cells they infect. Viruses lack their own metabolism, and therefore have to give precise instructions to the cell to manipulate it for their own use. As viruses are limited in size and can carry only a limited amount of genes, they often directly interfere with biological key nodes to reach highest efficiency. This makes viruses ideal tools to study cellular principles. Detailed analyses of these interactions has led to the discovery of many of the cells basic features and mechanisms. For example, the genetic origin of mutations, discovery of host controlled restriction and modification, definition of a gene, demonstration of the triplet nature of the genetic code, RNA polyadenylation, arrangement of genes into introns and exons, the nuclear localization signal and the discovery of gene silencing by double-stranded RNA as antiviral response were discovered through study of viruses, to name only a few examples (reviewed in (Enquist, 2009)). For sure this list will continue to grow as new powerful techniques and methods allow a more and more detailed view into the cells structure and processes. One advantage of viruses is their size: They can be visualized by EM, and after fluorescent-tagging also by light microscopy.

1.2 Viruses as pathogens

Although viruses proved to be very useful for basic research, a major motivation to study viruses comes from the fact that they are responsible for many human diseases. Smallpox, for example, is known as one of humankind’s greatest killers. It decimated the human population over the course of history. As an example, during the European conquest of the New World, imported smallpox

infections had a large impact on the indigenous population. The outbreak of the “Spanish Flu” at the end of World War I was responsible for more casualties then the war itself. This influenza pandemic killed an estimated 20 to 40 million people. Ironically but not surprising the high relevance for human health and associated social and economic consequences catalyzed also some of the largest triumphs in the history of virology and medicine. In 1796 Edward Jenner demonstrated that inoculation with cowpox lesions provided protection against the more virulent variola major virus, the causative agent of smallpox. The subsequent development of vaccines against many different pathogens had its tentative climax by the eradication of smallpox after a concerted worldwide vaccination campaign of the World Health Organization in 1979. Nevertheless, we will be confronted with new emerging viral threats, now and in the future. For example, the acquired immune deficiency syndrome (AIDS) caused by the human immunodeficiency virus (HIV) has since its discovery in 1981 (Marx, 1982) become one of the biggest medical challenges of our time. It has a deep social and economical impact worldwide, but especially in Sub-Saharan Africa.

1.3 Viruses as oncogenic agents

More recently viruses gained attention because of their association with human cancer. Since the early demonstration of viral causation of murine leukemias by Gross (Gross, 1951) or the recognition of Adenovirus type 12 as first human virus to be oncogenic (Trentin, Yabe, & Taylor, 1962) many viruses have been identified to account for different cancers in mammals. Medical records indicate that 12-20% of the human cancer incidences worldwide are associated with viral infections (Parkin, 2006). Human papilloma virus, for example, is known to be present in 100% of all analyzed cervix cancers and vaccination efforts are therefore underway with the hope to reduce the amount of incidences. Other examples are Epstein-Barr virus (EBV) responsible for Burkitt’s lymphoma, human T lymphotropic virus type 1 (HTLV-1) associated with adult T-cell leukemia, human herpesvirus type 8 (HHV-8) known to induce body cavity lymphoma or hepatitis B virus (HBV) for hepatocellular carcinoma. New viruses most certainly will be added to the list of cancer-causing viruses emphasizing

the high importance of this field and the need of detailed knowledge about the underlying mechanism. More information on the role of DNA-tumor viruses in cancer can be found in the review embedded in this thesis (DNA-tumor virus entry – From the plasma membrane to the nucleus (Greber & Puntener, 2009)).

1.4 Viruses as tools in gene therapy

An emerging field in virology is the use of viruses as tools in gene therapy (Bangari & Mittal, 2006). In particular, adenoviruses have obtained much attention in this regard as they are well studied, of low pathogenicity, can be grown easily to high titers, have a broad tropism and posses a low oncogenic potential as genomes are rarely integrated into the host chromosome. Gene therapy approaches aim to deliver genes into target cells in order to correct or compensate the absence or mutation of a specific gene or eliminate cancer cells by selective infection. Although the idea is intriguing there are still a lot of problems to overcome. Most importantly the efficacy of host defenses is still one of the major challenges in the field. Adenoviruses are highly immunogenic. Not only the humoral but also the cell-mediated immune responses are activated upon infection (Dai, et al., 1995). This dramatically reduces success rates in gene therapy trials because the low efficiency of gene transfer often requires repeated treatment with vectors. In addition there is a high prevalence of neutralizing antibodies against species C adenoviruses on which most vectors are based (Nwanegbo, et al., 2004). Although a lot of progress has been made in recent years and a large number of clinical trials are underway it remains to be seen if the substantial problems can be solved.

Therefore, continuous basic virological research is important. Not only because viruses are an ongoing threat causing infections and cancer, but also because many of the underlying mechanisms remain to be discovered and these mechanisms are the basis for new virus-mediated gene therapies.

2. Adenoviruses

2.1 Adenoviridae

In this research, properties of a GFP-insertion mutant of Adenovirus type 2 (Ad2) were studied in some detail. Ad2 belongs to the family of Adenoviridae which is classified into four major genera comprising Atadenovirus, Aviadenovirus, Mastadenovirus and Siadenovirus (Davison, Benko, & Harrach, 2003). Recently, a fifth genus infecting fish was proposed (Benko, et al., 2002). The genera of Mastadenovirus comprise all Adenoviruses known to infect mammals, including humans. Human adenoviruses are further divided into species A to F including 51 serotypes. Many of them are known to cause respiratory infections (species B, C and E) but also gastroenteritis (species F) as well as keratoconjunctivitis (species B, D and E) are frequently associated with adenoviral infections in humans. Although adenovirus infections cause normally mild diseases, severe complications can occur in immunocompromised patients (Kojaoghlanian, Flomenberg, & Horwitz, 2003).

2.2 Adenovirus structure and composition

Adenoviruses are composed of a non-enveloped capsid of about 90 nm in diameter surrounding and protecting the core consisting of the 36 kbp genome and associated proteins (Fig.1). From the 13 known polypeptides forming the viral particle, hexon (pII) is the most abundant. It forms 240 homotrimeric capsomers that build up the icosahedral capsid together with homopentamers of penton base (pIII) anchoring the 37 nm long fiber (trimer of pIV) to the capsid. Penton base and fibers constitute the penton capsomere which is present at each of the 12 vertices of the icosahedral capsid. The capsid is stabilized by minor capsid proteins IIIa, VI, VIII and IX. The exact position of these proteins is still discussed. However, four trimers of pIX are assumed to be embedded in large cavities in the upper surface of an assembly of 9 hexons also known as groups-of-nine (GON) cementing this structure into a highly-stable assembly (Furcinitti, van Oostrum, & Burnett, 1989). pIIIa, which also lies on the outside of the capsid connects two neighboring GONs (Fabry, et al., 2005). The position of

pVI is not clear. The current model locates pVI in the internal cavity of the hexon trimer. Data supporting this model come from biochemical studies (Everitt, Lutter, & Philipson, 1975) (Matthews & Russell, 1995) and from Cryo-EM structural studies (Silvestry, et al., 2009; Stewart, Fuller, & Burnett, 1993). However, the assignment of pVI to locations inside the hexon trimer is problematic, as there are 360 copies of pVI per virion but only 240 capsomers. Interestingly, unassigned structures around the 5-fold symmetry of the vertices projecting towards the DNA-core have been detected in cryo-EM studies, and these structures have been tentatively assigned to pVI (Fabry, et al., 2005).

While cryo-EM studies in combination with X-ray structures of individual component proteins resulted in a rather well defined model of the capsid structure (Nemerow, Pache, Reddy, & Stewart, 2009) the core is not well presented because it lacks symmetry (Stewart, Burnett, Cyrklaff, & Fuller, 1991). Although structural information of the precise organization of the genome inside the viral particle is missing, biochemical analysis of isolated cores of species C human Ad2 and the closely related Ad5 revealed five DNA-associated proteins. The basic proteins V, VII and X (pV, pVII, pX), the terminal protein covalently attached to the 5’ ends of the DNA (Rekosh, Russell, Bellet, & Robinson, 1977), and approximately 10 copies of the viral protease loosely associated with the core (Weber, 2003) (Mangel, Baniecki, & McGrath, 2003). A schematic of the present model is shown below. (from (Russell, 2009)).

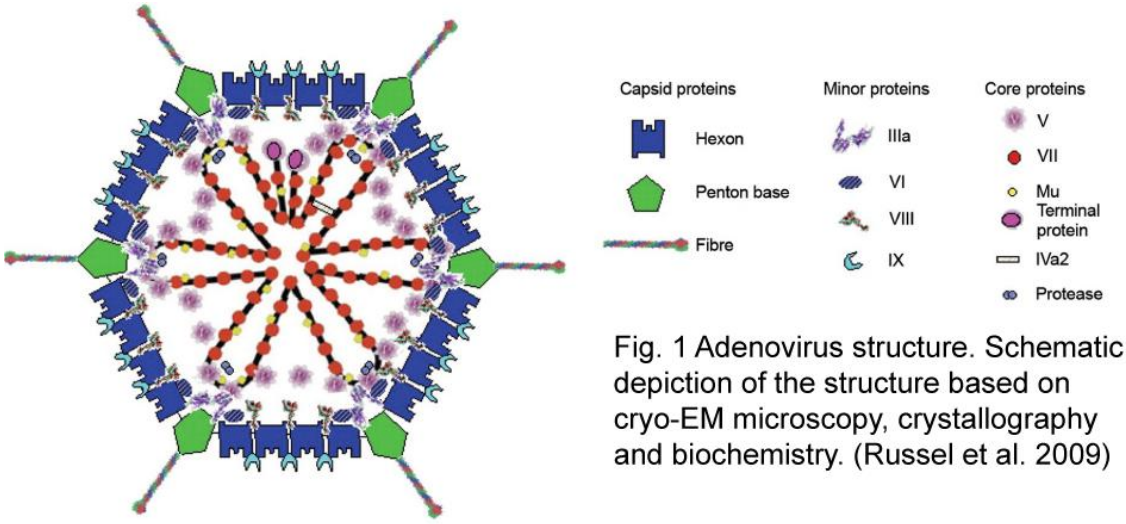

Fig. 1 Adenovirus structure. Schematic depiction of the structure based on cryo-EM microscopy, crystallography and biochemistry. (Russel et al. 2009)

3. Viral chromatin

3.1 Current model of adenovirus chromatin

Copy numbers of VII and V were measured to be 1070 and 180, respectively, in virus particles (Everitt, Sundquist, Pettersson, & Philipson, 1973). Based on this data together with results obtained by digestion of cores with staphylococcal nuclease which yielded 200 base pair DNA fragments (which was later also confirmed by Black et al. (Black & Center, 1979)), Corden et al. suggested a model in which viral DNA is organized into 180 nucleosome-like units where 200 bp DNA is condensed by hexamer of protein VII and associated with one copy of protein V (Corden, Engelking, & Pearson, 1976). However, micrococcal nuclease digestions and electron microscopy analysis of viral cores led Mirza et al. to conclude that the chromatin is organized into 200 nucleosome-like units with monomer cores of 150 bps and an average 30 bp linker region (Mirza & Weber, 1982). Furthermore, they could identify dimers of protein VII in crosslinking experiments in agreement to observations later made by Chatterjee et al. (Chatterjee, Vayda, & Flint, 1985) and also proposed by studies analyzing the binding of VII to DNA by partial proteolytic mapping of the sites of covalent-

attachment of 32P-labelled oligonucleotides (Chatterjee, Vayda, & Flint, 1986b). Therefore, it was proposed that the nucleosome-like cores are composed of three dimers of protein VII. As pV is present in a ratio of 1 copy to 1 nucleosome-like unit in Corden's model, it was speculated that protein V functions in bridging nucleosomes and thereby helps condensing to viral genome. In addition to its ability to bind DNA in a non specific manner, pV was also found to bind pVI and therefore a role for pV in connecting the core to the capsid is assumed (Matthews & Russell, 1998). It is interesting to note that a recombinant Ad5 in which protein V is deleted gave rise to low levels of viral particles, suggesting that pV was involved in the assembly of infectious virions (Ugai, Borovjagin, Le, Wang, & Curiel, 2007). The deletion, however, is compensated by mutations in mu (pX) indicating redundancy for core organization by molecular adaptation which is further supported by the fact that pV is specific for Mastadenoviruses, which exclusively infect mammals (http://www.vmri.hu/~harrach/ADENOSEQ.HTM).

In Corden's model the copy number of VII is predicted to be 1080 while in Mirza's model it is 1200. This seems to be in conflict with biochemically measured copy numbers of VII and V which are 833 +/- 33 and 157 +/- 1 respectively (van Oostrum & Burnett, 1985) or, to RP-HPLC-based estimations which gave, 633 +/- 59 and 170 +/- 15 for pVII and PV, respectively (Lehmberg, et al., 1999). However, this discrepancy could be explained by stretches in the viral genome lacking pVII and pV.

3.2 The role of cellular histones in adenoviral infections

The proposed model of the viral core is intriguing, especially because of its analogy to cellular chromatin: Eukaryotic cells package their DNA with histones and associated proteins into nucleosomes. Nucleosomes are octamers composed of two copies each of core histones H2A, H2B, H3 and H4 condensing 146 bp of DNA (Luger & Richmond, 1998). An additional protein, histone H1, dynamically interconnects individual nucleosomes with a short residence time of a few minutes on chromatin (Janicki & Spector, 2003) (Talbert

& Henikoff, 2010). While nucleosomes are invariant in structure and composition chromatin is highly dynamic as it switches between condensed and decondensed states in mitosis and interphase. Flexibility is necessary in addition for regulating access to specific DNA sequences during transcription and DNA replication and is mediated by posttranslational modifications of specific histone residues as well as the DNA itself. These modifications include acetylation, phosphorylation, methylation, ubiquitination, sumoylation and ADP-ribosylation of histones and base methylation of cytosine residues (Keppler & Archer, 2008; Strahl & Allis, 2000). It is worthwhile to note that several of these modifications are also found on the adenoviral core proteins V and VII suggesting a role of the cellular chromatin regulation system in viral transcription, replication and assembly (Dery, et al., 1986; Fedor & Daniell, 1980; Weber & Khittoo, 1983).

Although the viral genome is associated with virally coded proteins V, VII and X in the virion, it can be found condensed by cellular histones in specific phases of the viral life cycle. Upon nuclear entry pVII remains bound to the incoming DNA throughout early phase and the beginning of DNA replication (Chatterjee, Vayda, & Flint, 1986a) (Greber, Webster, Weber, & Helenius, 1996) (Haruki, Gyurcsik, Okuwaki, & Nagata, 2003) (Johnson, et al., 2004) (Xue, Johnson, Ornelles, Lieberman, & Engel, 2005). It is, however, released upon onset of transcription (J. Chen, Morral, & Engel, 2007). Besides the viral early gene product E1A, several cellular factors are involved in this viral chromatin remodeling process. The protein SET/template activating factor-Iβ (TAF-Iβ), for example, was found to associate with pVII (Haruki, et al., 2003) (Haruki, Okuwaki, Miyagishi, Taira, & Nagata, 2006) (Xue, et al., 2005) and stimulated transcription and DNA replication from adenovirus nucleoprotein preparations (Kawase, et al., 1996) (Okuwaki & Nagata, 1998). The cellular protein pp32 was also shown to associate with pVII *in vitro* (Xue, et al., 2005). Interestingly both proteins are components of the INHAT complex known to regulate histone acetylation and transcription (Seo, et al., 2001) (Seo, et al., 2002). It is tempting to assume that once pVII is released from the viral genome the DNA engages with cellular histones. Indeed newly synthesized viral DNA was found to be bound by cellular histones and served as template for transcription and

replication (Dery, et al., 1985). The use of histones in the cellular phase of the viral life cycle is not unique to adenoviruses. Herpesviruses, for example, condense the genome in viral particles with the help of polyamines but organizes it into regular histone-based nucleosomes during latency and irregularly spaced nucleosomes during productive infection (Paulus, Nitzsche, & Nevels, 2010). Genomes of SV40 and polyomavirus are condensed by cellular histones during the whole life cycle.

4. Adenovirus life-cycle

4.1 Endocytosis and transport to the nucleus

The first step in adenovirus entry is attachment to the target cell. This is mediated by cellular receptors, which in case of Ad2 is the primary Coxsackie and Adenovirus receptor (CAR) and secondary alpha v integrin co-receptors which bind to a RGD motif exposed at the surface of penton base (Bergelson, et al., 1997) (Meier & Greber, 2004; Wickham, Mathias, Cheresh, & Nemerow, 1993) (Burckhardt & Greber, 2009). These interactions not only induce various signaling events such as activation of protein kinase A (PKA) and mitogen activated protein kinase (MAPK) (Suomalainen, Nakano, Boucke, Keller, & Greber, 2001) but also leads to the shedding of fiber and therefore initiates the stepwise disassembly of the viral capsid during entry (Greber, Willetts, Webster, & Helenius, 1993; Nakano, Boucke, Suomalainen, Stidwill, & Greber, 2000). Adenoviruses are then internalized by clathrin-mediated endocytosis or macropinocytosis (Meier, et al., 2002) and accumulate in endosomes. It was suggested that further disassembly in this compartment results in the exposure of pVI which harbors an amphipathic alpha-helix with membrane lytic activity and therefore triggers membrane lysis and ultimately escape of viral particles into the cytosol (Wiethoff, Wodrich, Gerace, & Nemerow, 2005) (Maier, Galan, Wodrich, & Wiethoff, 2010). However, the precise mechanism is not known. The cytosolic Ad2 are then transported along microtubules by the dynein/dynactin motor complex to the microtubule organizing center (MTOC) (Suomalainen, et

al., 1999) (Mabit, et al., 2002) from where they reach the nuclear pore complex (NPC) and bind to the CAN/Nup214 receptor (Trotman, Mosberger, Fornerod, Stidwill, & Greber, 2001). How exactly the particles are transported from the MTOC to the NPC is not known. However, this process is sensitive to the macrolide antibiotic leptomycin B (LMB), which inhibits nuclear protein export and prevents the attachment of incoming virions to the NPC (Strunze, Trotman, Boucke, & Greber, 2005). Figure 2 depicts the described entry process.

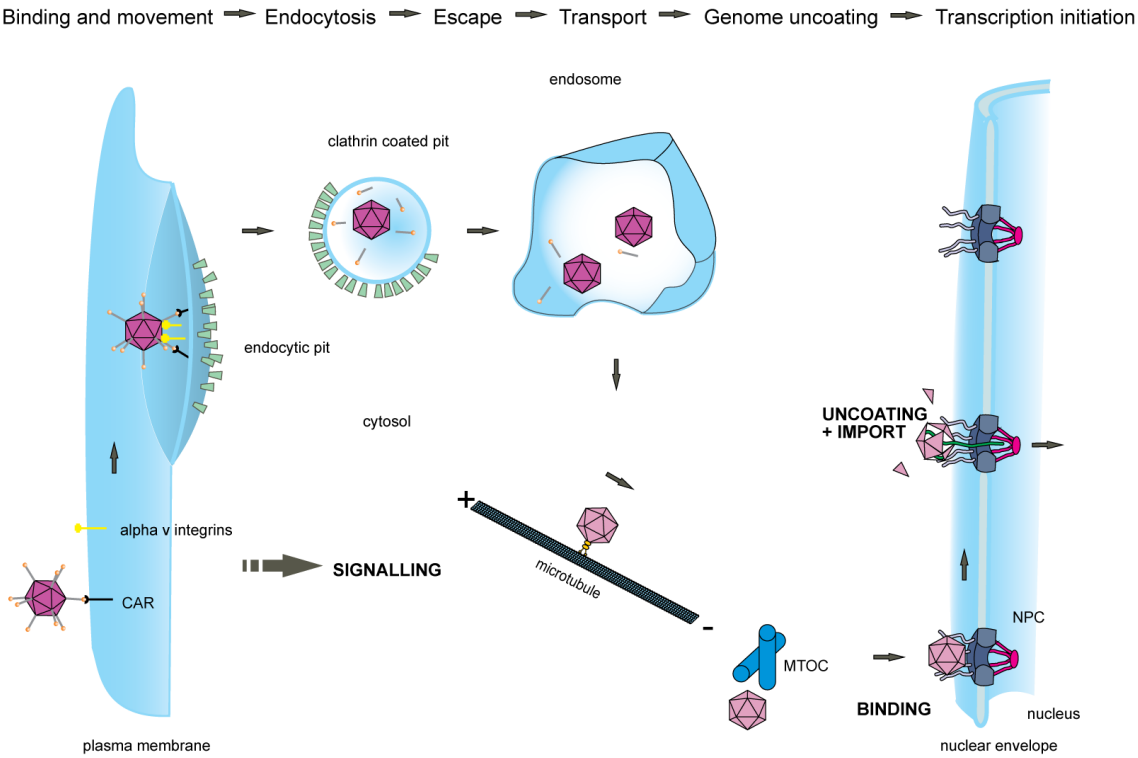

Figure 2. Schematic presentation of Ad2 entry. Adapted from Puntener & Greber 2009

4.2 Adenovirus DNA import

(Note: A compacted version of this chapter can be found in the review embedded in this thesis)

Replication of adenovirus occurs in the nucleus, and therefore delivery of the viral DNA into this cellular compartment is a prerequisite for productive infection. The nucleoplasm is separated from the cytoplasm by the nuclear envelope, which is composed of the inner and outer nuclear membranes enclosing the perinuclear space, which is an extension of the ER lumen. While

the ONM is continuous with the ER and studded with ribosomes, the INM is characterized by a set of integral membrane proteins. Exchange of molecules through the two concentric lipid bilayers is maintained by multiprotein structures known as nuclear pore complexes at sites at which the INM and ONM are fused. NPCs of Saccharomyces cerevisiae contain at least 456 individual protein molecules and are composed of a set of ~30 distinct proteins with a total mass of ~50 MDa. The molecular architecture of NPCs is highly conserved among all eukaryotes and a detailed view of NPCs of Saccharomyces cerevisiae has recently been published (Alber, et al., 2007). Briefly, the NPCs are made up of a core scaffold that forms an interlaced network coating the entire curved surface of the nuclear envelope membrane. The inner face of this scaffold serves as the anchor site for proteins with large disordered regions containing characteristic repetitive sequence motifs known as FG repeats forming the aqueous channel and contributing to the selectivity of nucleocytoplasmic transport. On top of the two inner rings of the core scaffold are the cytoplasmic ring to which long cytoplasmic filaments are attached and the nuclear ring forming a basket-like structure consisting of nuclear filaments. The diameter of the central channel is ~39 nm, which is also the size limit for transported particles (Pante & Kann, 2002). The NPC has been intensively reviewed and for further reading the following reviews are suggested (D'Angelo & Hetzer, 2008) (Lim, Ullman, & Fahrenkrog, 2008) (Cook, Bono, Jinek, & Conti, 2007).

Kinetic studies of nuclear transport have shown that each NPC can accommodate up to 1000 translocation events per second, and despite the huge traffic, transport is highly selective and regulated (Ribbeck & Gorlich, 2001). While small molecules such as ions or metabolites can pass the NPC by diffusion, cargos larger than ~40 kDa require specific transport receptors (Talcott & Moore, 1999). FG-proteins play an important role in the translocation of cargo but the biophysical properties of the pore necessary for selective translocation is still controversial. There are two main models discussed: 1) FG-proteins form a gelatinous meshwork, which would allow small molecules to passively diffuse. Transport receptors bound to larger cargoes would locally interact with FG-sequences and dissolve the barrier to permit passage through

the pore (Frey, Richter, & Gorlich, 2006). 2) The NPC forms an entropic barrier, which repels non-FG-binding molecules. Binding of receptors would concentrate transport complexes and thereby increase the probability of transport (Lim, Aebi, & Stoffler, 2006).

In both models transport receptors play a critical role. Most of the nucleocytoplasmic transport factors belong to the family of karyopherin-β also known as importin-β like proteins. Depending on its directionality they are grouped as importins, exportins or transportins. Karyopherins bind cargo either directly or via an adaptor. For example, isoforms of importin-α are often used as adaptors for importin-β. Translocation is driven by the guanosine triphosphatase (GTPase) Ran: In its GTP bound form (RanGTP), Ran binds to karyopherins and either triggers the dissociation of import complexes or promotes the assembly of export complexes. In the cytoplasm Ran GTPase-activating factor 1 (RanGAP1) induces hydrolysis of GTP causing the dissociation of export complexes whereas RanGDP/GTP exchange factor (RanGEF) localized in the nucleoplasm stimulates exchange of GDP for GTP resulting in dissociation of import complexes. Ran in its GDP or GTP bound form is asymmetrically distributed with the first concentrated in the cytoplasm and the latter in the nucleoplasm creating a gradient, which provides the necessary energy for the transport processes. For detailed reviews of nucleocytoplasmic transport, see also (Cook, et al., 2007) (Terry, Shows, & Wente, 2007).

Cargos imported into the nucleus are recognized by their karyopherins by the nuclear localization signal (NLS) for import and the nuclear export signal (NES) for export. A monopartite NLS consist of a cluster of 3 to 5 positively charged amino acids such as the SV40 T antigen NLS whereas in case of a bipartite NLS a smaller lysine/arginine cluster is separated from the monopartite-like cluster by a linker of 10 to 12 residues.

Studying virus nuclear import has proven to be difficult. Although some progress has been made the last decade, the lack of suitable live probes for DNA/RNA is still a major hurdle. While DNA virus nuclear import is often visualized using semiquantitative Fluorescent *in situ* hybridization (FISH) a live assay for poliovirus was recently developed where the viral genome was labeled by the

RNA binding dye Syto82 (Brandenburg, et al., 2007). To date, unfortunately, there is no such technique available for DNA viruses including adenovirus. Attempts undertaken in our lab by either inserting a series of 40 lac operator sequences in a recombinant Ad5 capable of binding fluorescently tagged lac repressor or labeling of viral DNA by the DNA intercalating dye TOTO-3 failed (unpublished).

Since all DNA viruses make use of the host cells, nuclear import machinery analysis of the corresponding interactions shed some light on the mechanisms of viral import. Information on the role of NLSs for nuclear import of DNA-tumor viruses can be found in the review *DNA-tumor virus entry – from plasma membrane to the nucleus* embedded in this thesis. Adenovirus disruption at the NPC, nuclear import of adenovirus DNA associated proteins and their role in DNA import are also described.

4.3 Adenovirus replication

Once the viral genome has been imported into the nucleus a well timed series of events is initiated which is roughly divided into an early and a late phase. The later phase starts upon onset of viral DNA replication and subsequent late gene expression. In the early phase mRNA is transcribed from seven different locations in the viral genome, designated early regions 1A (E1A), E1B, E2A, E2B, E3, E4 and a late region 1 (L1). Translated proteins interact with viral and host cell proteins in order to optimize synthesis of new virions. The first protein to be expressed is E1A (Nevins, Ginsberg, Blanchard, Wilson, & Darnell, 1979). It induces the host to enter the S phase of the cell cycle and also stimulates expression from the other early transcription units. Viral proteins E1B-55K and E4orf6 inhibit p53 function and thereby prevent apoptosis of the cell (Cathomen & Weitzman, 2000). Proteins transcribed from the E3 region mainly provide protection from the immune system (Lichtenstein, Toth, Doronin, Tollefson, & Wold, 2004). Finally, terminal protein (pTP), DNA binding protein (DBP) and the viral polymerase are transcribed from the E2 region preparing the cell for replication of viral DNA. DNA replication is initiated at either terminus of the double-stranded viral genome. At each replication fork only one of the two

parental strands is replicated, producing a daughter duplex and a displaced single-strand DNA (Dery, et al., 1985). Viral DNA replication occurs at discrete intranuclear locations which are often visualized by staining of DBP as the displaced single-stranded DNA is bound by this protein. Focal viral inclusions with the shape of rings, crescents or spheres are thereby observed which were named ssDNA accumulation sites (Puvion-Dutilleul, Pedron, & Cajean-Feroldi, 1984). While early in replication these sites are active for both replication and transcription, these activities become compartmentalized as replication proceeds. ssDNA continues to be accumulated at the DBP positive sites while dsDNA is released to the surrounding nucleoplasm, where it is used as template for transcription (Pombo, Ferreira, Bridge, & Carmo-Fonseca, 1994). Interestingly we were able to locate pV and GFP-pV expressed from Ad2 and Ad2-GFP-pV to ssDNA accumulation sites at early times and adjacent to them at late time points of infection. This suggests a role for pV in transcription, replication or assembly of new particles (unpublished). In this context it is worthwhile to note that it was speculated that only the single-stranded DNA is used for encapsidation. A premature chromatinization of viral dsDNA by pV and pVII would therefore not be beneficial as chromatinized viral genome is not a optimal template for transcription and replication (Johnson, et al., 2004; Korn & Horwitz, 1986). Indeed, expression of pV, which harbors NLSs targeting the protein to the nucleus and nucleolus (Matthews, 2001), was found to redistribute nucleolin/C23 and nucleophosmin/B23 from the nucleus to the cytoplasm (Matthews, 2001). B23 in turn interacts with pV and pre-pVII und suppresses the formation of aggregates between DNA and the core proteins (Samad, Okuwaki, Haruki, & Nagata, 2007) (Okuwaki, Matsumoto, Tsujimoto, & Nagata, 2001) (Okuwaki, Iwamatsu, Tsujimoto, & Nagata, 2001). This data suggest that spatial and temporal separation of viral components might be important for correct transcription, replication and assembly of new viral particles.

4.4 Cell lysis and egress

At the end of the viral replication cycle, newly synthesized viral particles have to be released from the infected cell in order to spread and infect new cells. A major challenge, therefore is tricking the immune system as viruses in the extracellular space are readily recognized and cleared by components of the immune system. Two principle routes are known. Some viruses have chosen to avoid a direct exposure to immunocompetent factors by spreading through cell-cell contacts. Neurotropic viruses such as herpesvirus and rhabdovirus were found to spread along neuronal networks and are transmitted via neurological synapses. Retroviruses use so called virological synapses, which closely resemble immunological synapses, for their cell-to-cell spread (Mothes, Sherer, Jin, & Zhong, 2010). If viruses do not make use of cell-assisted spreading they have to meet several requirements in order to be successful. Large numbers must be released that are sufficiently stable to reach distant areas by diffusion. Once particles reach the target cell, strong binding to receptors is necessary for efficient infection. There are several indications that adenoviruses support such a cell-free transmission mechanism. The adenovirus protease, for example, was found to cleave the cellular cytokeratin K18 thereby disrupting the intermediate filament system, which is thought to make infected cells more susceptible to lysis by mild mechanical forces (P. H. Chen, Ornelles, & Shenk, 1993). However, cleavage of cytokeratin K 18 alone is not sufficient to destabilize the cellular integrity, since the synthesis of new keratin readily repairs the intermediate filaments. Only at late stages of infection when translation of cellular proteins is inhibited does the lack of filament repair lead to a sufficient breakdown of the cytokeratin network, which facilitates release of newly synthesized infectious virus particles (Zhang & Schneider, 1994). Besides cytokeratin, actin and microtubules have also been identified as substrates for the viral protease suggesting that disruption of the cellular filament system is important for cell lysis (Mangel, et al., 2003).

The second mechanism involves the virally encoded E3 11.6 kDa adenovirus death protein (ADP) (Tollefson, Scaria, et al., 1996). ADP is an integral membrane protein shown to localize to the endoplasmatic reticulum where it is synthesized, the Golgi apparatus where it is glycosylated (Scaria, Tollefson,

Saha, & Wold, 1992) and the nuclear membrane. While only small amounts of this protein are synthesized at early times of infection under the control of the E3 promotor, expression of ADP is greatly amplified at late stages of infection through transcription from the viral major late promoter (MLP) (Tollefson, Scaria, Saha, & Wold, 1992). At this time ADP accumulates at the nuclear membrane and the Golgi apparatus. Interestingly in EM studies with a mutant adenovirus lacking the gene for ADP, infected cells showed an extremely swollen nucleus with apparently intact nuclear envelope at late time points of infection and no cytosolic virus, whereas the nuclear envelope could not be readily defined in wt infected cells at the same time point (Tollefson, Ryerse, Scaria, Hermiston, & Wold, 1996). The authors therefore suggested that ADP might function in the disruption of the cell nucleus.

Interestingly, adenovirus particles were found in the cytoplasm of infected Hela cells at late stages of infection, while the nuclear membrane was seemingly intact (Puvion-Dutilleul, Besse, Pichard, & Cajean-Feroldi, 1998). In addition infected cells were shown to be able to transmit penton to neighboring cells probably through a cell contact-assisted mechanism as no free penton could be detected in the extracellular medium (Trotman, Achermann, Keller, Straub, & Greber, 2003). This could indicate that viral components or even whole particles might be transmitted to adjacent cells in the absence of lysis. Since Ad2-GFP-pV is able to complete a full replication cycle, this virus can be used for live imaging of virus adenovirus egress, and thus as a tool to unravel mechanisms of progeny virus release from adenovirus-infected cells.

5. References

Alber, F., Dokudovskaya, S., Veenhoff, L. M., Zhang, W., Kipper, J., Devos, D., et al. (2007). The molecular architecture of the nuclear pore complex. *Nature, 450*(7170), 695-701.

Bangari, D. S., & Mittal, S. K. (2006). Current strategies and future directions for eluding adenoviral vector immunity. *Curr Gene Ther, 6*(2), 215-226.

Benko, M., Elo, P., Ursu, K., Ahne, W., LaPatra, S. E., Thomson, D., et al. (2002). First molecular evidence for the existence of distinct fish and snake adenoviruses. *J Virol, 76*(19), 10056-10059.

Bergelson, J. M., Cunningham, J. A., Droguett, G., Kurt-Jones, E. A., Krithivas, A., Hong, J. S., et al. (1997). Isolation of a common receptor for Coxsackie B viruses and adenoviruses 2 and 5. *Science, 275*(5304), 1320-1323.

Black, B. C., & Center, M. S. (1979). DNA-binding properties of the major core protein of adenovirus 2. *Nucleic Acids Res, 6*(6), 2339-2353.

Brandenburg, B., Lee, L. Y., Lakadamyali, M., Rust, M. J., Zhuang, X., & Hogle, J. M. (2007). Imaging poliovirus entry in live cells. *PLoS Biol, 5*(7), e183.

Burckhardt, C. J., & Greber, U. F. (2009). Virus movements on the plasma membrane support infection and transmission between cells. *PLoS Pathog, 5*(11), e1000621.

Cathomen, T., & Weitzman, M. D. (2000). A functional complex of adenovirus proteins E1B-55kDa and E4orf6 is necessary to modulate the expression level of p53 but not its transcriptional activity. *J Virol, 74*(23), 11407-11412.

Chatterjee, P. K., Vayda, M. E., & Flint, S. J. (1985). Interactions among the three adenovirus core proteins. *J Virol, 55*(2), 379-386.

Chatterjee, P. K., Vayda, M. E., & Flint, S. J. (1986a). Adenoviral protein VII packages intracellular viral DNA throughout the early phase of infection. *Embo J, 5*(7), 1633-1644.

Chatterjee, P. K., Vayda, M. E., & Flint, S. J. (1986b). Identification of proteins and protein domains that contact DNA within adenovirus nucleoprotein cores by ultraviolet light crosslinking of oligonucleotides 32P-labelled in vivo. *J Mol Biol, 188*(1), 23-37.

Chen, J., Morral, N., & Engel, D. A. (2007). Transcription releases protein VII from adenovirus chromatin. *Virology, 369*(2), 411-422.

Chen, P. H., Ornelles, D. A., & Shenk, T. (1993). The adenovirus L3 23-kilodalton proteinase cleaves the amino-terminal head domain from cytokeratin 18 and disrupts the cytokeratin network of HeLa cells. *J Virol, 67*(6), 3507-3514.

Cook, A., Bono, F., Jinek, M., & Conti, E. (2007). Structural biology of nucleocytoplasmic transport. *Annu Rev Biochem, 76*, 647-671.

Corden, J., Engelking, H. M., & Pearson, G. D. (1976). Chromatin-like organization of the adenovirus chromosome. *Proc Natl Acad Sci U S A, 73*(2), 401-404.

D'Angelo, M. A., & Hetzer, M. W. (2008). Structure, dynamics and function of nuclear pore complexes. *Trends Cell Biol, 18*(10), 456-466.

Dai, Y., Schwarz, E. M., Gu, D., Zhang, W. W., Sarvetnick, N., & Verma, I. M. (1995). Cellular and humoral immune responses to adenoviral vectors containing factor IX gene: tolerization of factor IX and vector antigens allows for long-term expression. *Proc Natl Acad Sci U S A, 92*(5), 1401-1405.

Davison, A. J., Benko, M., & Harrach, B. (2003). Genetic content and evolution of adenoviruses. *J Gen Virol, 84*(Pt 11), 2895-2908.

Dery, C. V., de Murcia, G., Lamarre, D., Morin, N., Poirier, G. G., & Weber, J. (1986). Possible role of ADP-ribosylation of adenovirus core proteins in virus infection. *Virus Res, 4*(4), 313-329.

Dery, C. V., Toth, M., Brown, M., Horvath, J., Allaire, S., & Weber, J. M. (1985). The structure of adenovirus chromatin in infected cells. *J Gen Virol, 66 (Pt 12)*, 2671-2684.

Enquist, L. W. (2009). Virology in the 21st century. *J Virol, 83*(11), 5296-5308.

Everitt, E., Lutter, L., & Philipson, L. (1975). Structural proteins of adenoviruses. XII. Location and neighbor relationship among proteins of adenovirion type 2 as revealed by enzymatic iodination, immunoprecipitation and chemical cross-linking. *Virology, 67*(1), 197-208.

Everitt, E., Sundquist, B., Pettersson, U., & Philipson, L. (1973). Structural proteins of adenoviruses. X. Isolation and topography of low molecular weight antigens from the virion of adenovirus type 2. *Virology, 52*(1), 130-147.

Fabry, C. M., Rosa-Calatrava, M., Conway, J. F., Zubieta, C., Cusack, S., Ruigrok, R. W., et al. (2005). A quasi-atomic model of human adenovirus type 5 capsid. *Embo J, 24*(9), 1645-1654.

Fedor, M. J., & Daniell, E. (1980). Acetylation of histone-like proteins of adenovirus type 5. *J Virol, 35*(3), 637-643.

Frey, S., Richter, R. P., & Gorlich, D. (2006). FG-rich repeats of nuclear pore proteins form a three-dimensional meshwork with hydrogel-like properties. *Science, 314*(5800), 815-817.

Furcinitti, P. S., van Oostrum, J., & Burnett, R. M. (1989). Adenovirus polypeptide IX revealed as capsid cement by difference images from electron microscopy and crystallography. *EMBO J, 8*(12), 3563-3570.

Greber, U. F., & Puntener, D. (2009). DNA-tumor virus entry--from plasma membrane to the nucleus. *Semin Cell Dev Biol, 20*(5), 631-642.

Greber, U. F., Webster, P., Weber, J., & Helenius, A. (1996). The role of the adenovirus protease on virus entry into cells. *EMBO J, 15*(8), 1766-1777.

Greber, U. F., Willetts, M., Webster, P., & Helenius, A. (1993). Stepwise dismantling of adenovirus 2 during entry into cells. *Cell, 75*(3), 477-486.

Gross, L. (1951). Pathogenic properties, and "vertical" transmission of the mouse leukemia agent. *Proc Soc Exp Biol Med, 78*(1), 342-348.

Haruki, H., Gyurcsik, B., Okuwaki, M., & Nagata, K. (2003). Ternary complex formation between DNA-adenovirus core protein VII and TAF-Ibeta/SET, an acidic molecular chaperone. *FEBS Lett, 555*(3), 521-527.

Haruki, H., Okuwaki, M., Miyagishi, M., Taira, K., & Nagata, K. (2006). Involvement of template-activating factor I/SET in transcription of adenovirus early genes as a positive-acting factor. *J Virol, 80*(2), 794-801.

Janicki, S. M., & Spector, D. L. (2003). Nuclear choreography: interpretations from living cells. *Curr Opin Cell Biol, 15*(2), 149-157.

Johnson, J. S., Osheim, Y. N., Xue, Y., Emanuel, M. R., Lewis, P. W., Bankovich, A., et al. (2004). Adenovirus protein VII condenses DNA, represses transcription, and associates with transcriptional activator E1A. *J Virol, 78*(12), 6459-6468.
Kawase, H., Okuwaki, M., Miyaji, M., Ohba, R., Handa, H., Ishimi, Y., et al. (1996). NAP-I is a functional homologue of TAF-I that is required for replication and transcription of the adenovirus genome in a chromatin-like structure. *Genes Cells, 1*(12), 1045-1056.
Keppler, B. R., & Archer, T. K. (2008). Chromatin-modifying enzymes as therapeutic targets--Part 2. *Expert Opin Ther Targets, 12*(11), 1457-1467.
Kojaoghlanian, T., Flomenberg, P., & Horwitz, M. S. (2003). The impact of adenovirus infection on the immunocompromised host. *Rev Med Virol, 13*(3), 155-171.
Korn, R., & Horwitz, M. S. (1986). Adenovirus DNA synthesis in vitro is inhibited by the virus-coded major core protein. *Virology, 150*(2), 342-351.
Lehmberg, E., Traina, J. A., Chakel, J. A., Chang, R. J., Parkman, M., McCaman, M. T., et al. (1999). Reversed-phase high-performance liquid chromatographic assay for the adenovirus type 5 proteome. *J Chromatogr B Biomed Sci Appl, 732*(2), 411-423.
Lichtenstein, D. L., Toth, K., Doronin, K., Tollefson, A. E., & Wold, W. S. (2004). Functions and mechanisms of action of the adenovirus E3 proteins. *Int Rev Immunol, 23*(1-2), 75-111.
Lim, R. Y., Aebi, U., & Stoffler, D. (2006). From the trap to the basket: getting to the bottom of the nuclear pore complex. *Chromosoma, 115*(1), 15-26.
Lim, R. Y., Ullman, K. S., & Fahrenkrog, B. (2008). Biology and biophysics of the nuclear pore complex and its components. *Int Rev Cell Mol Biol, 267*, 299-342.
Luger, K., & Richmond, T. J. (1998). DNA binding within the nucleosome core. *Curr Opin Struct Biol, 8*(1), 33-40.
Mabit, H., Nakano, M. Y., Prank, U., Saam, B., Dohner, K., Sodeik, B., et al. (2002). Intact microtubules support adenovirus and herpes simplex virus infections. *J Virol, 76*(19), 9962-9971.
Maier, O., Galan, D. L., Wodrich, H., & Wiethoff, C. M. (2010). An N-terminal domain of adenovirus protein VI fragments membranes by inducing positive membrane curvature. *Virology*.
Mangel, W. F., Baniecki, M. L., & McGrath, W. J. (2003). Specific interactions of the adenovirus proteinase with the viral DNA, an 11-amino-acid viral peptide, and the cellular protein actin. *Cell Mol Life Sci, 60*(11), 2347-2355.
Marx, J. L. (1982). New disease baffles medical community. *Science, 217*(4560), 618-621.
Matthews, D. A. (2001). Adenovirus protein V induces redistribution of nucleolin and B23 from nucleolus to cytoplasm. *J Virol, 75*(2), 1031-1038.
Matthews, D. A., & Russell, W. C. (1995). Adenovirus protein-protein interactions: molecular parameters governing the binding of protein VI to hexon and the activation of the adenovirus 23K protease. *J Gen Virol, 76 (Pt 8)*, 1959-1969.
Matthews, D. A., & Russell, W. C. (1998). Adenovirus core protein V is delivered by the invading virus to the nucleus of the infected cell and later in infection is associated with nucleoli. *J Gen Virol, 79 (Pt 7)*, 1671-1675.
Meier, O., Boucke, K., Hammer, S. V., Keller, S., Stidwill, R. P., Hemmi, S., et al. (2002). Adenovirus triggers macropinocytosis and endosomal leakage together with its clathrin-mediated uptake. *J Cell Biol, 158*(6), 1119-1131.
Meier, O., & Greber, U. F. (2004). Adenovirus endocytosis. *J Gene Med, 6 Suppl 1*, S152-163.
Mirza, M. A., & Weber, J. (1982). Structure of adenovirus chromatin. *Biochim Biophys Acta, 696*(1), 76-86.
Mothes, W., Sherer, N. M., Jin, J., & Zhong, P. (2010). Virus cell-to-cell transmission. *J Virol*.
Nakano, M. Y., Boucke, K., Suomalainen, M., Stidwill, R. P., & Greber, U. F. (2000). The first step of adenovirus type 2 disassembly occurs at the cell surface, independently of endocytosis and escape to the cytosol. *J Virol, 74*(15), 7085-7095.
Nemerow, G. R., Pache, L., Reddy, V., & Stewart, P. L. (2009). Insights into adenovirus host cell interactions from structural studies. *Virology, 384*(2), 380-388.
Nevins, J. R., Ginsberg, H. S., Blanchard, J. M., Wilson, M. C., & Darnell, J. E., Jr. (1979). Regulation of the primary expression of the early adenovirus transcription units. *J Virol, 32*(3), 727-733.
Nwanegbo, E., Vardas, E., Gao, W., Whittle, H., Sun, H., Rowe, D., et al. (2004). Prevalence of neutralizing antibodies to adenoviral serotypes 5 and 35 in the adult populations of The Gambia, South Africa, and the United States. *Clin Diagn Lab Immunol, 11*(2), 351-357.
Okuwaki, M., Iwamatsu, A., Tsujimoto, M., & Nagata, K. (2001). Identification of nucleophosmin/B23, an acidic nucleolar protein, as a stimulatory factor for in vitro replication of adenovirus DNA complexed with viral basic core proteins. *J Mol Biol, 311*(1), 41-55.
Okuwaki, M., Matsumoto, K., Tsujimoto, M., & Nagata, K. (2001). Function of nucleophosmin/B23, a nucleolar acidic protein, as a histone chaperone. *FEBS Lett, 506*(3), 272-276.
Okuwaki, M., & Nagata, K. (1998). Template activating factor-I remodels the chromatin structure and stimulates transcription from the chromatin template. *J Biol Chem, 273*(51), 34511-34518.
Pante, N., & Kann, M. (2002). Nuclear pore complex is able to transport macromolecules with diameters of about 39 nm. *Mol Biol Cell, 13*(2), 425-434.
Parkin, D. M. (2006). The global health burden of infection-associated cancers in the year 2002. *Int J Cancer, 118*(12), 3030-3044.
Paulus, C., Nitzsche, A., & Nevels, M. (2010). Chromatinisation of herpesvirus genomes. *Rev Med Virol, 20*(1), 34-50.
Pombo, A., Ferreira, J., Bridge, E., & Carmo-Fonseca, M. (1994). Adenovirus replication and transcription sites are spatially separated in the nucleus of infected cells. *EMBO J, 13*(21), 5075-5085.
Puvion-Dutilleul, F., Besse, S., Pichard, E., & Cajean-Feroldi, C. (1998). Release of viruses and viral DNA from nucleus to cytoplasm of HeLa cells at late stages of productive adenovirus infection as revealed by electron microscope in situ hybridization. *Biol Cell, 90*(1), 5-38.
Puvion-Dutilleul, F., Pedron, J., & Cajean-Feroldi, C. (1984). Identification of intranuclear structures containing the 72K DNA-binding protein of human adenovirus type 5. *Eur J Cell Biol, 34*(2), 313-322.
Rekosh, D. M., Russell, W. C., Bellet, A. J., & Robinson, A. J. (1977). Identification of a protein linked to the ends of adenovirus DNA. *Cell, 11*(2), 283-295.
Ribbeck, K., & Gorlich, D. (2001). Kinetic analysis of translocation through nuclear pore complexes. *EMBO J, 20*(6), 1320-1330.
Russell, W. C. (2009). Adenoviruses: update on structure and function. *J Gen Virol, 90*(Pt 1), 1-20.

Samad, M. A., Okuwaki, M., Haruki, H., & Nagata, K. (2007). Physical and functional interaction between a nucleolar protein nucleophosmin/B23 and adenovirus basic core proteins. *FEBS Lett, 581*(17), 3283-3288.
Scaria, A., Tollefson, A. E., Saha, S. K., & Wold, W. S. (1992). The E3-11.6K protein of adenovirus is an Asn-glycosylated integral membrane protein that localizes to the nuclear membrane. *Virology, 191*(2), 743-753.
Seo, S. B., Macfarlan, T., McNamara, P., Hong, R., Mukai, Y., Heo, S., et al. (2002). Regulation of histone acetylation and transcription by nuclear protein pp32, a subunit of the INHAT complex. *J Biol Chem, 277*(16), 14005-14010.
Seo, S. B., McNamara, P., Heo, S., Turner, A., Lane, W. S., & Chakravarti, D. (2001). Regulation of histone acetylation and transcription by INHAT, a human cellular complex containing the set oncoprotein. *Cell, 104*(1), 119-130.
Silvestry, M., Lindert, S., Smith, J. G., Maier, O., Wiethoff, C. M., Nemerow, G. R., et al. (2009). Cryo-electron microscopy structure of adenovirus type 2 temperature-sensitive mutant 1 reveals insight into the cell entry defect. *J Virol, 83*(15), 7375-7383.
Stewart, P. L., Burnett, R. M., Cyrklaff, M., & Fuller, S. D. (1991). Image reconstruction reveals the complex molecular organization of adenovirus. *Cell, 67*(1), 145-154.
Stewart, P. L., Fuller, S. D., & Burnett, R. M. (1993). Difference imaging of adenovirus: bridging the resolution gap between X-ray crystallography and electron microscopy. *EMBO J, 12*(7), 2589-2599.
Strahl, B. D., & Allis, C. D. (2000). The language of covalent histone modifications. *Nature, 403*(6765), 41-45.
Strunze, S., Trotman, L. C., Boucke, K., & Greber, U. F. (2005). Nuclear targeting of adenovirus type 2 requires CRM1-mediated nuclear export. *Mol Biol Cell, 16*(6), 2999-3009.
Suomalainen, M., Nakano, M. Y., Boucke, K., Keller, S., & Greber, U. F. (2001). Adenovirus-activated PKA and p38/MAPK pathways boost microtubule-mediated nuclear targeting of virus. *EMBO J, 20*(6), 1310-1319.
Suomalainen, M., Nakano, M. Y., Keller, S., Boucke, K., Stidwill, R. P., & Greber, U. F. (1999). Microtubule-dependent plus- and minus end-directed motilities are competing processes for nuclear targeting of adenovirus. *J Cell Biol, 144*(4), 657-672.
Talbert, P. B., & Henikoff, S. (2010). Histone variants--ancient wrap artists of the epigenome. *Nat Rev Mol Cell Biol, 11*(4), 264-275.
Talcott, B., & Moore, M. S. (1999). Getting across the nuclear pore complex. *Trends Cell Biol, 9*(8), 312-318.
Terry, L. J., Shows, E. B., & Wente, S. R. (2007). Crossing the nuclear envelope: hierarchical regulation of nucleocytoplasmic transport. *Science, 318*(5855), 1412-1416.
Tollefson, A. E., Ryerse, J. S., Scaria, A., Hermiston, T. W., & Wold, W. S. (1996). The E3-11.6-kDa adenovirus death protein (ADP) is required for efficient cell death: characterization of cells infected with adp mutants. *Virology, 220*(1), 152-162.
Tollefson, A. E., Scaria, A., Hermiston, T. W., Ryerse, J. S., Wold, L. J., & Wold, W. S. (1996). The adenovirus death protein (E3-11.6K) is required at very late stages of infection for efficient cell lysis and release of adenovirus from infected cells. *J Virol, 70*(4), 2296-2306.
Tollefson, A. E., Scaria, A., Saha, S. K., & Wold, W. S. (1992). The 11,600-MW protein encoded by region E3 of adenovirus is expressed early but is greatly amplified at late stages of infection. *J Virol, 66*(6), 3633-3642.
Trentin, J. J., Yabe, Y., & Taylor, G. (1962). The quest for human cancer viruses. *Science, 137*, 835-841.
Trotman, L. C., Achermann, D. P., Keller, S., Straub, M., & Greber, U. F. (2003). Non-classical export of an adenovirus structural protein. *Traffic, 4*(6), 390-402.
Trotman, L. C., Mosberger, N., Fornerod, M., Stidwill, R. P., & Greber, U. F. (2001). Import of adenovirus DNA involves the nuclear pore complex receptor CAN/Nup214 and histone H1. *Nat Cell Biol, 3*(12), 1092-1100.
Ugai, H., Borovjagin, A. V., Le, L. P., Wang, M., & Curiel, D. T. (2007). Thermostability/infectivity defect caused by deletion of the core protein V gene in human adenovirus type 5 is rescued by thermo-selectable mutations in the core protein X precursor. *J Mol Biol, 366*(4), 1142-1160.
van Oostrum, J., & Burnett, R. M. (1985). Molecular composition of the adenovirus type 2 virion. *J Virol, 56*(2), 439-448.
Weber, J. M. (2003). Adenain, the adenovirus endoprotease (a review). *Acta Microbiol Immunol Hung, 50*(1), 95-101.
Weber, J. M., & Khittoo, G. (1983). The role of phosphorylation and core protein V in adenovirus assembly. *J Gen Virol, 64 (Pt 9)*, 2063-2068.
Wickham, T. J., Mathias, P., Cheresh, D. A., & Nemerow, G. R. (1993). Integrins alpha v beta 3 and alpha v beta 5 promote adenovirus internalization but not virus attachment. *Cell, 73*(2), 309-319.
Wiethoff, C. M., Wodrich, H., Gerace, L., & Nemerow, G. R. (2005). Adenovirus protein VI mediates membrane disruption following capsid disassembly. *J Virol, 79*(4), 1992-2000.
Xue, Y., Johnson, J. S., Ornelles, D. A., Lieberman, J., & Engel, D. A. (2005). Adenovirus protein VII functions throughout early phase and interacts with cellular proteins SET and pp32. *J Virol, 79*(4), 2474-2483.
Zhang, Y., & Schneider, R. J. (1994). Adenovirus inhibition of cell translation facilitates release of virus particles and enhances degradation of the cytokeratin network. *J Virol, 68*(4), 2544-2555.

REVIEW

DNA-tumor virus entry – from plasma membrane to the nucleus.

Puntener, D. & U.F. Greber.

Seminars in Cell & Developmental Biology 2009

DNA-tumor virus entry - from plasma membrane to the nucleus

Daniel Puntener & Urs F. Greber[1)]

Institute of Zoology, University of Zürich, Winterthurerstrasse 190, CH-8057 Zürich, Switzerland

[1)] corresponding author

Abstract

DNA-tumor viruses comprise enveloped and nonenveloped agents that cause malignancies in a large variety of cell types and tissues by inferfering with cell cycle control and immortalization. Those DNA-tumor viruses that replicate in the nucleus use cellular mechanisms to transport their genome and newly synthesized viral proteins into the nucleus. This requires cytoplasmic transport and nuclear import of their genome. Agents that employ this strategy include adenoviruses, hepadnaviruses, herpesviruses, papillomaviruses, and polyomaviruses, but not poxviruses which replicate in the cytoplasm. Here, we discuss how DNA-tumor viruses enter cells, take advantage of cytoplasmic transport, and import their DNA genome through the nuclear pore complex into the nucleus. Remarkably, nuclear import of incoming genomes does not necessarily follow the same pathways used by the structural proteins of the viruses during the replication and assembly phases of the viral life cycle. Understanding the mechanisms of DNA nuclear import can identify new pathways of cell regulation and anti-viral therapies.

Key words

nucleocytoplasmic transport, nuclear pore complex, cytoplasmic transport, cell transformation, virus entry

List of virus abbreviations

Duck hepatitis virus (dHBV)
Epstein Barr virus (EBV)
Hepatitis B virus (HBV)
Herpes simplex virus 1 (HSV1)
Human adenovirus (Ad)
Human herpesvirus (HHV)
Human papillomavirus (HPV)
Kaposi's sarcoma-associated herpesvirus (KSHV)
Merkel cell polyomavirus (MCPyV)
Papovaviruses (polyoma and papilloma viruses)
Varizella zoster virus (VZV)

Contents

Contributions: [1] D. Puntener, [2] U.F. Greber

1. Introduction

Medical and epidemiologic records indicate that 12–20% of the human cancer incidences worldwide are associated with viral infections (Parkin, 2006). These infections are mostly due to DNA-tumor viruses, the flavivirus hepatitis C virus (HCV), and retroviruses, such as the human T lymphotropic virus type 1 (HTLV-1), a slow transforming RNA retrovirus associated with adult T-cell leukemia (Javier & Butel, 2008; McLaughlin-Drubin & Munger, 2008; Pagano, et al., 2004; zur Hausen, 2002). A variety of viruses induce tumors in animals and a few of them have been recognized by the International Agency for Research in Cancer (IARC) as human carcinogens (Carbone & Barbanti-Brodano, 2006). DNA-tumor viruses are a diverse group of agents grouped into twenty-two families of double-stranded DNA-viruses infecting vertebrates and invertebrates but not plants (Tab. 1) (International Committee on Taxonomy of Viruses, http://www.ictvonline.org/index.asp). Their capsid sizes range from 30 nm in the case of Hepatits B virus (HBV) up to 150 nm for Epstein Barr virus (EBV). Their genomes are linear, for example adenovirus, or circular such as SV40. They can be non-enveloped, such as adenoviridae, papillomaviridae, polyomaviridae, or enveloped, such as herpesviruses and hepadnaviruses.

Human Adenovirus type 12 (Ad12) was the first human virus recognized to be oncogenic when it was found to cause malignant tumors after inoculation into newborn hamsters (Trentin, Yabe, & Taylor, 1962) (Tab. 1). Later, it was shown that Ad12 integrates its DNA into the host chromosomes (Dörfler, 1968). Up to now, no epidemiologic evidence has been reported of adenovirus-associated malignancies in humans, although a recent study detected Ad-DNA in pediatric brain tumors (Kosulin, et al., 2007).

Herpesviruses are classified into three subfamlies, alpha-, beta- and gamma-herpesviruses (Knipe & Cliffe, 2008), some of which have been associated with human cancers of epithelia and lymphatic cells (Cesarman & Mesri, 2007; Molho-Pessach & Lotem, 2007) (Tab. 1). The chicken alpha-herpesvirus Marek's disease virus causes T cell tumors, neurological disease and immune suppression in its natural host (Osterrieder, Kamil, Schumacher, Tischer, & Trapp, 2006). The beta-herpesvirus human cytomegalovirus (HCMV) is associated with glioblastoma (for a recent discussion, see G. Miller, 2009) but has so far not been observed to transform normal cells into cancerous cells. The gamma-herpesvirus Epstein Barr virus (EBV) was the first virus shown to induce human tumors, nasopharyngeal carcinoma (Epstein, Henle, Achong, & Barr, 1965).

Papillomaviruses are the causative agents of skin warts, laryngeal papillomas and cervical carcinoma, and occur in skin cancers and head and neck sarcomas (Hebner & Laimins, 2006) (Tab. 1). Sexually transmitted human HPVs infect the genital tract, and are classified as 'low risk' or 'high risk' based on their capability to cause cervical carcinoma. Among the high risk papilloma viruses, HPV16 is a major cause of cervical cancer (J. N. Roberts, et al., 2007) and infects basal keratinocytes of mucosal epithelia that undergo differentiation.

Members of the polyomavirus family have tumorigenic potential which was initially shown for SV40 (Girardi, Sweet, Slotnick, & Hilleman, 1962) (Tab. 1). SV40 causes oncogenic transformation in nonpermissive rodent hosts, although not in its natural host, the rhesus macaque. Other members of the polyomaviruses have been implicated in the etiology of rare neuronal tumors (White, et al., 2005). Most recently, an aggressive human skin cancer, Merkel cells carcinoma has been linked to a previously unknown polyomavirus, the Merkel cell polyomavirus (MCPyV) (Feng, Shuda, Chang, & Moore, 2008). In addition, hepadnaviruses that replicate through an RNA intermediate have been

associated with hepatocellular carcinoma (Pungpapong, Kim, & Poterucha, 2007) (Tab. 1).

Here we discuss the mechanims of nuclear transport and import of viral genomes during the early phases of DNA-tumor virus infections. Nuclear import of viral structural proteins and transforming proteins has been extensively reviewed in the recent past (Alvisi, Rawlinson, Ghildyal, Ripalti, & Jans, 2008; Fontoura, Faria, & Nussenzveig, 2005; Greber & Fassati, 2003; Pouton, Wagstaff, Roth, Moseley, & Jans, 2007). For nucleocytoplasmic transport of RNA from DNA-tumor viruses we refer to recent reviews on adenoviruses (Dobner & Kzhyshkowska, 2001; Fontoura, et al., 2005), herpesviruses (Mettenleiter, Klupp, & Granzow, 2006; Sandri-Goldin, 2001; Sommer & Heise, 2008), papillomaviruses and polyomaviruses (Jiang, Abend, Johnson, & Imperiale, 2008) and hepadnaviruses (Lopez-Bueno, Villarreal, & Almendral, 2006).

2. DNA-tumor virus entry into cells

Virus entry into cells is a stepwise process which has been studied in some detail in cultured cells (see e.g., Greber & Fassati, 2003; Marsh & Helenius, 2006; Sieczkarski & Whittaker, 2005). For a schematic view of a generic entry pathway, see Fig. 1. In certain primary cells or explant cultures, they have been more difficult to study due to strong innate host anti-virus responses, and the limited availability and batch-to-batch variations of these cells. Nonetheless, there are a number of entry steps that are universally required for infection of diverse cell types with human or prototypic DNA-tumor viruses, including virus attachment to a receptor at the cell surface (for recent reviews, see Dugan, Eash, & Atwood, 2006; Glebe & Urban, 2007; Greber & Gastaldelli, 2007;

Heldwein & Krummenacher, 2008; Pedersen & Hollsberg, 2006; Stanley, Pett, & Coleman, 2007; Young, Herbert, Barlow, Holers, & Hannan, 2008), and lateral movements of the virus-receptor complex to specialized sites on the plasma membrane (reviewed in Sattentau, 2008; Sherer & Mothes, 2008). These lateral movements can lead the virus particles, for example, to tight and adherens junctions, where additional receptors are localized, such as CAR for adenoviruses, or nectins for herpesviruses (Greber & Gastaldelli, 2007).

The lateral junctions not only maintain cell adhesion but also regulate epithelial and endothelial cell proliferation. This is reflected in the observation that deregulated cell adhesion is a hallmark of invasive tumors. Recently it has been suggested that a ubiquitin ligase of KSHV targets vascular endothelial cadherin for ubiquitin-mediated degradation (Mansouri, Rose, Moses, & Fruh, 2008). Cadherin degradation leads to rearrangements of the actin cytoskeleton and disregulated transendothelial barriers, which could open the gate for additional viruses and increase tumorigenicity. These features are reminescent of the HBV protein HBx which promotes hepatocellular carcinoma by enhancing the degradation of the extracellular matrix (Lara-Pezzi, et al., 2002) and downregulating cadherin (J. O. Lee, et al., 2005).

The surface-bound DNA-tumor viruses are in many cases taken up by endocytic processes or direct penetration through the plasma membrane (Akula, et al., 2003; Amstutz, et al., 2008; Damm & Pelkmans, 2006; Dugan, et al., 2006; Funk, Mhamdi, Hohenberg, Will, & Sirma, 2006; Gastaldelli, et al., 2008; Lin, et al., 1997; Meier & Greber, 2003; Querbes, O'Hara, Williams, & Atwood, 2006; Rappocciolo, et al., 2008; Spoden, et al., 2008), or they may fuse their envelope with the limiting endosomal membrane (Cooper, Paran, & Shaul, 2003; Heldwein & Krummenacher, 2008). Endocytozed nonenveloped viruses can penetrate the limiting endosomal membrane (Greber, 2002; Greber, Singh, & Helenius, 1994; Sieczkarski & Whittaker, 2005), or a membrane of the

endoplasmic reticulum (Burckhardt & Greber, 2008; Schelhaas, et al., 2007). For example, papillomaviruses are taken up by endocytosis, and released from endosomes upon proteolytic cleavage of the minor capsid protein L2 by cellular furin proteases (Richards, Lowy, Schiller, & Day, 2006; Selinka, Giroglou, & Sapp, 2002). L2 remains associated with the viral DNA and ends up in the nucleus near promyelocytic leukemia protein bodies (Day, Baker, Lowy, & Schiller, 2004).

3. Bidirectional cytoplasmic transport of incoming virus particles provides a mechanism to reach the nucleus

Cytoplasmic transport of DNA-tumor viruses or prototypic DNA-tumor viruses has been studied in some detail, most prominently with HSV1 (Mabit, et al., 2002; Sodeik, Ebersold, & Helenius, 1997) and Ad2/5 (Kelkar, Pfister, Crystal, & Leopold, 2004; J. G. Smith, Cassany, Gerace, Ralston, & Nemerow, 2008; Suomalainen, Nakano, Boucke, Keller, & Greber, 2001; Suomalainen, et al., 1999). These viruses take advantage of the microtubule-based motor protein complex dynein/dynactin to the minus ends of microtubules near the nucleus (for reviews, see Greber & Way, 2006; Leopold & Pfister, 2006; Radtke, Dohner, & Sodeik, 2006). EBV likely follows the same route on microtubules to the nucleus as HSV1 because its capsid protein BFRF3, a homologue of the HSV capsid protein UL35, associates with dynein light chains similar to HSV1 (Douglas, et al., 2004). Bidirectional transport towards and away from the nucleus allows fine-tuning and precise delivery of capsids to avoid unproductive situations, such as accumulations at the microtubule organzing centers (Greber & Way, 2006). For DNA-tumor viruses it may ensure nuclear targeting in cells with divergent orientations of microtubules, such as polarized epithelial cells where microtubule minus ends are near the apical membrane, or basal cells where minus ends are near the nucleus.

3.1. Viral determination of the transport direction or no transport bias?

There are several possibilities how viruses might achieve their delivery to the nuclear membrane. One is that they themselves define a transport preference by exposing proteins on the capsid that preferentially associate with a plus end or a minus end directed microtubule motor (Greber, 2005). For example, the gamma-herpesvirus murine herpesvirus 4 which lacks the ORF75c tegument protein failed to be transported to the nucleus of murine cells although it was delivered into the cytosol (Gaspar, Gill, Losing, May, & Stevenson, 2008). Incoming HSV1 capsids preferentially recruit the dynein/dynactin motor complex as opposed to a plus end-directed motor, whereas newly assembled capsids recruit a periphery directed motor (Luxton, et al., 2005; Nagel, et al., 2008).

An important question is the nature of the viral binding partner for motor proteins. Limited proteolysis of incoming HSV capsid or tegument proteins is part of a stepwise uncoating programme to make virions competent for engagement with cytoplasmic motors, such as the minor capsid protein VP26 or the tegument protein UL36 (VP1/2) (Wolfstein, et al., 2006). For incoming viruses, it was suggested that proteasomal degradation but not ubiquitin is required for HSV localization to the nucleus (Delboy, Roller, & Nicola, 2008). Alternatively, cytoplasmic processing of incoming capsids might make them competent for docking to the nuclear pore complex (NPC) as observed shortly after infection (Mabit, et al., 2002). This suggests that nuclear accumulation occurs by retention, not requiring a transport bias. In support of this, incoming Ad2/5 particles were found to be enriched at the nucleus in certain cell types without a detectable transport bias to the nucleus (Suomalainen, et al., 1999).

3.2. Regulated transport

Other aspects of cytoplasmic virus transport are subject to regulation by cell signalling. It has been observed, for example, that signalling through protein kinase A and p38/MAPK enhanced the nuclear delivery of incoming Ad2/5 by

stimulating minus end–directed transport (Suomalainen, et al., 2001). Likewise, the activation of Rac1 during Ad2/5 entry, which stabilizes peripheral microtubules (Gundersen, 2002) increased the loading of Ad2/5 to microtubules (Warren & Cassimeris, 2007). This is consistent with the observation that microtubule stabilizing compounds at very low concentrations enhanced nuclear targeting of Ad2/5 (Giannakakou, et al., 2002), and incoming Ad2/5 stabilized microtubules (Warren, Rutkowski, & Cassimeris, 2006).

Similar results have also been reported for KSHV, which activates Rho GTPases (Naranatt, Krishnan, Smith, & Chandran, 2005). Activation of RhoA and Rac GTPase alters the dynamics by increasing the acetylation of microtubules thereby enhancing the dynein motor dependent transport of KSHV to the nucleus. Interestingly, both Ad2/5 and KSHV use RGD peptides in one of their virion proteins to bind integrins for upstream signalling and endocytic uptake (Akula, Pramod, Wang, & Chandran, 2002; Meier & Greber, 2003; Stewart & Nemerow, 2007). Integrin activation by the incoming viruses may lead to activation of Rho GTPases and PI3K activation (Raghu, et al., 2007), and local stabilization of microtubules, and thereby enhance the loading of viruses to the tracks. It is possible that similar mechanisms are used by EBV, which encodes BFRF3, a homologue of the HSV UL35 (VP26) capsid protein which associates with dynein light chains (Douglas, et al., 2004). The upstream signalling events for EBV are however not known, despite the notion that EBV enters B-cells through an endocytic pathway and fuses with the endosomal membrane at low pH (N. Miller & Hutt-Fletcher, 1992; Nemerow & Cooper, 1984).

Although the mechanisms of motor loading to the cytosolic virus particles are not known, components of the dynein motor in complex with the dynactin subunit have been observed on a number of cytoplasmic DNA-tumor viruses, including adenoviruses, herpesviruses, and papillomaviruses (Dohner, et al.,

2002; Florin, et al., 2006; Leopold, et al., 2000; Schroer, 2004; J. G. Smith, et al., 2008; Suomalainen, et al., 1999). Interestingly, interference with the dynein/dynactin motor not only reduced viral transport towards the nucleus, but also decreased the transport rate to the periphery in some instances. This suggests that dynactin and components of the dynein motor complex enable high activities of both dynein and kinesin motors on DNA-tumor viruses. This interpretation is supported by trafficking studies of cellular cargoes where dynactin interference inhibited bidirectional (Gross, Welte, Block, & Wieschaus, 2002), and overexpression of p50/dynamitin reduced both dynein- and kinesin II-mediated transport of melanosomes in Xenopus laevis (Deacon, et al., 2003). Possibly, yet unknown proteins coordinate the activities of minus and plus end directed motors on the viral cargo, as suggested for lipid droplets in drosophila (Shubeita, et al., 2008), or bidirectional transport is simply a consequence of the properties of the motors, as suggested for the transport of peroxisomes (Ally, Larson, Barlan, Rice, & Gelfand, 2008).

4. From microtubules to the nucleus

Incoming DNA-tumor viruses can reach the nuclear envelope by several mechanisms. One is that the viruses must pass through the microtubule-organizing center (MTOC) (pathway A, Fig. 1), or that they detach from the microtubules proximal to the nucleus (pathway B, Fig. 1). Detachment could, for example, occur by virus modification at the MTOC, or by an activity gradient of a nuclear factor leading to motor detachment from the tracks or the virus. For Ad2/5 it has been shown that treating cells with inhibitors or siRNAs against the nuclear export factor CRM1 reduced the targeting of incoming Ad2/5 to the nucleus but did not affect viral transport on microtubules (Strunze, Trotman, Boucke, & Greber, 2005), and this requires the capsid protein hexon as suggested by antibody interference (J. G. Smith, et al., 2008). CRM1 or a nuclear protein exported by CRM1 to the cytoplasm could hence provide a cue

for virus detachment from microtubules. Alternatively, CRM1, which binds Nup214/CAN could be involved in maintaining a functional binding site for the virus on the NPC.

A second possibility to localize viruses to the nucleus is by stochastic detachment from microtubule tracks and cytoplasmic diffusion of the free particles until a binding site at the nuclear envelope, for example the NPC is reached. This mechanism would be expected to be less rapid and less efficient than regulated detachment.

A third, intermediate strategy is to detach the incoming DNA-tumor viruses from microtubules directly at the NPC thereby bypassing a diffusion step through the cytoplasm. This model is attractive because the most distal NPC protein RanBP2 (NUP358) has a binding site for microtubules (Joseph & Dasso, 2008), and could thereby connect cytoplasmic transport with nuclear import. In this model viruses could either traffic all the way to the minus ends of microtubules near the centrosome, and revert transport direction towards the periphery to approach the nuclear envelope, or they could directly reach the nucleus by microtubules that lead from the periphery to the centrosome in close proximity to the nuclear envelope.

A fourth possibility to access the nucleoplasm has been suggested for polyomaviruses. These viruses are targeted to the endoplasmic reticulum and nuclear envelope lumen, from where they could penetrate the inner nuclear membrane (Magnuson, et al., 2005; Schelhaas, et al., 2007). To what extent this unconventional pathway into the nucleus is used is, however, unknown. Infectious incoming SV40 particles have been found in the cytosol on the other hand (reviewed in Greber & Kasamatsu, 1996; Whittaker, Kann, & Helenius, 2000) which implies that these viruses can use a pathway from the cytosol to the NPC into the nucleus for infection.

5. The nuclear pore complex - gate keeper of nucleocytoplasmic exchange

DNA-tumor viruses infect nondividing cells and effectively utilize and manipulate the NPC. NPCs are large macromolecular complexes, which control all known nucleocytoplasmic exchange of nondividing cells (reviewed in D'Angelo & Hetzer, 2008; Terry, Shows, & Wente, 2007). There are multiple pathways for a large variety of cargoes through the NPC. The general transport mechanism involves affinity gating on natively unfolded phenylalanine-glycine (FxFG and GLFG) rich nucleoporins (NUPs, Frey & Gorlich, 2007; Lim, et al., 2007; Patel, Belmont, Sante, & Rexach, 2007). The affinity of transport receptors to the natively unfolded proteins provides selectivity for passage of the receptor-cargo complex through the NPC. Stability and hence directionality of the receptor-cargo complex is controlled by the small GTP binding protein Ran (Gorlich & Kutay, 1999).

Within the NPC, the cytoplasmic filament protein Nup214/CAN and its associated protein Nup88 are involved in nuclear export of preribosomal complexes (Bernad, Engelsma, Sanderson, Pickersgill, & Fornerod, 2006), and NES bearing proteins (Hutten & Kehlenbach, 2006). The cytoplasmic filament protein RanBP2/Nup358 provides a docking platform for export complexes that are being disassembled, and for binding of cargo-free export receptors before they return to the nucleus (Engelsma, Bernad, Calafat, & Fornerod, 2004). It is also involved in import of NLS containing proteins, and its absence can be compensated by overexpression of import receptors (Hutten, Flotho, Melchior, & Kehlenbach, 2008). In single round import reactions, neither RanBP2 nor Nup214/CAN are required for import of model proteins (Walther, et al., 2002). This supports the notion that NPC proteins, and in particular the FG-repeat proteins have a high degree of redundancy (Strawn, Shen, Shulga, Goldfarb, & Wente, 2004).

Finally, an important aspect of NPC function for DNA-tumor virus infections is that the pore diameter can be gated. Kinetic studies have shown that within time frames typical for the entry phase of most viruses, the permeability diameter of the pore is in the range of 40 nm (Pante & Kann, 2002). Although this is still too small for the passage of adenovirus, herpesvirus, or papovavirus (polyoma and papilloma) capsids, it is large enough for the passage of hepadnaviruses and also parvoviruses.

6. Adenovirus docks and disassembles at the NPC, and releases the viral chromatin into the nucleus

6.1. Adenovirus disruption

In vitro and *in vivo* studies have shown that Ad2/5 bind to NPCs independently of cytosolic factors including NLS-containing proteins or nuclear import or export receptors (Trotman, Mosberger, Fornerod, Stidwill, & Greber, 2001; Wisnivesky, Leopold, & Crystal, 1999). The major viral capsid protein hexon binds to the NPC protein Nup214/CAN located at the base of the cytoplasmic filaments. This is reminescent of the Stat1 transcription factor binding to FG-nucleoporins Nup153 and Nup214 (Marg, et al., 2004). Unlike Stat1, only 5% of the incoming hexon is found to be imported into the nucleus (Greber, Willetts, Webster, & Helenius, 1993). This is equivalent to the amount of one facette of the icosahedral capsid, and indicates that hexon itself does not have a functional NLS. Accordingly, newly synthesized hexon protein enters the nucleus for viral capsid assembly only by chaperone-mediated folding (Hong, et al., 2005) and binding to the nucleophilic protein VI (D.A. Matthews & Russell, 1994; Wodrich, et al., 2003). Noteably, the large majority of incoming protein VI remains within endosomes (Greber, Webster, Weber, & Helenius, 1996) where it supports

virus escape to the cytosol (Gastaldelli, et al., 2008; Wiethoff, Wodrich, Gerace, & Nemerow, 2005). The NPC-docked virions bind the highly mobile nuclear histone H1 (Misteli, Gunjan, Hock, Bustin, & Brown, 2000), either via the acidic clusters of hexon facing towards the outside of the virion (Rux & Burnett, 2000), or the viral DNA (Fig. 2). This together with the H1-import factors importin (karyopherin) β and importin 7, and additional factors contributes to capsid disruption and uncoating of the DNA-nucleoprotein complex for import (Saphire, Guan, Schirmer, Nemerow, & Gerace, 2000; Trotman, et al., 2001).

6.2. Nuclear import of adenovirus DNA associated proteins

The viral chromatin enters the nucleus, yet the composition of the core, which is translocated through the NPC is not well defined. The covalent interaction of the preterminal protein (pTP) with the 5' ends of the viral genome predicts that the pTP is imported together with the DNA (Zhao & Padmanabhan, 1988) (Fig. 2). It is also likely that pVII and possibly histone H1 accompany the DNA through the NPC (Trotman, et al., 2001; Xue, Johnson, Ornelles, Lieberman, & Engel, 2005). In contrast, the composition of the core in the virus is well known. It is made up of four viral proteins, protein V (pV, 368 amino acids, 157 copies per genome (van Oostrum & Burnett, 1985)), pVII (174 amino acids, about 800 copies per genome, (Sung, Lischwe, Richards, & Hosokawa, 1977)), mu (19 amino acids, Hosokawa & Sung, 1976)) and two copies of the terminal protein (671 amino acids) covalently attached to the 5' ends of the linear viral DNA (Berk, 2007).

pV, pVII and mu are positively charged and condense the viral DNA. The most abundant core protein pVII is tightly bound to the DNA in a manner similar to the core histones of eucaryotic chromatin (Johnson, et al., 2004), and remains associated with the viral DNA throughout the early phase of the viral life cycle (Chatterjee, Vayda, & Flint, 1986; Xue, et al., 2005). It is thought to attenuate viral gene expression, and is associated with the chromatin-modifying

complexes SET and INHAT. The precursor of pVII has basic NLS sequences that target the protein to the nucleus by interacting with importin alpha/beta (Hindley, Lawrence, & Matthews, 2007; T. W. Lee, Blair, & Matthews, 2003). It has also been shown that pVII isolated from recombinant *E. coli* is imported into the nucleus of digitonin permeabilized cells by binding to the import factor transportin which recognizes M9-type sequences (Hindley, et al., 2007). Whether pVII contains an M9-like sequence is unknown. *In vitro* assays further suggested that nuclear import of the viral DNA required transportin, as it could be competed for by excess of soluble M9-GST fusion proteins (Hindley, et al., 2007). Surprisingly, an excess of pVII was not able to compete for DNA-import which suggests that pVII is not sufficient. If transportin is involved in nuclear import of the incoming viral DNA and infection remains unknown. It is also unknown if and how the terminal protein is involved in import of the viral DNA (Zhao & Padmanabhan, 1988).

Regardless, the incoming viral DNA-protein complex is remodeled in the nucleus, which involves several host factors of the chromatin remodeling complex, template-activating factor-I (TAF-I), TAF-II, TAF-III and the acidic protein pp32 (Haruki, Okuwaki, Miyagishi, Taira, & Nagata, 2006; Spector, 2007). TAF-I forms a ternary complex with pVII (Haruki, Gyurcsik, Okuwaki, & Nagata, 2003; Xue, et al., 2005), and this is required for rapid onset of early viral gene transcription as suggested by siRNA knock-down experiments (Haruki, et al., 2006). Later in the infection cycle, nucleophosmin/B23 interacts with newly synthesized precursor of pVII and suppresses aggregation of viral DNA with core proteins in the nucleus, and thereby supports viral assembly (Samad, Okuwaki, Haruki, & Nagata, 2007).

Unlike pVII and terminal protein, the other core protein pV is less tightly bound to the DNA, and may be released before or during DNA import into the nucleus, as suggested by chromatin immunoprecipitations (Spector, Johnson, Baird, &

Engel, 2003). It is not known if pV enters the nucleus on its own or in complex with other factors (D. A. Matthews & Russell, 1998b), or if it stays in the cytoplasm in association with the mitochondrial protein p32 implicated in ARF-mediated apoptosis (Itahana & Zhang, 2008; D. A. Matthews & Russell, 1998a). Remarkably, a pV knock-out virus is viable in the presence of compensatory mutations in the mu protein (Ugai, Borovjagin, Le, Wang, & Curiel, 2007). This suggests that pV has no unique functions in the replication cycle of mastadenoviruses, at least in cultured cells, which is further supported by the observation that pV does not occur in atadenoviruses, aviadenoviruses and siadenoviruses.

7. Herpesviruses dock to the NPC and release their DNA into the nucleus

7.1. Herpes simplex virus type 1 docking to the NPC

Similar to adenoviruses, herpesviruses uncoat their DNA at the NPC (see Fig. 2). This strategy precludes that the naked viral chromatin travels through the cytoplasm, which could trigger DNA-sensing innate immune responses including the TBK-IRF pathway or inflammasome (Barchet, Wimmenauer, Schlee, & Hartmann, 2008; Muruve, et al., 2008). *In vitro* experiments showed that HSV-1 capsids purified from extracellular virions by detergent and high salt treatments bound to NPCs of rat liver nuclear envelopes depending on soluble importin β, Ran-GTP and other factors (Ojala, Sodeik, Ebersold, Kutay, & Helenius, 2000). Experiments with the hamster mutant cell line tsBN2 (Dickmanns, et al., 1996) at the restrictive temperature confirmed that the Ran guanine nucleotide exchange factor RCC1 (regulator of chromosome condensation 1) was required for genome delivery to the nucleus or gene expression (Strang & Stow, 2007).

Although the components of the viral capsid recognized by importin beta are not known, it has been shown trypsin-treated capsids, which lost the inner tegument proteins including UL47 (VP13/14), UL48 (VP16) and UL49 (VP22) poorly bound to the isolated nuclei. While the UL48 (VP16) transcription factor associated with UL49 (VP22) and supported virus assembly (Hafezi, Bernard, Cook, & Elliott, 2005), the knock out of UL49 (VP22) had no effects on the expression levels of the immediate early viral protein ICP0 (Elliott, Hafezi, Whiteley, & Bernard, 2005), indicating that UL49 (VP22) has no important role for nuclear import of HSV1 DNA. Interestingly, the 32 kDa tegument protein UL14 has been implicated in enhancing nuclear import of UL48 (VP16), and it enhanced nuclear targeting of incoming HSV1 (Yamauchi, et al., 2008). In the nucleus, it forms a regulatory complex with HCF1 and the POU-domain transcription factor Oct1, and thereby activates transcription of immediate early viral genes (Wysocka & Herr, 2003). It is possible that UL14 is involved in cytoplasmic transport or docking of incoming virions to the NPC, and thereby facilitates the uncoating of the viral DNA for nuclear import.

7.2. Herpes simplex type 1 mutants dissect uncoating and nuclear import

The recent developments of viral mutants have allowed progress in understanding viral mechanisms of capsid disassembly. Experiments with the classical HSV1 temperature sensitive mutant tsB7 and a similar pseudorabies virus mutant indicated that viral DNA is released at the NPC (Batterson, Furlong, & Roizman, 1983; Feldman, Blankenship, & Ben-Porat, 1981). At the non-permissive temperature tsB7 capsids containing DNA accumulated at the NPC, whereas upon temperature shift, DNA was released. This was consistant with early electron microscopy studies showing that empty capsids of incoming viruses accumulated at the nuclear membrane and persisted for several hours (Miyamoto & Morgan, 1971; Morgan, Rose, & Mednis, 1968). Mutational mapping of tsB7 showed that the UL36 gene encoding the VP1/2 tegument

protein was involved in releasing the DNA from the capsid (Zhou, Chen, Jakana, Rixon, & Chiu, 1999). UL36 (VP1/2) is conserved in beta- and gamma-herpesviruses (reviewed in Mettenleiter, 2004). UL36 (VP1/2) together with UL37 and UL25 is one of the innermost capsid associated tegument proteins that remain associated with the incoming capsids until docking at the NPC. UL36 deletion mutants failed to spread the infection to uninfected nuclei in experimentally induced syncitia indicating that UL36 was required for capsid transport to, or DNA import into the nucleus (A. P. Roberts, et al., 2009). Interestingly, proteolytic cleavage of VP1/2 was required for DNA import into the nucleus but not for capsid docking to the NPC (Jovasevic, Liang, & Roizman, 2008).

While UL37 was not required for delivery of HSV1 DNA into the nucleus (A. P. Roberts, et al., 2009) – although it was involved in pseudorabiesvirus transport to the nucleus (Krautwald, Fuchs, Klupp, & Mettenleiter, 2009), another inner tegument protein UL25 was specifically implicated in DNA uncoating, as indicated by the temperature sensitive HSV1 ts1249 mutant which had an uncoating defect at the restrictive temperature but was transported to the nucleus (Preston, Murray, Preston, McDougall, & Stow, 2008). Interestingly, the EBV may use similar mechanisms since its protein BVRF1 is a homologue of UL25 (Johannsen, et al., 2004) which remains capsid associated and localizes to microtubules as well as to nuclear membrane with incoming capsids (Kaelin, Dezelee, Masse, Bras, & Flamand, 2000). Since UL25 is also required for DNA packaging and associates with the portal complex at a single capsid vertex (Cockrell, Sanchez, Erazo, & Homa, 2009), it is possible that the DNA is extruded through the portal structure of the capsid (Cardone, et al., 2007; Chang, Schmid, Rixon, & Chiu, 2007; Newcomb, Booy, & Brown, 2007; Newcomb, et al., 2001). The portal is part of a ring structure made up by the UL6 protein, and has a 5 nm pore through which the viral DNA is packaged into the procapsid during replication of both herpesviruses and double-stranded DNA bacteriophages (Lander, et al., 2006). UL6 is conserved among other

alpha- herpesviruses, such as varizella zoster virus (VZV), which causes varicella (chickenpox, primary infection) and zoster (shingles, a secondary infection upon reactivation of VZV from latency). Future measurements of herpesvirus DNA uncoating on isolated nuclear envelopes in combination with specific orientations of single virus particles may unveil if the portal needs to be oriented towards the NPC for DNA release into the nucleus or if the orientation of the particles can be random. All this provides strong evidence that the inner tegument proteins UL25 and UL36 (VP1/2) and the portal are parts of capsid-associated complexes that interact with the NPC, and trigger the release of viral DNA from the capsid.

In the herpesvirus capsid, the DNA is tightly packed in a paracristalline array and thought to be protein-free, similar to bacteriophage DNA (Oh & Fraser, 2008). Studies of DNA ejection from bacteriophages had argued that DNA release can be attenuated by surrounding osmotic pressure implying that the process is independent of ATP consuming enzymes, such as motor proteins (Evilevitch, Lavelle, Knobler, Raspaud, & Gelbart, 2003). Recent studies have extended this concept showing that DNA condensation by osmotic stress and DNA binding proteins enhances the ejection process from the phages (Jeembaeva, Castelnovo, Larsson, & Evilevitch, 2008). For HSV1, atomic force microscopy experimentation suggested that the incoming genome is translocated through the NPC as a condensed rod-like structure with a diameter of 35-40 nm and a length of 130-160 nm (Shahin, et al., 2006). It is thus possible that the herpesvirus DNA picks up DNA condensing proteins, such as cellular histones after its release from the capsids. Histones would not only condense and neutralize negative charges on the DNA backbone, they would also be a template for import factors, such as importin beta- and importin 7 (Jakel, et al., 1999), and thereby increase the probability for DNA passage through the NPC, as suggested for adenovirus DNA (Trotman, et al., 2001). That histones could be involved in herpesvirus infection is also supported by the finding that incoming viral DNA was complexed with histones as early as 1 h

post infection, although it is not known how and where histones associate with the incoming DNA (Kent, et al., 2004). Whether tegument proteins with functional NLSs, such as UL36 (VP1/2) (Abaitua & O'Hare, 2008) mediate nuclear import of the DNA is not known.

8. Nuclear import of papillomaviruses and polyomaviruses

Human papillomaviruses (HPV) uptake is a slow process and not well defined, although it seems to be acid dependent (Day, Lowy, & Schiller, 2003; Selinka, et al., 2002; J. L. Smith, Campos, & Ozbun, 2007; Spoden, et al., 2008). Some HPVs bind to heparansulfate-proteoglycans (Giroglou, Florin, Schafer, Streeck, & Sapp, 2001) and possibly secondary receptor(s), such as alpha-6 integrin, laminin or tetraspanin proteins (Culp, Budgeon, Marinkovich, Meneguzzi, & Christensen, 2006; Evander, et al., 1997). Factors and signals that lead to nuclear import of nonstructural and structural HPV proteins are listed in Tab. 2. It is unknown, however, how the viruses reach the cytosol, and the genomes imported into the nucleus.

Similar to papillomaviruses, the polyomaviruses SV40, JC virus and BK virus access the nucleus after endocytic uptake (see Fig. 2) (Eash, Querbes, & Atwood, 2004; Pelkmans, Kartenbeck, & Helenius, 2001; Pho, Ashok, & Atwood, 2000). SV40 has a double-stranded closed circular DNA of 5000 base pairs, three structural proteins VP1, VP2, and VP3, and four core histones, H2A, H2B, H3 and H4 (Imperiale & Major, 2007). VP1 forms 72 pentameric capsomers (Yan, Stehle, Liddington, Zhao, & Harrison, 1996), incorporating the minor proteins, VP2 and VP3 that are thought to contact the minichromosome and the VP1 pentamer (Clever, Dean, & Kasamatsu, 1993). It is thought that

polyomaviruses undergo limited conformational changes at the plasma membrane, in endosomes or the endoplasmic reticulum (ER). In the case of SV40, the reducing environment and the protein folding machinery of the ER may lead to the release of DNA-containing subviral particles into the cytosol (Schelhaas, et al., 2007). This may also lead to the exposure of the NLS in the amino-terminus of the capsid protein VP1 (reviewed in Greber & Kasamatsu, 1996; Kasamatsu & Nakanishi, 1998).

Experiments with microinjected SV40 favor the notion that infectious viral DNA passes through the cytosol (Clever, Yamada, & Kasamatsu, 1991). SV40 subviral particles were found to be imported into the nucleus, as concluded from the observation that the injection of neutralizing antibodies against the VP1 amino-terminus or against VP3 into infected cells blocked infection (Nakanishi, Clever, Yamada, Li, & Kasamatsu, 1996) (Fig. 2). These subviral particles are thought to contain the core histones, yet the histone-complexed minichromosomes were poorly targeted to the nucleus (Nakanishi, et al., 1996). This indicates a role for the VP1,2,3 proteins in cytoplasmic transport or NPC binding.

Interestingly, VP1,2,3 can each be independently imported into the nucleus (Ishii, et al., 1996). VP1 has a bipartite amino-terminal NLS whereas VP2 and VP3 have a classical SV40 T-antigen-like signal in the carboxy-terminus (Ishii, Nakanishi, Yamada, Macalalad, & Kasamatsu, 1994). Recently, cytosolic virus was found to bind importin α and β (Nakanishi, Li, Qu, Jafri, & Kasamatsu, 2007). Only a small fraction of the incoming DNA was, however, recovered in immune complexes with VP1 and the minor capsid protein VP3. The DNA was sensitive to DNase, unlike the DNA of intact purified SV40 particles. This suggests that SV40 entry into the cytosol is slow, rather inefficient, and coupled to partial DNA uncoating.

A similar process of NLS exposure and importin binding may operate for JC virus entry, which may reflect a similar use of NLS sequences for nuclear import of newly synthesized proteins (Shishido-Hara, Ichinose, Higuchi, Hara, & Yasui, 2004). Unlike SV40, JC virions were apparently imported into the nucleus in a more intact form than the SV40 subviral particles, as suggested by analyses of particles loaded with free fluorescent dye molecules (Qu, et al., 2004).

9. Nuclear import of hepadnaviruses

HBV is an enveloped DNA-virus with an icosahedral capsid of 180 or 240 core proteins (Crowther, et al., 1994). HBV infects primary human hepatocytes and a few cell lines at low efficiency, which makes it difficult to study the infectious entry of this virus. Lipofection has been used to deliver HBV capsids into the cytoplasm (Rabe, Glebe, & Kann, 2006). In these experiments capsids were transported by microtubule dependent motors to the nuclear membrane where they bound to NPCs, and they released their genome into the nucleus. These results were similar to studies with duck hepatitis virus (dHBV) (Funk, et al., 2006; Funk, Mhamdi, Lin, Will, & Sirma, 2004; Stoeckl, et al., 2006). dHBV core proteins have an internal NLS as the carboxy-terminus of the HBV core (Mabit, Breiner, Knaust, Zachmann-Brand, & Schaller, 2001). A dHBV knock-out mutant lacking the core NLS was not found at the NPC suggesting that this NLS was directly or indirectly required for capsid localization to the NPC. Biochemical studies suggested that attachment of HBV capsids to the NPC and transport through the NPC involved importins and the NLS in the carboxy-terminus of the HBV core protein (Kann, Sodeik, Vlachou, Gerlich, & Helenius, 1999; Steven, et al., 2005) (Fig. 2). In native capsids, this NLS is not exposed at the surface, which implies that conformational changes of the capsid during entry are required for importin binding, capsid uncoating and DNA import into the nucleus (Kann, Schmitz, & Rabe, 2007). An alternative nuclear import

model for HBV suggested that the capsids could very transiently interact with the NPC in an importin-independent manner (Lill, et al., 2006). These results suggested that binding of HBV initially occurs on one of the cytoplasmic filaments, off-centered from the central axis of the NPC towards the edges by about 45 nm. How uncoating of the viral DNA occurs is unknown.

10. Conclusions and outlook

Nuclear import of DNA-tumor virus genomes depends on cell type and virus specific steps, such as binding to receptors, uptake and signaling into cells. Subsequent events, including rupture of endomembranes, cytoplasmic transport, uncoating and nuclear import of the genome involve virus family-specific mechanisms, and can be studied with prototypic DNA-tumor viruses and the tumor viruses. In the past years, signals and host factors for nuclear import have been identified for a considerable number of DNA-tumor virus capsid proteins. These studies have so far not resulted in novel anti-viral treatments, possibly due to a strong similarity of viral protein import with host protein import into the nucleus. Ongoing analyses of viral genome uncoating and nuclear import may, in contrast, identify exquisite host factors for viral DNA import. If such factors are dispensible for normal cell functions in cells that are infected by DNA-tumor viruses, they constitute a new class of targets for anti-viral compounds. Mechanistic cell biological analyses combined with interference experiments in cells and animal models will be necessary to elucidate the complex interplay between the tumor viruses and the host.

Acknowledgements

Work in the Greber laboratory was supported by the Swiss National Science Foundation, the Cancer League of the Canton of Zurich and Oncoswiss.

Figures and Tables

Fig. 1: Prototypic entry pathway of a DNA-tumor virus

An intact virus particle (red) attaches to a primary and secondary receptor(s), which can elicit signalling into the cell. Viral transport on the cell surface is followed by confinement and endocytosis (or direct penetration of the plasma membrane in some cases), which coincides with initiation of a stepwise viral uncoating programme (or membrane fusion). Virus is taken into primary vesicles and transported to intracellular compartments where penetration to the cytosol occurs. Bidirectional microtubule-dependent transport moves viruses to the microtubule-organizing center (MTOC) (A), or along the nuclear envelope (B), from where viruses reach the nuclear pore complex (NPC) by unknown mechanisms. They bind to the NPC, uncoat their DNA and release it into the nucleus.

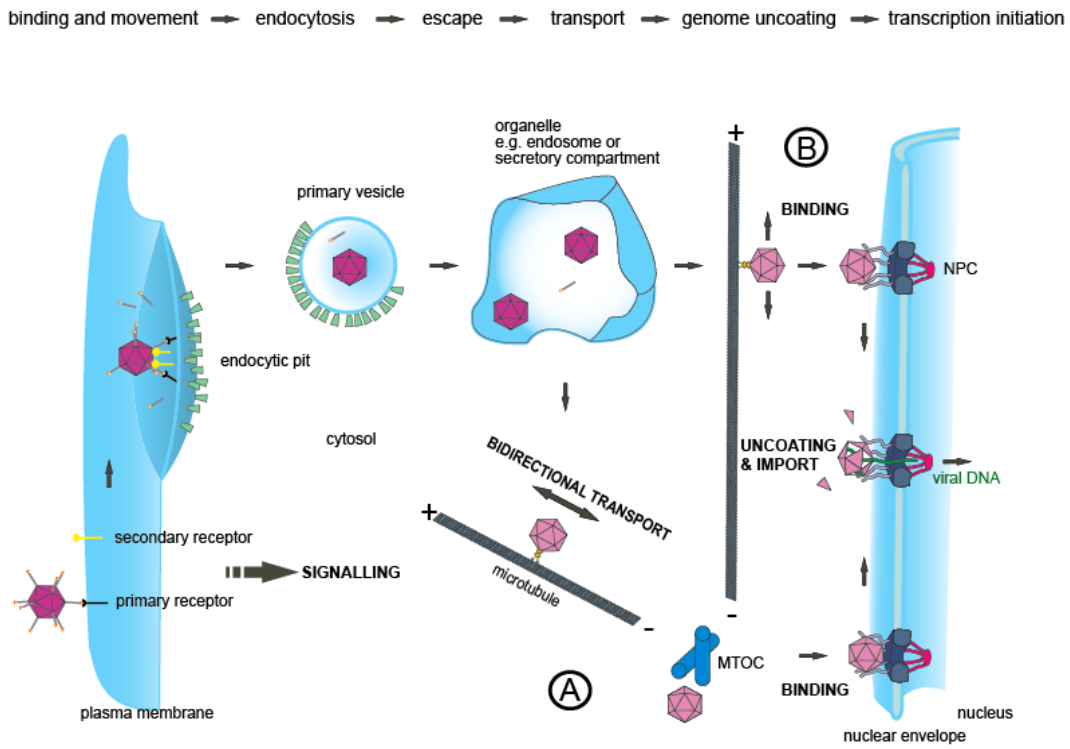

Fig. 2: Disassembly and nuclear import strategies of DNA-tumor viruses

Adenoviruses, herpesviruses, polyomaviruses and hepadnaviruses import cores with linear or circular genomic DNA and viral proteins into the nucleus of post-mitotic cells. A) Schematic representation of four prototypic nuclear import mechanisms for viral cores containing genome and viral proteins. Adenoviruses employ a capsid disruption strategy at the nuclear pore complex to release the core from the capsid. Herpesviruses use a capsid unplugging mechanism, and polyomaviruses and hepadnaviruses a mechanism which delivers capsids or subcapsid particles into the nucleus. The table of panel B) lists the NLS-containing viral core proteins and the host factors (importins) recognizing these NLSs.

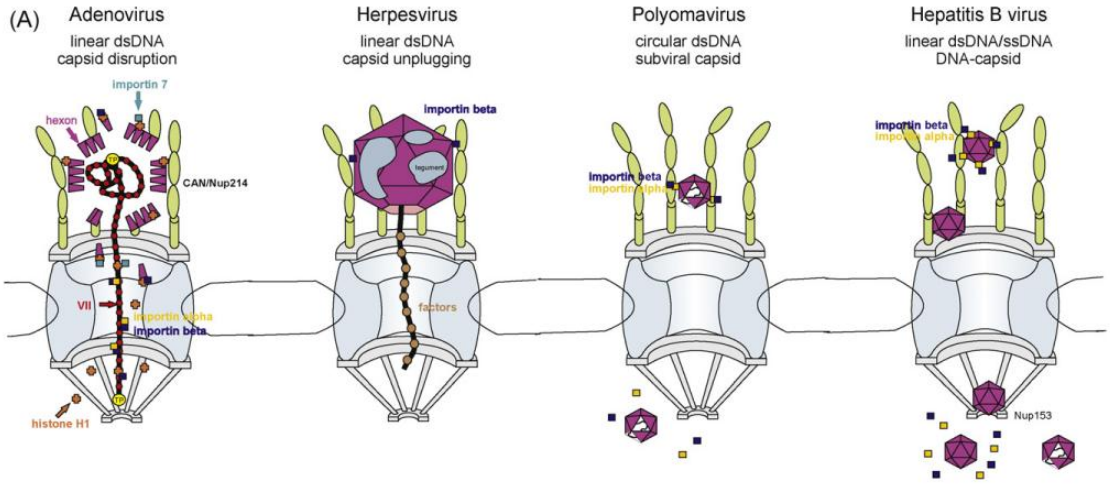

(B) Cellular and viral factors for nuclear import of DNA-containing tumor virus cores

Virus	DNA	Viral NLS-factor	Importin	References
Ad2/5	linear dsDNA	protein VII	imp α/β	(117, 127, 136)
			transportin	(137)
		terminal protein	?	(128)
		linker histone H1	imp β, imp 7	(117, 178)
HSV-1	linear dsDNA	UL36 (VP1/2)	imp β	(149, 160, 163, 180)
		UL47 (VP13/14)	?	(149, 162)
		UL14	?	(154)
		core histones?	?	(179)
SV40	circular dsDNA	VP1, VP3	imp α/β	(194, 195, 197)
		core histones?	?	(209)
JCV	circular dsDNA	VP1	imp α/β	(198, 199)
		core histones?	?	in analogy to SV40?
HBV	dsDNA, partly ssDNA	core protein	imp α/β	(205, 206)
HBV GFP-capsid		core protein	no importin	(208)
dHBV	dsDNA, partly ssDNA	core protein	imp α/β	(204)

Table 1

Table 1
The most common mammalian DNA-tumor viruses.

Family	Genus Species	Serotype	Size (nm)	Oncogene	Tumor	References
Adenoviridae			90	E1A, E1B, E4orf1		[133,210]
	Mastadenoviruses	Ad12			Experimental tumors in rodents	[7,8]
		Various serotypes from subspecies A, B, C, D			Candidate tumor viruses	
Herpesviridae			150			
	Alpha-herpesviruses					
	Mardivirus	Gallid herpesvirus 2 (Marek's disease virus)				[13]
		Gamma-herpesviruses				[211]
	Lymphocryptovirus	Human herpesvirus 4 (HHV4, Epstein–Barr virus, EBV)	EBNA-2,3		Burkitt's lymphoma	[212]
	Rhadinovirus	Saimiriine herpesvirus 2 (Herpesvirus saimiri)				[213]
		Murid herpesvirus 4 (Murid herpesvirus 68)				[214]
		Human herpesvirus 8 (HHV8, Kaposi's sarcoma virus KSHV)	K1, vGPCR	Kaposi's sarcoma		[215]
Papillomaviridae			55	E6, E7	Squamous cell carcinomas	[2,216]
	Alpha-papillomaviruses	Human papillomavirus 16, 18, 31, 45 Rhesus papillomavirus type 1 (RhPV1)				
	Gamma-papillomaviruses	Human papillomavirus 4				
	Delta-papillomaviruses	Bovine papillomavirus 1, 2				
	European elk papillomavirus					
	Kappa-papillomaviruses	Cottontail rabbit papillomavirus				
	Lambda-papillomaviruses	Canine oral papillomavirus				
	Mu-papillomaviruses	Human papillomavirus 1				
	Xi-papillomaviruses	Bovine papillomavirus 4				
Polyomaviridae			40	T-antigen		[189,209]
	Simian virus 40 (SV40)				Sarcomas in juvenile hamsters	[217]
	BK virus				Brain tumors	[218])
	JC virus				Gliomas, medulloblastomas	[219]
	Merkel cell polyomavirus (MCPyV)				Human skin cancer	[20]
	Murine polyomavirus				Mesotheliomas	[220]
	Hamster polyomavirus				Cutaneous tumors	[221]
Hepadnaviridae			30–34	HBx	Hepatocellular carcinoma	[222]
	Orthohepadnaviruses	Hepatitis B virus (HBV)				
		Woodchuck hepatitis virus (WHV)			Animal model virus	[223]
Poxviridae			200 × 300			[224]
	Chordopoxviruses					[225]
	Molluscipoxviruses	Molluscum contagiosum virus			Epidermal tumors	[226]
	Leporipoxviruses	Shope fibroma virus	SFGF		Benign cutaneous tumors	[227]
	Yatapoxviruses	Yaba monkey tumor virus			Subcutaneous histicytomas	[228]
	Avipoxviruses	Fowlpoxvirus				[229]

Table 2

Table 2
Nucleocytoplasmic shuttling of human papillomavirus proteins.

Protein	Import	Export	Function	Literature
Non-structural, regulatory				
E1	Imp α3/4/5/E2	CRM1	DNA strand separation	[1–6]
E2	Strong NLS in hinge region		E1 assembly, tethering factor Transcriptional activator	[1,6,7]
E4	Putative classical NLS		Host replication inhibition Interaction with keratin network	[8,9]
E5	Cytoplasmic protein		Growth stimulation	[10]
E6	Various importins	CRM1?	Inactivation of p53	[11,12]
E7	Ran-dependent, large NLS	NES	Inactivation of tumor supressors Importin-independent?	[13,14]
Structural, capsid				
L1	α2/β1		Main capsid component	[15–18]
L2	α2/β1, β2, β3, Hsc70		Membrane destabilisation	[15,19–22]

A recent report indicated that HPV16 requires host cells to go through early prophase of the cell cycle for successful onset of transcription of the viral capsid associated genes [230].
Literature for the Table.

[1] Howley P, Lowy D. Papillomaviruses. In Knipe DM, Howley PM, editors. Fields virology. Philadelphia, PA, USA: Lippincott Williams & Wilkins; 2007. p. 2299–2354.
[2] Bian XL, Rosas-Acosta G, Wu YC, Wilson VG. Nuclear import of bovine papillomavirus type 1 E1 protein is mediated by multiple alpha importins and is negatively regulated by phosphorylation near a nuclear localization signal. J Virol 2007;81(6):2899–2908.
[3] Rosas-Acosta G, Wilson VG. Identification of a nuclear export signal sequence for bovine papillomavirus E1 protein. Virology 2008;373(1):49–162.
[4] Yu JH, Lin BY, Deng W, Broker TR, Chow LT. Mitogen-activated protein kinases activate the nuclear localization sequence of human papillomavirus type 11 E1 DNA helicase to promote efficient nuclear import. J Virol 2007;81(10):5066–78.
[5] Florin L, Sapp C, Streeck RE, Sapp M. Assembly and translocation of papillomavirus capsid proteins. J Virol 2002;76(19):10009–14.
[6] Wu YC, Deyrieux AF, Wilson VG. Papillomaviruses and the host SUMOylation system. Biochem Soc Trans 2007;35(Pt 6):1433–35.
[7] Zou N, Lin BY, Duan F, Lee KY, Jin G, Guan R, et al. The hinge of the human papillomavirus type 11 E2 protein contains major determinants for nuclear localization and nuclear matrix association. J Virol 2000;74(8):3761–70.
[8] Roberts S, Kingsbury SR, Stoeber K, Knight GL, Gallimore PH, Williams GH. Identification of an arginine-rich motif in human papillomavirus type 1 E1;E4 protein necessary for E4-mediated inhibition of cellular DNA synthesis in vitro and in cells. J Virol 2008;82(18):9056–64.
[9] Davy CE, Jackson DJ, Wang Q, Raj K, Masterson PJ, Fenner NF, et al. Identification of a G(2) arrest domain in the E1 wedge E4 protein of human papillomavirus type 16. J Virol 2002;76(19):9806–18.
[10] Thomsen P, van Deurs B, Norrild B, Kayser L. The HPV16 E5 oncogene inhibits endocytic trafficking. Oncogene 2000;19(52):6023–32.
[11] Le Roux LG, Moroianu J. Nuclear entry of high-risk human papillomavirus type 16 E6 oncoprotein occurs via several pathways. J Virol 2003;77(4):2330–37.
[12] Freedman DA, Levine AJ. Nuclear export is required for degradation of endogenous p53 by MDM2 and human papillomavirus E6. Mol Cell Biol 1998;18(12):7288–93.
[13] Angeline M, Merle E, Moroianu J. The E7 oncoprotein of high-risk human papillomavirus type 16 enters the nucleus via a nonclassical Ran-dependent pathway. Virology 2003;317(1):13–23.
[14] Knapp AA, McManus PM, Bockstall K, Moroianu J. Identification of the nuclear localization and export signals of high risk HPV16 E7 oncoprotein. Virology 2009;383(1):60–8.
[15] Chen XS, Garcea RL, Goldberg I, Casini G, Harrison SC. Structure of small virus-like particles assembled from the L1 protein of human papillomavirus 16. Mol Cell 2000;5(3):557–567.
[16] Paintsil J, Muller M, Picken M, Gissmann L, Zhou J. Carboxyl terminus of bovine papillomavirus type-1 L1 protein is not required for capsid formation. Virology 1996;223(1):238–244.
[17] Nelson LM, Rose RC, Moroianu J. Nuclear import strategies of high risk HPV16 L1 major capsid protein. J Biol Chem 2002;277(26):23958–64.
[18] Bird G, O'Donnell M, Moroianu J, Garcea RL. Possible role for cellular karyopherins in regulating polyomavirus and papillomavirus capsid assembly. J Virol 2008;82(20):9848–57.
[19] Bordeaux J, Forte S, Harding E, Darshan MS, Klucevsek K, Moroianu J. The l2 minor capsid protein of low-risk human papillomavirus type 11 interacts with host nuclear import receptors and viral DNA. J Virol 2006;80(16):8259–62.
[20] Darshan MS, Lucchi J, Harding E, Moroianu J. The l2 minor capsid protein of human papillomavirus type 16 interacts with a network of nuclear import receptors. J Virol 2004;78(22):12179–88.
[21] Klucevsek K, Daley J, Darshan MS, Bordeaux J, Moroianu J. Nuclear import strategies of high-risk HPV18 L2 minor capsid protein. Virology 2006;352(1):200–8.
[22] Florin L, Becker KA, Sapp C, Lambert C, Sirma H, Muller M, et al. Nuclear translocation of papillomavirus minor capsid protein L2 requires Hsc70. J Virol 2004;78(11):5546–53.

References

Abaitua, F., & O'Hare, P. (2008). Identification of a highly conserved, functional nuclear localization signal within the N-terminal region of herpes simplex virus type 1 VP1-2 tegument protein. *J Virol, 82*(11), 5234-5244.

Akula, S. M., Naranatt, P. P., Walia, N. S., Wang, F. Z., Fegley, B., & Chandran, B. (2003). Kaposi's sarcoma-associated herpesvirus (human herpesvirus 8) infection of human fibroblast cells occurs through endocytosis. *J Virol, 77*(14), 7978-7990.

Akula, S. M., Pramod, N. P., Wang, F. Z., & Chandran, B. (2002). Integrin alpha3beta1 (CD 49c/29) is a cellular receptor for Kaposi's sarcoma-associated herpesvirus (KSHV/HHV-8) entry into the target cells. *Cell, 108*(3), 407-419.

Ally, S., Larson, A. G., Barlan, K., Rice, S., & Gelfand, V. (2008). Mechanical Cross-Talk between Kinesin-1 and Cytoplasmic Dynein In Vivo. *Mol Cell Biol, 19 (suppl)*, abstract no 1547.

Alvisi, G., Rawlinson, S. M., Ghildyal, R., Ripalti, A., & Jans, D. A. (2008). Regulated nucleocytoplasmic trafficking of viral gene products: a therapeutic target? *Biochim Biophys Acta, 1784*(1), 213-227.

Amstutz, B., Gastaldelli, M., Kälin, S., Imelli, N., Boucke, K., Wandeler, E., et al. (2008). Subversion of CtBP1 controlled macropinocytosis by human Adenovirus serotype 3. *EMBO J., 27*(7), 956-966.

Barchet, W., Wimmenauer, V., Schlee, M., & Hartmann, G. (2008). Accessing the therapeutic potential of immunostimulatory nucleic acids. *Curr Opin Immunol, 20*(4), 389-395.

Batterson, W., Furlong, D., & Roizman, B. (1983). Molecular genetics of Herpes simplex virus. VIII. Further characterization of a temperature-sensitive mutant defective in release of viral DNA and in other stages of the viral reproductive cycle. *J. Virol., 45*, 397-407.

Berk, A. J. (2007). Adenoviridae: the viruses and their replication. In D. M. Knipe & P. M. Howley (Eds.), *Fields Virology* (5 ed., Vol. 2, pp. 2355-2436). Philadelphia, PA, USA: Lippincott Williams & Wilkins.

Bernad, R., Engelsma, D., Sanderson, H., Pickersgill, H., & Fornerod, M. (2006). Nup214-Nup88 nucleoporin subcomplex is required for CRM1-mediated 60 S preribosomal nuclear export. *J Biol Chem, 281*(28), 19378-19386.

Burckhardt, C. J., & Greber, U. F. (2008). Redox rescues virus from ER trap. *Nat Cell Biol, 10*(1), 9-11.

Carbone, M., & Barbanti-Brodano, M. G. (2006). Viral carcinogenesis. In A. E. C. e. al. (Ed.), *Oncology, an evidence-based approach* (pp. 214-232). New York: Springer.

Cardone, G., Winkler, D. C., Trus, B. L., Cheng, N., Heuser, J. E., Newcomb, W. W., et al. (2007). Visualization of the herpes simplex virus portal in situ by cryo-electron tomography. *Virology, 361*(2), 426-434.

Cesarman, E., & Mesri, E. A. (2007). Kaposi sarcoma-associated herpesvirus and other viruses in human lymphomagenesis. *Curr Top Microbiol Immunol, 312*, 263-287.

Chang, J. T., Schmid, M. F., Rixon, F. J., & Chiu, W. (2007). Electron cryotomography reveals the portal in the herpesvirus capsid. *J Virol, 81*(4), 2065-2068.

Chatterjee, P. K., Vayda, M. E., & Flint, S. J. (1986). Adenoviral protein VII packages intracellular viral DNA throughout the early phase of infection. *Embo Journal, 5*(7), 1633-1644.

Clever, J., Dean, D. A., & Kasamatsu, H. (1993). Identification of a DNA binding domain in simian virus 40 capsid proteins Vp2 and Vp3. *J. Biol. Chem., 268*(28), 20877-20883.

Clever, J., Yamada, M., & Kasamatsu, H. (1991). Import of simian virus 40 virions through nuclear pore complexes. *Proc. Natl. Acad. Sci. U.S.A., 88*(16), 7333-7337.

Cockrell, S. K., Sanchez, M. E., Erazo, A., & Homa, F. L. (2009). Role of the UL25 protein in herpes simplex virus DNA encapsidation. *J Virol, 83*(1), 47-57.

Cooper, A., Paran, N., & Shaul, Y. (2003). The earliest steps in hepatitis B virus infection. *Biochim Biophys Acta, 1614*(1), 89-96.

Crowther, R. A., Kiselev, N. A., Bottcher, B., Berriman, J. A., Borisova, G. P., Ose, V., et al. (1994). Three-dimensional structure of hepatitis B virus core particles determined by electron cryomicroscopy. *Cell, 77*(6), 943-950.

Culp, T. D., Budgeon, L. R., Marinkovich, M. P., Meneguzzi, G., & Christensen, N. D. (2006). Keratinocyte-secreted laminin 5 can function as a transient receptor for human papillomaviruses by binding virions and transferring them to adjacent cells. *J Virol, 80*(18), 8940-8950.

D'Angelo, M. A., & Hetzer, M. W. (2008). Structure, dynamics and function of nuclear pore complexes. *Trends Cell Biol, 18*(10), 456-466.

Damm, E. M., & Pelkmans, L. (2006). Systems biology of virus entry in mammalian cells. *Cell Microbiol, 8*(8), 1219-1227.

Day, P. M., Baker, C. C., Lowy, D. R., & Schiller, J. T. (2004). Establishment of papillomavirus infection is enhanced by promyelocytic leukemia protein (PML) expression. *Proc Natl Acad Sci U S A, 101*(39), 14252-14257.

Day, P. M., Lowy, D. R., & Schiller, J. T. (2003). Papillomaviruses infect cells via a clathrin-dependent pathway. *Virology, 307*(1), 1-11.

Deacon, S. W., Serpinskaya, A. S., Vaughan, P. S., Lopez Fanarraga, M., Vernos, I., Vaughan, K. T., et al. (2003). Dynactin is required for bidirectional organelle transport. *J Cell Biol, 160*(3), 297-301.

Delboy, M. G., Roller, D. G., & Nicola, A. V. (2008). Cellular proteasome activity facilitates herpes simplex virus entry at a postpenetration step. *J Virol, 82*(7), 3381-3390.

Dickmanns, A., Bischoff, F. R., Marshallsay, C., Luhrmann, R., Ponstingl, H., & Fanning, E. (1996). The thermolability of nuclear protein import in tsBN2 cells is suppressed by microinjected Ran-GTP or Ran-GDP, but not by RanQ69L or RanT24N. *J Cell Sci, 109 (Pt 6)*, 1449-1457.

Dobner, T., & Kzhyshkowska, J. (2001). Nuclear export of adenovirus RNA. *Curr Top Microbiol Immunol, 259*, 25-54.

Dohner, K., Wolfstein, A., Prank, U., Echeverri, C., Dujardin, D., Vallee, R., et al. (2002). Function of dynein and dynactin in herpes simplex virus capsid transport. *Molecular Biology of the Cell, 13*(8), 2795-2809.

Dörfler, W. (1968). The fate of the DNA of adenovirus type 12 in baby hamster kidney cells. *60*, 636-643.

Douglas, M. W., Diefenbach, R. J., Homa, F. L., Miranda-Saksena, M., Rixon, F. J., Vittone, V., et al. (2004). Herpes simplex virus type 1 capsid protein VP26 interacts with dynein light chains RP3 and Tctex1 and plays a role in retrograde cellular transport. *J Biol Chem, 279*(27), 28522-28530.

Dugan, A. S., Eash, S., & Atwood, W. J. (2006). Update on BK virus entry and intracellular trafficking. *Transpl Infect Dis, 8*(2), 62-67.

Eash, S., Querbes, W., & Atwood, W. J. (2004). Infection of vero cells by BK virus is dependent on caveolae. *J Virol, 78*(21), 11583-11590.
Elliott, G., Hafezi, W., Whiteley, A., & Bernard, E. (2005). Deletion of the herpes simplex virus VP22-encoding gene (UL49) alters the expression, localization, and virion incorporation of ICP0. *J Virol, 79*(15), 9735-9745.
Engelsma, D., Bernad, R., Calafat, J., & Fornerod, M. (2004). Supraphysiological nuclear export signals bind CRM1 independently of RanGTP and arrest at Nup358. *Embo J, 23*(18), 3643-3652.
Epstein, M. A., Henle, G., Achong, B. G., & Barr, Y. M. (1965). Morphological and Biological Studies on a Virus in Cultured Lymphoblasts from Burkitt's Lymphoma. *J Exp Med, 121*, 761-770.
Evander, M., Frazer, I. H., Payne, E., Qi, Y. M., Hengst, K., & McMillan, N. A. (1997). Identification of the alpha6 integrin as a candidate receptor for papillomaviruses. *J Virol, 71*(3), 2449-2456.
Evilevitch, A., Lavelle, L., Knobler, C. M., Raspaud, E., & Gelbart, W. M. (2003). Osmotic pressure inhibition of DNA ejection from phage. *Proc Natl Acad Sci U S A, 100*(16), 9292-9295.
Feldman, L., Blankenship, M. L., & Ben-Porat, T. (1981). Isolation and characterization of a temperature-sensitive uncoating mutant of pseudorabies virus. *J Gen Virol, 54*(Pt 2), 333-342.
Feng, H., Shuda, M., Chang, Y., & Moore, P. S. (2008). Clonal integration of a polyomavirus in human Merkel cell carcinoma. *Science, 319*(5866), 1096-1100.
Florin, L., Becker, K. A., Lambert, C., Nowak, T., Sapp, C., Strand, D., et al. (2006). Identification of a dynein interacting domain in the papillomavirus minor capsid protein l2. *J Virol, 80*(13), 6691-6696.
Fontoura, B. M., Faria, P. A., & Nussenzveig, D. R. (2005). Viral interactions with the nuclear transport machinery: discovering and disrupting pathways. *IUBMB Life, 57*(2), 65-72.
Frey, S., & Gorlich, D. (2007). A saturated FG-repeat hydrogel can reproduce the permeability properties of nuclear pore complexes. *Cell, 130*(3), 512-523.
Funk, A., Mhamdi, M., Hohenberg, H., Will, H., & Sirma, H. (2006). pH-independent entry and sequential endosomal sorting are major determinants of hepadnaviral infection in primary hepatocytes. *Hepatology, 44*(3), 685-693.
Funk, A., Mhamdi, M., Lin, L., Will, H., & Sirma, H. (2004). Itinerary of hepatitis B viruses: delineation of restriction points critical for infectious entry. *J Virol, 78*(15), 8289-8300.
Gaspar, M., Gill, M. B., Losing, J. B., May, J. S., & Stevenson, P. G. (2008). Multiple functions for ORF75c in murid herpesvirus-4 infection. *PLoS ONE, 3*(7), e2781.
Gastaldelli, M., Imelli, N., Boucke, K., Amstutz, B., Meier, O., & Greber, U. F. (2008). Infectious Adenovirus Type 2 Transport Through Early but not Late Endosomes. *Traffic, 9*(12), 2265-2278.
Giannakakou, P., Nakano, M., Nicolaou, K. C., O'Brate, A., Yu, J., Blagosklonny, M. V., et al. (2002). Enhanced microtubule-dependent trafficking and p53 nuclear accumulation by suppression of microtubule dynamics. *Proc Natl Acad Sci U S A, 99*(16), 10855-10860.
Girardi, A. J., Sweet, B. H., Slotnick, V. B., & Hilleman, M. R. (1962). Development of tumors in hamsters inoculated in the neonatal period with vacuolating virus, SV-40. *Proc Soc Exp Biol Med, 109*, 649-660.
Giroglou, T., Florin, L., Schafer, F., Streeck, R. E., & Sapp, M. (2001). Human papillomavirus infection requires cell surface heparan sulfate. *J Virol, 75*(3), 1565-1570.
Glebe, D., & Urban, S. (2007). Viral and cellular determinants involved in hepadnaviral entry. *World J Gastroenterol, 13*(1), 22-38.
Gorlich, D., & Kutay, U. (1999). Transport between the cell nucleus and the cytoplasm. *Annu Rev Cell Dev Biol, 15*, 607-660.
Greber, U. F. (2002). Signalling in viral entry. *Cell Mol Life Sci, 59*, 608-626.
Greber, U. F. (2005). Viral trafficking violations in axons - the herpes virus case. [review]. *Proc. Natl. Acad. Sci. USA, 102*((16)), 5639-5640.
Greber, U. F., & Fassati, A. (2003). Nuclear import of viral DNA genomes. *Traffic, 4*, 136-143.
Greber, U. F., & Gastaldelli, M. (2007). Junctional gating: the Achilles' heel of epithelial cells in pathogen infection. *Cell Host and Microbe, 2*, 143-146.
Greber, U. F., & Kasamatsu, H. (1996). Nuclear targeting of adenovirus and simian virus SV40. *Trends Cell Biol., 6*, 189-195.
Greber, U. F., Singh, I., & Helenius, A. (1994). Mechanisms of virus uncoating. *Trends Microbiol., 2*, 52-56.
Greber, U. F., & Way, M. (2006). A super highway to virus infection. [review]. *Cell, 124(4)*, 741-754.
Greber, U. F., Webster, P., Weber, J., & Helenius, A. (1996). The role of the adenovirus protease in virus entry into cells. *EMBO J., 15*, 1766-1777.
Greber, U. F., Willetts, M., Webster, P., & Helenius, A. (1993). Stepwise dismantling of adenovirus 2 during entry into cells. *Cell, 75*, 477-486.
Gross, S. P., Welte, M. A., Block, S. M., & Wieschaus, E. F. (2002). Coordination of opposite-polarity microtubule motors. *J Cell Biol, 156*(4), 715-724.
Gundersen, G. G. (2002). Microtubule capture: IQGAP and CLIP-170 expand the repertoire. *Curr Biol, 12*(19), R645-647.
Hafezi, W., Bernard, E., Cook, R., & Elliott, G. (2005). Herpes simplex virus tegument protein VP22 contains an internal VP16 interaction domain and a C-terminal domain that are both required for VP22 assembly into the virus particle. *J Virol, 79*(20), 13082-13093.
Haruki, H., Gyurcsik, B., Okuwaki, M., & Nagata, K. (2003). Ternary complex formation between DNA-adenovirus core protein VII and TAF-Ibeta/SET, an acidic molecular chaperone. *FEBS Lett, 555*(3), 521-527.
Haruki, H., Okuwaki, M., Miyagishi, M., Taira, K., & Nagata, K. (2006). Involvement of template-activating factor I/SET in transcription of adenovirus early genes as a positive-acting factor. *J Virol, 80*(2), 794-801.
Hebner, C. M., & Laimins, L. A. (2006). Human papillomaviruses: basic mechanisms of pathogenesis and oncogenicity. *Rev Med Virol, 16*(2), 83-97.
Heldwein, E. E., & Krummenacher, C. (2008). Entry of herpesviruses into mammalian cells. *Cell Mol Life Sci, 65*(11), 1653-1668.
Hindley, C. E., Lawrence, F. J., & Matthews, D. A. (2007). A role for transportin in the nuclear import of adenovirus core proteins and DNA. *Traffic, 8*(10), 1313-1322.
Hong, S. S., Szolajska, E., Schoehn, G., Franqueville, L., Myhre, S., Lindholm, L., et al. (2005). The 100K-chaperone protein from adenovirus serotype 2 (Subgroup C) assists in trimerization and nuclear localization of hexons from subgroups C and B adenoviruses. *J Mol Biol, 352*(1), 125-138.

Hosokawa, K., & Sung, M. T. (1976). Isolation and characterization of an extreme basic protein from adenovirus type 5. *J. Virol., 17*, 924-934.
Hutten, S., Flotho, A., Melchior, F., & Kehlenbach, R. H. (2008). The Nup358-RanGAP Complex Is Required for Efficient Importin {alpha}/{beta}-dependent Nuclear Import. *Mol Biol Cell, 19*(5), 2300-2310.
Hutten, S., & Kehlenbach, R. H. (2006). Nup214 is required for CRM1-dependent nuclear protein export in vivo. *Mol Cell Biol, 26*(18), 6772-6785.
Imperiale, M., & Major, E. (2007). Polyomaviruses. In D. M. Knipe & P. M. Howley (Eds.), *Fields Virology* (5 ed., Vol. 2, pp. 2263-2298). Philadelphia, PA, USA: Lippincott Williams & Wilkins.
Ishii, N., Minami, N., Chen, E. Y., Medina, A. L., Chico, M. M., & Kasamatsu, H. (1996). Analysis of a nuclear localization signal of simian virus 40 major capsid protein Vp1. *J Virol, 70*(2), 1317-1322.
Ishii, N., Nakanishi, A., Yamada, M., Macalalad, M. H., & Kasamatsu, H. (1994). Functional complementation of nuclear targeting-defective mutants of simian virus 40 structural proteins. *J. Virol., 68*(12), 8209-8216.
Itahana, K., & Zhang, Y. (2008). Mitochondrial p32 is a critical mediator of ARF-induced apoptosis. *Cancer Cell, 13*(6), 542-553.
Jakel, S., Albig, W., Kutay, U., Bischoff, F. R., Schwamborn, K., Doenecke, D., et al. (1999). The importin beta/importin 7 heterodimer is a functional nuclear import receptor for histone H1. *Embo J, 18*(9), 2411-2423.
Javier, R. T., & Butel, J. S. (2008). The history of tumor virology. *Cancer Res, 68*(19), 7693-7706.
Jeembaeva, M., Castelnovo, M., Larsson, F., & Evilevitch, A. (2008). Osmotic pressure: resisting or promoting DNA ejection from phage? *J Mol Biol, 381*(2), 310-323.
Jiang, M., Abend, J. R., Johnson, S. F., & Imperiale, M. J. (2008). The role of polyomaviruses in human disease. *Virology*.
Johannsen, E., Luftig, M., Chase, M. R., Weicksel, S., Cahir-McFarland, E., Illanes, D., et al. (2004). Proteins of purified Epstein-Barr virus. *Proc Natl Acad Sci U S A, 101*(46), 16286-16291.
Johnson, J. S., Osheim, Y. N., Xue, Y., Emanuel, M. R., Lewis, P. W., Bankovich, A., et al. (2004). Adenovirus protein VII condenses DNA, represses transcription, and associates with transcriptional activator E1A. *J Virol, 78*(12), 6459-6468.
Joseph, J., & Dasso, M. (2008). The nucleoporin Nup358 associates with and regulates interphase microtubules. *FEBS Lett, 582*(2), 190-196.
Jovasevic, V., Liang, L., & Roizman, B. (2008). Proteolytic cleavage of VP1-2 is required for release of herpes simplex virus 1 DNA into the nucleus. *J Virol, 82*(7), 3311-3319.
Kaelin, K., Dezelee, S., Masse, M. J., Bras, F., & Flamand, A. (2000). The UL25 protein of pseudorabies virus associates with capsids and localizes to the nucleus and to microtubules. *J Virol, 74*(1), 474-482.
Kann, M., Schmitz, A., & Rabe, B. (2007). Intracellular transport of hepatitis B virus. *World J Gastroenterol, 13*(1), 39-47.
Kann, M., Sodeik, B., Vlachou, A., Gerlich, W. H., & Helenius, A. (1999). Phosphorylation-dependent binding of hepatitis B virus core particles to the nuclear pore complex. *J Cell Biol, 145*(1), 45-55.
Kasamatsu, H., & Nakanishi, A. (1998). How do animal DNA viruses get to the nucleus? *Annu Rev Microbiol, 52*, 627-686.
Kelkar, S. A., Pfister, K. K., Crystal, R. G., & Leopold, P. L. (2004). Cytoplasmic dynein mediates adenovirus binding to microtubules. *J Virol, 78*(18), 10122-10132.
Kent, J. R., Zeng, P. Y., Atanasiu, D., Gardner, J., Fraser, N. W., & Berger, S. L. (2004). During lytic infection herpes simplex virus type 1 is associated with histones bearing modifications that correlate with active transcription. *J Virol, 78*(18), 10178-10186.
Knipe, D. M., & Cliffe, A. (2008). Chromatin control of herpes simplex virus lytic and latent infection. *Nat Rev Microbiol, 6*(3), 211-221.
Kosulin, K., Haberler, C., Hainfellner, J. A., Amann, G., Lang, S., & Lion, T. (2007). Investigation of adenovirus occurrence in pediatric tumor entities. *J Virol, 81*(14), 7629-7635.
Krautwald, M., Fuchs, W., Klupp, B. G., & Mettenleiter, T. C. (2009). Translocation of incoming pseudorabies virus capsids to the cell nucleus is delayed in the absence of tegument protein pUL37. *J Virol*.
Lander, G. C., Tang, L., Casjens, S. R., Gilcrease, E. B., Prevelige, P., Poliakov, A., et al. (2006). The structure of an infectious P22 virion shows the signal for headful DNA packaging. *Science, 312*(5781), 1791-1795.
Lara-Pezzi, E., Gomez-Gaviro, M. V., Galvez, B. G., Mira, E., Iniguez, M. A., Fresno, M., et al. (2002). The hepatitis B virus X protein promotes tumor cell invasion by inducing membrane-type matrix metalloproteinase-1 and cyclooxygenase-2 expression. *J Clin Invest, 110*(12), 1831-1838.
Lee, J. O., Kwun, H. J., Jung, J. K., Choi, K. H., Min, D. S., & Jang, K. L. (2005). Hepatitis B virus X protein represses E-cadherin expression via activation of DNA methyltransferase 1. *Oncogene, 24*(44), 6617-6625.
Lee, T. W., Blair, G. E., & Matthews, D. A. (2003). Adenovirus core protein VII contains distinct sequences that mediate targeting to the nucleus and nucleolus, and colocalization with human chromosomes. *J Gen Virol, 84*(Pt 12), 3423-3428.
Leopold, P. L., Kreitzer, G., Miyazawa, N., Rempel, S., Pfister, K. K., Rodriguez-Boulan, E., et al. (2000). Dynein- and microtubule-mediated translocation of adenovirus serotype 5 occurs after endosomal lysis. *Hum Gene Ther, 11*(1), 151-165.
Leopold, P. L., & Pfister, K. K. (2006). Viral strategies for intracellular trafficking: motors and microtubules. *Traffic, 7*(5), 516-523.
Lill, Y., Lill, M. A., Fahrenkrog, B., Schwarz-Herion, K., Paulillo, S., Aebi, U., et al. (2006). Single hepatitis-B virus core capsid binding to individual nuclear pore complexes in Hela cells. *Biophys J, 91*(8), 3123-3130.
Lim, R. Y., Fahrenkrog, B., Koser, J., Schwarz-Herion, K., Deng, J., & Aebi, U. (2007). Nanomechanical basis of selective gating by the nuclear pore complex. *Science, 318*(5850), 640-643.
Lin, C. T., Lin, C. R., Tan, G. K., Chen, W., Dee, A. N., & Chan, W. Y. (1997). The mechanism of Epstein-Barr virus infection in nasopharyngeal carcinoma cells. *Am J Pathol, 150*(5), 1745-1756.
Lopez-Bueno, A., Villarreal, L. P., & Almendral, J. M. (2006). Parvovirus variation for disease: a difference with RNA viruses? *Curr Top Microbiol Immunol, 299*, 349-370.
Luxton, G. W., Haverlock, S., Coller, K. E., Antinone, S. E., Pincetic, A., & Smith, G. A. (2005). Targeting of herpesvirus capsid transport in axons is coupled to association with specific sets of tegument proteins. *Proc Natl Acad Sci U S A, 102*(16), 5832-5837.
Mabit, H., Breiner, K. M., Knaust, A., Zachmann-Brand, B., & Schaller, H. (2001). Signals for bidirectional nucleocytoplasmic transport in the duck hepatitis B virus capsid protein. *J. Virol., 75*(4), 1968-1977.

Mabit, H., Nakano, M. Y., Prank, U., Saam, B., Döhner, K., Sodeik, B., et al. (2002). Intact microtubules support Adenovirus and Herpes simplex virus infections. *J. Virol., 76*, 9962-9971.
Magnuson, B., Rainey, E. K., Benjamin, T., Baryshev, M., Mkrtchian, S., & Tsai, B. (2005). ERp29 triggers a conformational change in polyomavirus to stimulate membrane binding. *Mol Cell, 20*(2), 289-300.
Mansouri, M., Rose, P. P., Moses, A. V., & Fruh, K. (2008). Remodeling of endothelial adherens junctions by Kaposi's sarcoma-associated herpesvirus. *J Virol, 82*(19), 9615-9628.
Marg, A., Shan, Y., Meyer, T., Meissner, T., Brandenburg, M., & Vinkemeier, U. (2004). Nucleocytoplasmic shuttling by nucleoporins Nup153 and Nup214 and CRM1-dependent nuclear export control the subcellular distribution of latent Stat1. *J Cell Biol, 165*(6), 823-833.
Marsh, M., & Helenius, A. (2006). Virus entry: open sesame. *Cell, 124*(4), 729-740.
Matthews, D. A., & Russell, W. C. (1994). Adenovirus protein-protein interactions: hexon and protein VI. *J. Gen. Virol., 75*, 3365-3374.
Matthews, D. A., & Russell, W. C. (1998a). Adenovirus core protein V interacts with p32--a protein which is associated with both the mitochondria and the nucleus. *J Gen Virol, 79*(Pt 7), 1677-1685.
Matthews, D. A., & Russell, W. C. (1998b). Adenovirus Core Protein V Is Delivered By the Invading Virus to the Nucleus Of the Infected Cell and Later In Infection Is Associated With Nucleoli. *Journal of General Virology, 79*(Part 7), 1671-1675.
McLaughlin-Drubin, M. E., & Munger, K. (2008). Viruses associated with human cancer. *Biochim Biophys Acta, 1782*(3), 127-150.
Meier, O., & Greber, U. F. (2003). Adenovirus endocytosis. *J. Gene Med., 5*, 451–462.
Mettenleiter, T. C. (2004). Budding events in herpesvirus morphogenesis. *Virus Res, 106*(2), 167-180.
Mettenleiter, T. C., Klupp, B. G., & Granzow, H. (2006). Herpesvirus assembly: a tale of two membranes. *Curr Opin Microbiol, 9*(4), 423-429.
Miller, G. (2009). Brain cancer. A viral link to glioblastoma? *Science, 323*(5910), 30-31.
Miller, N., & Hutt-Fletcher, L. M. (1992). Epstein-Barr virus enters B cells and epithelial cells by different routes. *66*, 3409-3414.
Misteli, T., Gunjan, A., Hock, R., Bustin, M., & Brown, D. T. (2000). Dynamic binding of histone H1 to chromatin in living cells. *Nature, 408*(6814), 877-881.
Miyamoto, K., & Morgan, C. (1971). Structure and development of viruses as observed in the electron microscope. XI. Entry and uncoating of herpes simplex virus. *J Virol, 8*(6), 910-918.
Molho-Pessach, V., & Lotem, M. (2007). Viral carcinogenesis in skin cancer. *Curr Probl Dermatol, 35*, 39-51.
Morgan, C., Rose, H. M., & Mednis, B. (1968). Electron Microscopy of Herpes simplex virus. I. Entry. *J. Virol., 2*, 507-516.
Muruve, D. A., Petrilli, V., Zaiss, A. K., White, L. R., Clark, S. A., Ross, P. J., et al. (2008). The inflammasome recognizes cytosolic microbial and host DNA and triggers an innate immune response. *Nature, 452*(7183), 103-107.
Nagel, C. H., Dohner, K., Fathollahy, M., Strive, T., Borst, E. M., Messerle, M., et al. (2008). Nuclear egress and envelopment of herpes simplex virus capsids analyzed with dual-color fluorescence HSV1(17+). *J Virol, 82*(6), 3109-3124.
Nakanishi, A., Clever, J., Yamada, M., Li, P. P., & Kasamatsu, H. (1996). Association With Capsid Proteins Promotes Nuclear Targeting Of Simian Virus 40 Dna. *Proceedings of the National Academy of Sciences of the United States of America, 93*(1), 96-100.
Nakanishi, A., Li, P. P., Qu, Q., Jafri, Q. H., & Kasamatsu, H. (2007). Molecular dissection of nuclear entry-competent SV40 during infection. *Virus Res, 124*(1-2), 226-230.
Naranatt, P. P., Krishnan, H. H., Smith, M. S., & Chandran, B. (2005). Kaposi's sarcoma-associated herpesvirus modulates microtubule dynamics via RhoA-GTP-diaphanous 2 signaling and utilizes the dynein motors to deliver its DNA to the nucleus. *J Virol, 79*(2), 1191-1206.
Nemerow, G. R., & Cooper, N. R. (1984). Early events in the infection of human B lymphocytes by Epstein-Barr virus: the internalization process. *Virology, 132*(1), 186-198.
Newcomb, W. W., Booy, F. P., & Brown, J. C. (2007). Uncoating the herpes simplex virus genome. *J Mol Biol, 370*(4), 633-642.
Newcomb, W. W., Juhas, R. M., Thomsen, D. R., Homa, F. L., Burch, A. D., Weller, S. K., et al. (2001). The UL6 gene product forms the portal for entry of DNA into the herpes simplex virus capsid. *J Virol, 75*(22), 10923-10932.
Oh, J., & Fraser, N. W. (2008). Temporal association of the herpes simplex virus genome with histone proteins during a lytic infection. *J Virol, 82*(7), 3530-3537.
Ojala, P. M., Sodeik, B., Ebersold, M. W., Kutay, U., & Helenius, A. (2000). Herpes simplex virus type 1 entry into host cells: reconstitution of capsid binding and uncoating at the nuclear pore complex in vitro. *Mol Cell Biol, 20*(13), 4922-4931.
Osterrieder, N., Kamil, J. P., Schumacher, D., Tischer, B. K., & Trapp, S. (2006). Marek's disease virus: from miasma to model. *Nat Rev Microbiol, 4*(4), 283-294.
Pagano, J. S., Blaser, M., Buendia, M. A., Damania, B., Khalili, K., Raab-Traub, N., et al. (2004). Infectious agents and cancer: criteria for a causal relation. *Semin Cancer Biol, 14*(6), 453-471.
Pante, N., & Kann, M. (2002). Nuclear pore complex is able to transport macromolecules with diameters of about 39 nm. *Molecular Biology of the Cell, 13*(2), 425-434.
Parkin, D. M. (2006). The global health burden of infection-associated cancers in the year 2002. *Int J Cancer, 118*(12), 3030-3044.
Patel, S. S., Belmont, B. J., Sante, J. M., & Rexach, M. F. (2007). Natively unfolded nucleoporins gate protein diffusion across the nuclear pore complex. *Cell, 129*(1), 83-96.
Pedersen, S. M., & Hollsberg, P. (2006). Complexities in human herpesvirus-6A and -6B binding to host cells. *Virology, 356*(1-2), 1-3.
Pelkmans, L., Kartenbeck, J., & Helenius, A. (2001). Caveolar endocytosis of simian virus 40 reveals a new two-step vesicular-transport pathway to the ER. *Nat Cell Biol, 3*(5), 473-483.
Pho, M. T., Ashok, A., & Atwood, W. J. (2000). JC virus enters human glial cells by clathrin-dependent receptor-mediated endocytosis. *Journal of Virology, 74*(5), 2288-2292.
Pouton, C. W., Wagstaff, K. M., Roth, D. M., Moseley, G. W., & Jans, D. A. (2007). Targeted delivery to the nucleus. *Adv Drug Deliv Rev, 59*(8), 698-717.

Preston, V. G., Murray, J., Preston, C. M., McDougall, I. M., & Stow, N. D. (2008). The UL25 gene product of herpes simplex virus type 1 is involved in uncoating of the viral genome. *J Virol, 82*(13), 6654-6666.
Pungpapong, S., Kim, W. R., & Poterucha, J. J. (2007). Natural history of hepatitis B virus infection: an update for clinicians. *Mayo Clin Proc, 82*(8), 967-975.
Qu, Q., Sawa, H., Suzuki, T., Semba, S., Henmi, C., Okada, Y., et al. (2004). Nuclear entry mechanism of the human polyomavirus JC virus-like particle: role of importins and the nuclear pore complex. *J Biol Chem, 279*(26), 27735-27742.
Querbes, W., O'Hara, B. A., Williams, G., & Atwood, W. J. (2006). Invasion of host cells by JC virus identifies a novel role for caveolae in endosomal sorting of noncaveolar ligands. *J Virol, 80*(19), 9402-9413.
Rabe, B., Glebe, D., & Kann, M. (2006). Lipid-mediated introduction of hepatitis B virus capsids into nonsusceptible cells allows highly efficient replication and facilitates the study of early infection events. *J Virol, 80*(11), 5465-5473.
Radtke, K., Dohner, K., & Sodeik, B. (2006). Viral interactions with the cytoskeleton: a hitchhiker's guide to the cell. *Cell Microbiol, 8*(3), 387-400.
Raghu, H., Sharma-Walia, N., Veettil, M. V., Sadagopan, S., Caballero, A., Sivakumar, R., et al. (2007). Lipid rafts of primary endothelial cells are essential for Kaposi's sarcoma-associated herpesvirus/human herpesvirus 8-induced phosphatidylinositol 3-kinase and RhoA-GTPases critical for microtubule dynamics and nuclear delivery of viral DNA but dispensable for binding and entry. *J Virol, 81*(15), 7941-7959.
Rappocciolo, G., Hensler, H. R., Jais, M., Reinhart, T. A., Pegu, A., Jenkins, F. J., et al. (2008). Human herpesvirus 8 infects and replicates in primary cultures of activated B lymphocytes through DC-SIGN. *J Virol, 82*(10), 4793-4806.
Richards, R. M., Lowy, D. R., Schiller, J. T., & Day, P. M. (2006). Cleavage of the papillomavirus minor capsid protein, L2, at a furin consensus site is necessary for infection. *Proc Natl Acad Sci U S A, 103*(5), 1522-1527.
Roberts, A. P., Abaitua, F., O'Hare, P., McNab, D., Rixon, F. J., & Pasdeloup, D. (2009). Differing roles of inner tegument proteins pUL36 and pUL37 during entry of herpes simplex virus type 1. *J Virol, 83*(1), 105-116.
Roberts, J. N., Buck, C. B., Thompson, C. D., Kines, R., Bernardo, M., Choyke, P. L., et al. (2007). Genital transmission of HPV in a mouse model is potentiated by nonoxynol-9 and inhibited by carrageenan. *Nat Med, 13*(7), 857-861.
Rux, J. J., & Burnett, R. M. (2000). Type-specific epitope locations revealed by X-ray crystallographic study of adenovirus type 5 hexon. *Mol Ther, 1*(1), 18-30.
Samad, M. A., Okuwaki, M., Haruki, H., & Nagata, K. (2007). Physical and functional interaction between a nucleolar protein nucleophosmin/B23 and adenovirus basic core proteins. *FEBS Lett, 581*(17), 3283-3288.
Sandri-Goldin, R. M. (2001). Nuclear export of herpes virus RNA. *Curr Top Microbiol Immunol, 259*, 2-23.
Saphire, A. C. S., Guan, T. L., Schirmer, E. C., Nemerow, G. R., & Gerace, L. (2000). Nuclear import of adenovirus DNA in vitro involves the nuclear protein import pathway and hsc70. *J. Biol. Chem., 275*(6), 4298-4304.
Sattentau, Q. (2008). Avoiding the void: cell-to-cell spread of human viruses. *Nat Rev Microbiol, 6*(11), 815-826.
Schelhaas, M., Malmstrom, J., Pelkmans, L., Haugstetter, J., Ellgaard, L., Grunewald, K., et al. (2007). Simian Virus 40 depends on ER protein folding and quality control factors for entry into host cells. *Cell, 131*(3), 516-529.
Schroer, T. A. (2004). Dynactin. *Annu Rev Cell Dev Biol, 20*, 759-779.
Selinka, H. C., Giroglou, T., & Sapp, M. (2002). Analysis of the infectious entry pathway of human papillomavirus type 33 pseudovirions. *Virology, 299*(2), 279-287.
Shahin, V., Hafezi, W., Oberleithner, H., Ludwig, Y., Windoffer, B., Schillers, H., et al. (2006). The genome of HSV-1 translocates through the nuclear pore as a condensed rod-like structure. *J Cell Sci, 119*(Pt 1), 23-30.
Sherer, N. M., & Mothes, W. (2008). Cytonemes and tunneling nanotubules in cell-cell communication and viral pathogenesis. *Trends Cell Biol, 18*(9), 414-420.
Shishido-Hara, Y., Ichinose, S., Higuchi, K., Hara, Y., & Yasui, K. (2004). Major and minor capsid proteins of human polyomavirus JC cooperatively accumulate to nuclear domain 10 for assembly into virions. *J Virol, 78*(18), 9890-9903.
Shubeita, G. T., Tran, S. L., Xu, J., Vershinin, M., Cermelli, S., Cotton, S. L., et al. (2008). Consequences of motor copy number on the intracellular transport of kinesin-1-driven lipid droplets. *Cell, 135*(6), 1098-1107.
Sieczkarski, S. B., & Whittaker, G. R. (2005). Viral entry. *Curr Top Microbiol Immunol, 285*, 1-23.
Smith, J. G., Cassany, A., Gerace, L., Ralston, R., & Nemerow, G. R. (2008). A Neutralizing Antibody Blocks Adenovirus Infection by Arresting Microtubule-Dependent Cytoplasmic Transport. *J Virol*.
Smith, J. L., Campos, S. K., & Ozbun, M. A. (2007). Human papillomavirus type 31 uses a caveolin 1- and dynamin 2-mediated entry pathway for infection of human keratinocytes. *J Virol, 81*(18), 9922-9931.
Sodeik, B., Ebersold, M. W., & Helenius, A. (1997). Microtubule-mediated transport of incoming Herpes Simplex Virus 1 capsids to the nucleus. *J. Cell Biol., 136*(5), 1007-1021.
Sommer, G., & Heise, T. (2008). Posttranscriptional control of HBV gene expression. *Front Biosci, 13*, 5533-5547.
Spector, D. J. (2007). Default assembly of early adenovirus chromatin. *Virology, 359*(1), 116-125.
Spector, D. J., Johnson, J. S., Baird, N. L., & Engel, D. A. (2003). Adenovirus type 5 DNA-protein complexes from formaldehyde cross-linked cells early after infection. *Virology, 312*(1), 204-212.
Spoden, G., Freitag, K., Husmann, M., Boller, K., Sapp, M., Lambert, C., et al. (2008). Clathrin- and caveolin-independent entry of human papillomavirus type 16--involvement of tetraspanin-enriched microdomains (TEMs). *PLoS ONE, 3*(10), e3313.
Stanley, M. A., Pett, M. R., & Coleman, N. (2007). HPV: from infection to cancer. *Biochem Soc Trans, 35*(Pt 6), 1456-1460.
Steven, A. C., Conway, J. F., Cheng, N., Watts, N. R., Belnap, D. M., Harris, A., et al. (2005). Structure, assembly, and antigenicity of hepatitis B virus capsid proteins. *Adv Virus Res, 64*, 125-164.
Stewart, P. L., & Nemerow, G. R. (2007). Cell integrins: commonly used receptors for diverse viral pathogens. *Trends Microbiol, 15*(11), 500-507.
Stoeckl, L., Funk, A., Kopitzki, A., Brandenburg, B., Oess, S., Will, H., et al. (2006). Identification of a structural motif crucial for infectivity of hepatitis B viruses. *Proc Natl Acad Sci U S A, 103*(17), 6730-6734.
Strang, B. L., & Stow, N. D. (2007). Blocks to herpes simplex virus type 1 replication in a cell line, tsBN2, encoding a temperature-sensitive RCC1 protein. *J Gen Virol, 88*(Pt 2), 376-383.
Strawn, L. A., Shen, T., Shulga, N., Goldfarb, D. S., & Wente, S. R. (2004). Minimal nuclear pore complexes define FG repeat domains essential for transport. *Nat Cell Biol, 6*(3), 197-206.

Strunze, S., Trotman, L. C., Boucke, K., & Greber, U. F. (2005). Nuclear targeting of adenovirus type 2 requires CRM1-mediated nuclear export. *Mol Biol Cell, 16*(6), 2999-3009.
Sung, M. T., Lischwe, M. A., Richards, J. C., & Hosokawa, K. (1977). Adenovirus chromatin. I. Isolation and characterization of the major core protein VII and precursor pro-VII. *J. Biol. Chem., 252*, 4981-4987.
Suomalainen, M., Nakano, M. Y., Boucke, K., Keller, S., & Greber, U. F. (2001). Adenovirus-activated PKA and p38/MAPK pathways boost microtubule-mediated nuclear targeting of virus. *Embo J, 20*(6), 1310-1319.
Suomalainen, M., Nakano, M. Y., Boucke, K., Keller, S., Stidwill, R. P., & Greber, U. F. (1999). Microtubule-dependent minus and plus end-directed motilities are competing processes for nuclear targeting of adenovirus. *J. Cell Biol., 144*, 657-672.
Terry, L. J., Shows, E. B., & Wente, S. R. (2007). Crossing the nuclear envelope: hierarchical regulation of nucleocytoplasmic transport. *Science, 318*(5855), 1412-1416.
Trentin, J. J., Yabe, Y., & Taylor, G. (1962). The quest for human cancer viruses. *Science, 137*, 835-841.
Trotman, L. C., Mosberger, N., Fornerod, M., Stidwill, R. P., & Greber, U. F. (2001). Import of adenovirus DNA involves the nuclear pore complex receptor CAN/Nup214 and histone H1. *Nature Cell Biology, 3*, 1092-1100.
Ugai, H., Borovjagin, A. V., Le, L. P., Wang, M., & Curiel, D. T. (2007). Thermostability/infectivity defect caused by deletion of the core protein V gene in human adenovirus type 5 is rescued by thermo-selectable mutations in the core protein X precursor. *J Mol Biol, 366*(4), 1142-1160.
van Oostrum, J., & Burnett, R. M. (1985). Molecular composition of the adenovirus type 2 virion. *J. Virol., 56*, 439-448.
Walther, T. C., Pickersgill, H. S., Cordes, V. C., Goldberg, M. W., Allen, T. D., Mattaj, I. W., et al. (2002). The cytoplasmic filaments of the nuclear pore complex are dispensable for selective nuclear protein import. *J Cell Biol, 158*(1), 63-77.
Warren, J. C., & Cassimeris, L. (2007). The contributions of microtubule stability and dynamic instability to adenovirus nuclear localization efficiency. *Cell Motil Cytoskeleton, 64*(9), 675-689.
Warren, J. C., Rutkowski, A., & Cassimeris, L. (2006). Infection with replication-deficient adenovirus induces changes in the dynamic instability of host cell microtubules. *Mol Biol Cell, 17*(8), 3557-3568.
White, M. K., Gordon, J., Reiss, K., Del Valle, L., Croul, S., Giordano, A., et al. (2005). Human polyomaviruses and brain tumors. *Brain Res Brain Res Rev, 50*(1), 69-85.
Whittaker, G. R., Kann, M., & Helenius, A. (2000). Viral entry into the nucleus. *Annu Rev Cell Dev Biol, 16*, 627-651.
Wiethoff, C. M., Wodrich, H., Gerace, L., & Nemerow, G. R. (2005). Adenovirus Protein VI Mediates Membrane Disruption following Capsid Disassembly. *J Virol, 79*(4), 1992-2000.
Wisnivesky, J. P., Leopold, P. L., & Crystal, R. G. (1999). Specific binding of the adenovirus capsid to the nuclear envelope. *Hum Gene Ther, 10*(13), 2187-2195.
Wodrich, H., Guan, T., Cingolani, G., Von Seggern, D., Nemerow, G., & Gerace, L. (2003). Switch from capsid protein import to adenovirus assembly by cleavage of nuclear transport signals. *Embo J, 22*(23), 6245-6255.
Wolfstein, A., Nagel, C. H., Radtke, K., Dohner, K., Allan, V. J., & Sodeik, B. (2006). The inner tegument promotes herpes simplex virus capsid motility along microtubules in vitro. *Traffic, 7*(2), 227-237.
Wysocka, J., & Herr, W. (2003). The herpes simplex virus VP16-induced complex: the makings of a regulatory switch. *Trends Biochem Sci, 28*(6), 294-304.
Xue, Y., Johnson, J. S., Ornelles, D. A., Lieberman, J., & Engel, D. A. (2005). Adenovirus Protein VII Functions throughout Early Phase and Interacts with Cellular Proteins SET and pp32. *J Virol, 79*(4), 2474-2483.
Yamauchi, Y., Kiriyama, K., Kubota, N., Kimura, H., Usukura, J., & Nishiyama, Y. (2008). The UL14 tegument protein of herpes simplex virus type 1 is required for efficient nuclear transport of the alpha transinducing factor VP16 and viral capsids. *J Virol, 82*(3), 1094-1106.
Yan, Y., Stehle, T., Liddington, R. C., Zhao, H., & Harrison, S. C. (1996). Structure determination of simian virus 40 and murine polyomavirus by a combination of 30-fold and 5-fold electron-density averaging. *Structure, 4*(2), 157-164.
Young, K. A., Herbert, A. P., Barlow, P. N., Holers, V. M., & Hannan, J. P. (2008). Molecular basis of the interaction between complement receptor type 2 (CR2/CD21) and Epstein-Barr virus glycoprotein gp350. *J Virol, 82*(22), 11217-11227.
Zhao, L.-J., & Padmanabhan, R. (1988). Nuclear transport of adenovirus DNA polymerase is facilitated by interaction with preterminal protein. *Cell, 55*, 1005-1015.
Zhou, Z. H., Chen, D. H., Jakana, J., Rixon, F. J., & Chiu, W. (1999). Visualization of tegument-capsid interactions and DNA in intact herpes simplex virus type 1 virions. *Journal of Virology, 73*(4), 3210-3218.
zur Hausen, H. (2002). Papillomaviruses and cancer: from basic studies to clinical application. *Nat Rev Cancer, 2*(5), 342-350.

RESULTS

Manuscript:

Fluorescent DNA-core dynamics in entry and egress reveals nonisotropic hatching of viruses from infected cell nuclei

Daniel Puntener, Martin F. Engelke, Nicola Imelli,
Zsolt Ruzsics, Karin Boucke, Corinne Wilhelm and
Urs F. Greber.

Manuscript submitted to PLoS Pathogens.

Contributions:

Martin F. Engelke:	Particle recognition routine
Nicola Imelli:	Figure S2
Karin Boucke:	Figure 3B, 4A, 4E
Corinne Wilhelm:	Figure 2E, 2F, S4
Zsolt Ruzsics:	Recombineering
Urs F. Greber:	Manuscript

Fluorescent DNA-core dynamics in entry and egress reveals nonisotropic hatching of viruses from infected cell nuclei

Daniel Puntener[1], Martin F. Engelke[1], Nicola Imelli[1], Zsolt Ruzsics[2], Karin Boucke[1], Corinne Wilhelm[1] and Urs F. Greber[1, 3]

[1] Institute of Molecular Life Sciences, University of Zurich, Winterthurerstrasse 190, CH-8057 Zurich, Switzerland

[2] Max von Pettenkofer Institute, Department of Virology, Gene Center, Ludwig-Maximilians-University, 81377 Munich, Germany

[3] corresponding author:

E-mail: urs.greber@imls.uzh.ch, Telephone: +41 44 635 48 41, Fax: +41 44 635 68 22

running head: Cell entry and egress of a DNA-core tagged virus

Abstract: 156 words

Total text: 46396 characters (wo spaces)

Figure: 7 Table: 0

Abstract

DNA-viruses and retroviruses maintain and replicate their genomes in host cell nuclei using histone-based nucleosomes, similar to chromatin. Human adenoviruses (HAdVs, short Ad) replicate and assemble in the nucleus. They organise a linear double-strand DNA genome into a condensed core with about 180 nucleosomes by the viral protein VII (pVII), the small pX, and by pV attaching the DNA to the capsid. Using reverse genetics we replaced the genomic pV locus of Ad2 by GFP-pV. Purified Ad2-GFP-pV virions incorporated GFP-pV, had normal internalization and endosomal escape kinetics, and produced viral particles. Live cell imaging and electron microscopy revealed the release of both clusters and solitary Ad2-GFP-pV virions from the nucleus, indicating that egress of adenovirus from lytically infected cells is nonisotropic. Incoming Ad2-GPF-pV virions released GFP-pV in two steps, during entry into the cytosol, and at the nuclear membrane, suggesting nonhomogenous occurance of GFP-pV in virions. These results have implications for virus-cell transmission and disease mechanisms.

Keywords:

Histone H2B, lytic egress, stepwise disassembly, fluorescent virus, fluorescence microscopy

Introduction

Eucaryotic cells package their DNA with histones and associated proteins into nucleosomes, which are invariant in structure and composition and wrap 146 bp of DNA around a core of histones H2A, H2B, H3 and H4 (Luger & Richmond, 1998). The nucleosome cores are interconnected with the linker histone H1, which unlike the core histones has a short residence time of several minutes on chromatin (Janicki & Spector, 2003; Talbert & Henikoff, 2010). Similar to host chromatin, DNA viruses and RNA retroviruses replicate by employing cellular histones, or they encode their own DNA-binding and organizing proteins (Lieberman, 2008; Paulus, Nitzsche, & Nevels, 2010; Puntener & Greber, 2009). They assemble and maintain their genomes in different chromatin states by packaging the nucleic acids into proteinaceous capsids and sometimes lipid envelopes, and thereby traffic their genome within and transmit it between cells (Burckhardt & Greber, 2009; Mothes, Sherer, Jin, & Zhong, 2010). DNA of the oncogenic human adenovirus type 12 (HAdV12, short Ad12) was found to be integrated into host DNA and packaged around nucleosomes of transformed hamster cells, and was epigenetically silenced by DNA methylation and histone H3 and H4 hypo-acetylation in phenotypically reverted cells highlighting the high degree of viral genome plasticity in the nucleus (Hochstein, Muiznieks, Mangel, Brondke, & Doerfler, 2007).

Intracellular viral genome dynamics is essential for infection. Viruses that replicate in the nucleus are thought to release their genomes in isotropically, that is in continuous processes as individual assemblies of nucleic acids and proteins. Herpesviruses, for example, package their DNA-genome into an icosahedral capsid in the nucleoplasm and release it by a budding process across the inner and outer nuclear membranes (reviewed in Mettenleiter, Klupp, & Granzow, 2009). Retroviruses, such as immunodeficiency virus, negative sense RNA-viruses, such as influenza virus, or autonomous parvoviruses use

the nuclear export machineries of the cell to transport their replicated genomes from the nucleus to the cytoplasm as continuous processes (Boulo, Akarsu, Ruigrok, & Baudin, 2007; Cullen, 2003; Engelsma, et al., 2008).

Adenoviruses replicate and assemble particles in the nucleus, and they are well known to lyse cultured and primary cells (Berk, 2007). Adenoviruses encode their own histone-like proteins to condense a linear double-strand DNA genome of about 36 kbp into a proteinaceous DNA-core. Although it is unknown how the viral DNA is precisely organised in the virion, isolated cores of species C human adenovirus serotypes 2 or 5 (HAdV2/5, short Ad2/5) contain five viral proteins, the basic proteins V, VII and X (pV, pVII, pX), the terminal protein covalently attached to the 5' ends of the DNA, and a small number of protein IVa2 and L3/p23 protease, which are involved in DNA encapsidation and transcriptional regulation, or virion processing (reviewed in Berk, 2007; Russell, 2009). Proteins V, VII and X are tightly interconnected as indicated by chemical cross-linking experiments (Chatterjee, Vayda, & Flint, 1985). Digestion of virion cores with staphylococcal nuclease combined with electron microscopy (EM) analyses and stoichiometric calculations suggested a model where the viral DNA is organised into approximately 180 nucleosome-like units by three subunits of dimeric pVII interspersed with one copy of pV (Black & Center, 1979; Chatterjee, Vayda, & Flint, 1986b; Corden, Engelking, & Pearson, 1976; Mirza & Weber, 1982; Sung, Cao, Coleman, & Budelier, 1983; Vayda, Rogers, & Flint, 1983). This model predicts 1080 copies of pVII and 180 copies of pV, which is 10-20% higher than the experimentally determined amounts of pVII and pV in isolated virion DNA (Lehmberg, et al., 1999; van Oostrum & Burnett, 1985), suggesting that there are stretches in the viral genome lacking pVII and pV. pV not only binds the viral DNA in a sequence independent manner, it also bridges the DNA-core and the capsid by interacting with pVI on the inner side of the major capsid protein hexon (Chatterjee, et al., 1985; Lindert, Silvestry, Mullen, Nemerow, & Stewart, 2009; Matthews & Russell, 1998; Perez-Berna, et al., 2009; Saban, Silvestry, Nemerow, & Stewart, 2006). Interestingly, a pV-

deleted Ad5 gave rise to low levels of viral particles, suggesting that pV was involved in the assembly of infectious virions (Ugai, Borovjagin, Le, Wang, & Curiel, 2007). Mutations in the gene encoding the precursor of pX could compensate for the lack of pV suggesting redundancy for core organisation by molecular adaptation. This is also supported by the notion that pV is specific for Mastadenoviruses, which exclusively infect mammals (http://www.vmri.hu/~harrach/ADENOSEQ.HTM).

Viral infection starts with entry, which delivers subviral particles to the cytosol. Invariably, the condensed viral genomes have to be uncoated for infection to proceed (Greber, Singh, & Helenius, 1994). The uncoating process of Ad2/5 starts at the plasma membrane, when virion fibers bind their primary receptor, the coxsackievirus Ad receptor CAR, and alpha v integrin coreceptors bind to penton base, which anchors fiber to the capsid (Bergelson, et al., 1997; Burckhardt & Greber, 2009; Meier & Greber, 2003; Wickham, Mathias, Cheresh, & Nemerow, 1993). Ad2/5 release their fibers prior to or during endocytosis (Greber, Willetts, Webster, & Helenius, 1993; Nakano, Boucke, Suomalainen, Stidwill, & Greber, 2000). An early step of Ad2/5 uncoating is sensitive to defensins, which bind virions and preclude viral escape from endosomes to the cytosol (Nguyen, Nemerow, & Smith, 2010), phenotypically mimicking the fate of the uncoating and escape-defective Ad2 mutant Ad2-ts1 (Gastaldelli, et al., 2008; Imelli, Ruzsics, Puntener, Gastaldelli, & Greber, 2009). The cytosolic Ad2/5 capsids traffic on microtubules to the nuclear pore complex (NPC), where they bind to the CAN/Nup214 receptor, and release their genome into the nucleus (Greber & Way, 2006). This process is sensitive to the macrolide antibiotic leptomycin B (LMB), which inhibits nuclear protein export and prevents the attachment of incoming virions to the nuclear pore complex (Strunze, Trotman, Boucke, & Greber, 2005). The precise composition of the imported DNA is unknown (reviewed in Puntener & Greber, 2009). It is known, however, that pVII remains with the incoming viral genome in the nucleus during the early infection phase (Walkiewicz, Morral, & Engel, 2009; Xue, Johnson,

Ornelles, Lieberman, & Engel, 2005). pVII together with pV then assembles newly synthesised viral DNA into core structures that are packaged into virions and released upon nuclear disintegration (reviewed in Berk, 2007).

Results

Genetic construction and reconstitution of Ad2-GFP-pV

We generated recombinant Ad2 genomic DNA with an N-terminally eGFP-tagged core protein V (GFP-pV) using exposon mutagenesis of Ad2_BAC53 (Fig. 1A, B). The resulting bacterial artificial chromosome (BAC) DNA had the expected *in silico* predicted restriction fragments and correct sequence between GFP and pV (Fig. 1C, not shown). Linearised BAC_Ad2-GFP-pV DNA was transfected into HER-911 cells, and infectious particles were serially expanded in A549 cells through about 5 passages, and purified by double CsCl density gradient as described (Greber, et al., 1993). XhoI restriction enzyme digests of DNA from these particles yielded the expected fragments (Fig. 1B). This suggested that Ad2-GFP-pV was stable for at least 5 passages. At passages higher than 10, loss of GFP-pV expression by Ad2-GFP-pV was, however, observed and this coincided with genetic alterations in the pV locus (not shown).

Ad2-GFP-pV particles contain GFP-pV and are infectious

We next analysed the protein composition of CsCl-gradient purified Ad2-GFP-pV. SDS-PAGE and Coomassie blue analyses indicated that Ad2-GFP-pV had a protein band of about 75 kDa, which was absent in Ad2, and lacked a prominent band at about 48 kDa (Fig. 2A). Both of these bands were immunostained by an anti-pV antibody in Western blots, but only the 75 kDa band of Ad2-GFP-pV also reacted with an anti-GFP antibody (Fig. 2B). This

corresponded well with the calculated mass for this fusion protein, which is 70.409 kDa (Fig. 2C). The other major structural proteins of Ad2-GFP-pV and Ad2 were normal in SDS-PAGE (Fig. 2A). The relative abundance of the viral structural proteins was estimated by densitometry using Coomassie blue stained protein II (hexon, pI = 5.1) as an internal reference and bovine serum albumin (BSA, pI = 5.8, http://expasy.org/tools/) as a calibration standard (Fig. 2C, D). Each virion contains 720 copies of hexon, as indicated by structural and metabolic labeling analyses (Stewart, Fuller, & Burnett, 1993; van Oostrum & Burnett, 1985). The copy numbers of pVII and pV had been estimated by biochemical assays or reversed phase high performance liquid chromatography to be 833 +/- 33 or 633 +/- 59 for pVII, and 157 +/- 1 or 170 +/- 15 for pV, respectively (Lehmberg, et al., 1999; van Oostrum & Burnett, 1985). Our Coomassie blue analyses found 63 +/-5 copies of pIII (penton base, pI = 5.3, expected copy number 60), and 316 +/- 92 copies of pVI (pI = 9.6, expected copy number 360) per virion, which agrees well with the expected values. The basic proteins pV (pI = 10.3) and pVII (pI = 12.3, expected copy number 833) were overestimated by a factor of 1.5 and 3.3, respectively, compared to metabolic labeling (van Oostrum & Burnett, 1985). This was expected from the fact that Coomassie blue attaches better to highly positively charged proteins than to neutral proteins (Tal, Silberstein, & Nusser, 1985). Coomassie blue analyses indicated 38 +/- 6 copies of GFP-pV (pI = 9.5) per virion, which is about 25% of the pV levels in Ad2. Importantly, both GFP-pV and Ad2 pV segregated with the viral DNA core in pyridine-disrupted virions fractionated in sucrose density gradients, although we noticed some proteolysis in both of the pelleted core fractions (Fig. 2E, F).

Since pV links the viral DNA to the inside wall of the capsid (Matthews & Russell, 1998), we measured the thermostability of Ad2-GFP-V particles by spectrofluorometric measurements of the binding of the DNA-interchalating dye TOTO-3 to isolated virions (Fig. 2G). TOTO-3 binding to both Ad2-GFP-pV and Ad2 was constant in the range of 25° to 47°C, and sharply increased from 47 to

51°C where it reached a plateau at about 60°C. However, about 10-15% of the Ad2-GFP-pV particles bound the dye, indictive of defective particles, which could in part explain that 15-20% of the Ad2-GFP-pV particles bound to cells but did not endocytose (see Fig. 4A).

Ad2-GFP-pV enters cells but is attenuated at particle production

To track the incoming GFP-pV, we isolated Ad2-GFP-pV particles and labeled the capsids with the fluorophore Atto647 according to previously established protocols (Suomalainen, et al., 1999). The Atto647 dye was found to be specifically incorporated into the major capid protein hexon, as indicated by fluorography of SDS-PAGE fractionated virions (Fig. 3A). Purified Ad2-GFP-pV virions labeled with red Atto fluorophores retained their full infectivity compared to the non-labeled virions (not shown). Both, Atto-647-Ad2-GFP-pV and Ad2 were monodisperse as shown by negative-stain EM (Fig. 3B). Dual color fluorescence microscopy indicated that most of the Atto-647-Ad2-GFP-pV particles were positive for both colors (Fig. 3C, arrows) with Gaussian distributions for both colors, indicating the presence of a single species of dual-colored particles (Fig. 3D). Importantly, non-labeled Ad2 or Ad2-GFP-pV gave no signals in the red and green, or red channels, respectively, indicating specificity of detection (Fig. S1A, B).

Entry of Ad2-GFP-pV particles into HeLa-ATCC cells was analysed by transmission EM. Viral particle counts at the plasma membrane, endosomes and the cytosol indicated that Ad2-GFP-pV endocytosis occurred with similar kinetics as wild type Ad2, although 15-20% of the Ad2-GFP-pV particles were not endocytosis-competent (Fig. 4A). At 90 min pi, about 50% of the Ad2-GFP-pV particles were in the cytosol, 30% in endosomes and 20% at the plasma membrane. Endosomal escape of Ad2-GFP-pV was confirmed by fluid phase marker dextran-FITC (10 kDa) uptake showing that Ad2-GFP-pV infection not

only triggered dextran uptake but also release to the cytosol and the nucleoplasm, similar to Ad2 (Suppl. Fig. 1, Meier, et al., 2002).

Ad2-GFP-pV was delayed at expressing the immediate early transactivator E1A compared to Ad2 (Fig. 4B). This was more pronounced at 12 h than 20 h pi or at low moi than high moi, suggesting that Ad2-GFP-pV could compensate the defect with time and increased particle numbers, consistent with the notion that Ad2-GFP-pV had a lower infectious particle to particle ratio than Ad2. In lung epithelial A549 cells, Ad2-GFP-pV gave 10 to 100-fold lower yields of cell-associated infectious viruses compared to Ad2, although the amounts of cell-free infectious units were similar to Ad2 at 72 h pi (Fig. 4C), again suggesting that Ad2-GFP-pV compensates a growth defect with time. These results were confirmed by measurements of tissue culture infectious dose 50 (TCID50) and fluorescent focus forming units (fffu) (Fig. 4D). We speculate that Ad2-GFP-pV is slightly impaired at particle assembly, and perhaps at a step between endosomal escape and expression of the immediate early transactivator E1A. Despite the lower overall yields, Ad2-GFP-pV clusters of several hundred particles and also single Ad2-GFP-pV were readily detected by transmission EM in the nucleus and the cytoplasm 37 h pi, similar to Ad2 (Fig. 4E). In addition, these infected cells had crystalline inclusions both in the nuclei and cytoplasm, identical with Ad5 protein inclusions (Franqueville, et al., 2008). In addition, both newly synthesised GFP-pV and pV were found in similar subnuclear structures, devoid of the viral DNA binding protein (DBP) (Fig. S3A), as indicated by a pV specific antibody (Fig. S3B, C).

Lytic egress of Ad2-GFP-pV from infected cells

We employed live cell fluorescence microscopy to analyze the subcellular localization of GFP-pV. Projected z-stacks from HeLa cells infected with Ad2-GFP-pV at moi 0.2 confirmed that newly synthesised GFP-pV accumulated in histone H2B-mCherry positive nuclei and nucleoli 30 h pi (Fig. 5A, B, and Suppl.

Mov. 1 and 2). The cells stably expressed H2B-mCherry and grew normally, similar to H2B-GFP cells (not shown, Kanda, Sullivan, & Wahl, 1998). At 30 to 39 h pi, the localization of GFP-pV changed, initially by the increase of a diffuse GFP-pV signal in the cytosol, and then by GFP-pV clusters that were expelled from the nuclei (Fig. 5A, B, Suppl. Mov. 1 and 2). These clusters often contained H2B-cherry, and some H2B-cherry remained in the nuclei, suggesting that release of GFP-pV was not necessarily accompanied by complete nuclear disintegration (Fig. 5A). EM-analyses of infected HeLa cells at 35 h pi revealed clustered Ad2-GFP-pV particles in the cytoplasm (Fig. 4E), suggesting that the cytoplasmic GFP-pV patches were composed of newly synthesized viral particles. We found no evidence for H2B-mCherry in purified Ad2 by Western blots (Fig. S4). In addition to partial nuclear disintegration, we also found completely disintegrated H2B-mCherry nuclei disappearing from the infected cells along with the GFP-pV structures (Fig. 5B). This represented lysis of the nuclear membrane and the plasma membrane. Quantitative analyses from 8 different movies recorded between 30 and 45 h pi indicated that 5.5% of the Ad2-GFP-pV infected nuclei either partially or completely disintegrated (Fig. 5C). This amount of cell lysis was in agreement with the 50-fold higher levels of cell-associated Ad2-GFP-pV compared to extracellular viruses 48 h pi (see Fig. 4D). Together the data show that adenovirus induced cell lysis is nonisotropic, and releases large clusters of several hundred virions to the cytoplasm and extracellular medium.

GFP-pV dissociates from Ad2-GFP-pV particles during entry

We next analyzed entry of Ad2-GFP-pV and the major core protein pVII into cells by confocal microscopy in live and fixed cells. Spinning disc confocal microscopy indicated progressive attachment of dual-color Atto565-labeled Ad2-GFP-pV to the periphery of HER-911 cells (Fig. S5, and Suppl. Mov. 3). The number and average intensity of solitary Atto647-labeled capsid puncta remained approximately constant from 0 min (cold-binding of virions) until 240 min pi indicating that incoming virions were neither degraded in nor released

from the cells, consistent with earlier findings (Fig. 6A, B, Greber, Webster, Weber, & Helenius, 1996; Trotman, Mosberger, Fornerod, Stidwill, & Greber, 2001).

In contrast, the GFP-pV fluorescence of Atto647-labeled virion capsids rapidly dropped to about 35% of the original value at 30 min pi, and to almost background levels at 90 min pi (Fig. 6B, C). Individual GFP-pV puncta distinct from capsids were occasionally found at 30 min pi but not at 0 min pi, suggesting that GFP-pV separated from capsids during cell-binding, endocytosis or escape from endosomes. The cytoplasmic GFP-pV puncta were not stained with an anti-pVII antibody (Fig. 6A), although this antibody detected a small percentage of cell-bound Ad2-GFP-pV at 0 min pi (Fig. 6D), suggesting that these surface-bound capsids, but not the intracellular GFP-pV puncta contained viral DNA. We speculate that the pVII-positive particles at 0 min pi (Fig. 6A) belong to the 10-15% DNA-dye positive Ad2-GFP-pV particles detected in the virus inoculum (Fig. 2G). The pVII-positive particles were faintly positive for GFP-pV at 0 min but not 30 min pi, suggesting that GFP-pV disappeared from the broken particles (Fig. 6E).

In addition, we noticed that the average pVII fluorescence on the Atto647-capsids steadily decreased from 0 to 240 min pi, and the number of pVII-positive Atto647-capsids increased to about 11% at 90 min and decreased again after 150 min pi (Fig. 6D). Many of the strongly pVII-positive particles at the late time points were in the nuclear area, together with a significant number of pVII puncta lacking Atto-647 (Fig. 6A). Since incoming pVII but not capsids are delivered into the nucleus 1 to 3 h pi (Greber, et al., 1997; Strunze, et al., 2005; Xue, et al., 2005), and pVII is released from the viral DNA in the nucleus by ongoing transcription (Chen, Morral, & Engel, 2007), our data suggest that the nuclear pVII puncta represent infectious incoming genomes, in agreement

with recent analyses (Walkiewicz, et al., 2009). Remarkably, we did not find GFP-pV on pVII-positive puncta in the nucleus, suggesting that it dissociated prior to or during nuclear import of the viral genomes (Le, et al., 2006).

A fraction of GFP-pV dissociates from the incoming virus particles depending on leptomycin B

Single particle analyses indicated that GFP-pV dissociated from incoming Ad2-Atto647 in two steps, a rapid phase from 0 to 30 min and a slower phase 30 to 90 min pi (Fig. 6). The timing of the slower phase coincides with virus transport on microtubules to the nucleus (Suomalainen, et al., 1999). To address the nature of the second dissociation phase of GFP-pV from Ad2, we treated HER-911 cells with the nuclear export inhibitor LMB. LMB confines the incoming Ad2/5 particles to the cytosol or blocks them at the microtubule-organizing center depending on the cell type, and prevents Ad2/5 attachment to the nuclear pore complex, and nuclear import of pVII (Strunze, et al., 2005). Ratiometric analyses of GFP-pV / Atto647 fluorescence in image stacks recorded by automated fluorescence microscopy at constant illumination and with chromatic aberrations corrections (see Fig. S6) indicated that the ratio of GFP-pV to Atto647 was 0.105 at 30 min pi, and dropped to 0.085 at 150 min pi, close to background levels (Fig. 7A, B). At 0 min pi it was approximately 0.2 (see also Fig 5C). These numbers closely matched the ratios of GFP-pV to Atto647 determined by single slice confocal microscopy (see Fig. 6C, insert).

The data suggest that the second step of GFP-pV loss occurs at the nuclear pore complex. Although the GFP-pV / Atto647 ratio at 30 min pi was slightly increased in LMB-treated cells, the drug did not inhibit the first phase of GFP-pV release (not shown). The detection of double positive Atto647-Ad2-GFP-pV particles in the cytosol and at the POM121-mCherry-labeled nuclear pore complexes corroborated this notion (Fig. S7, Dultz, et al., 2008). These results imply that the early detachment of GFP-pV occurred before or shortly after virus

penetration into the cytosol, while the second step occurred at the nuclear membrane, suggesting that GFP-pV is not organized homogeneously in the viral particle.

Discussion

Imaging of subcellular localizations of viral DNA, RNA, proteins or particles at high resolution has greatly advanced concepts in molecular virology and cell biology. It has been significantly enhanced by labeling of viruses with chemical fluorophores or fluorescent proteins (reviewed in, Brandenburg & Zhuang, 2007; Burckhardt & Greber, 2009; Greber & Way, 2006). For adenoviruses, GFP had been fused to the capsid-stabilizing protein pIX (240 copies per virion, San Martin & Burnett, 2003), and purified virions were observed at the plasma membrane and the cytoplasm (Meulenbroek, Sargent, Lunde, Jasmin, & Parks, 2004). In addition, an adenovirus encoding pV-GFP, pre-pVII-GFP and a dual color Ad5 with pIX-RFP and pV-GFP were also reported (Le, et al., 2006; Ugai, et al., 2010). The utility of these viruses was, however, limited. Both pre-pVII-GFP and pV-GFP were expressed from an artificial promoter in the deleted E3 region of the genome, while endogenous pre-pVII and pV were also expressed, which resulted in low incorporation of pV-GFP in virus particles (Ugai, et al., 2010). In addition, the pV-GFP expressing Ad5 contained significant amounts of disrupted virions (Le, et al., 2006). The pIX-RFP / pV-GFP labeled virions on the other hand were heterogeneous with respect to green and red fluorescence, and it remained unknown how these viruses enter or exit cells.

Using a combination of live cell and quantitative fluorescence imaging of a DNA-core protein in the context of a complete viral genome, we visualize for the first time the dynamics of viral release from the nucleus at late times of the

adenoviral live cycle. Unexpectedly, we find that infected cells release clusters of Ad2-GFP-pV virions from the nuclei, indicating that lytic virus release is nonisotropic. This feature is reminiscent of a reverse process of Ostwald ripening observed in inorganic systems and macromolecule crystals, such as tabacco mosaic virus, where the minimization of total interfacial energy drives crystal growth from precipitate clusters of various sizes (Malkin & McPherson, 1993; Voorhees, 1992). Virus clusters from crystal-like assemblies in the cell nucleus are new feature for cell-free spreading of viruses, and extend the concept of viral spreading through aqueous medium. We suggest that extracellular virus clusters can not only adhere to noninfected cells by cumulative low affinity interactions, but these cells are then subject to high multiplicity infection, which proceeds faster than low multiplicity infections, since single viruses do not activate quiescent cells as efficiently as a cohort of viruses does. In addition, viruses within such clusters might be protected from stress or cellular inactivation.

Remarkably, before virus clusters were found to be released, a homogenous GFP-pV signal increased in the cytoplasm, suggesting that the nuclear membrane is leaky for small molecules, such as GFP-pV. The subsequent release of Ad2/5 from the nucleus likely involves the adenovirus death protein (ADP, 11.6 kD protein) (Wold, Tollefson, & Hermiston, 1995), and lamin proteolysis (Chiou & White, 1998). We speculate that a driving force in the nucleus expells virus clusters by osmotic pressure from protein and nucleic acid polymers that are built up during viral replication.

Interestingly, the virus clusters frequently remained associated with the cytoplasm, before they were displaced to the medium, which suggests disruption of the plasma membrane. The latter may be a consequence of nuclear disruption, which releases the viral protease L3/p23 to the cytosol, and thereby could enhance degradation of the cytoskeleton. L3/p23 cleaves

cytokeratin K18, microtubules and actin, and makes the infected cell more susceptible to mechanical stress (reviewed in, Greber, 1998; Mangel, Baniecki, & McGrath, 2003). Precisely how the plasma membrane is disrupted and the newly synthesized virus clusters are released from the cell can now be analysed with the cell-lytic Ad2-GFP-pV. We anticipate, however, that the virus clusters can be controlled in size and shape by cellular or viral factors, and that isotropic release of single viruses from cell-tethered clusters will give rise to infection along the conventional single particle entry pathway.

Our detailed entry studies of Ad2-GFP-pV revealed two new steps of virus uncoating. First, we showed that a large fraction of GFP-pV is lost from the particles at 30 min pi, when the majority of endocytosis-competent Ad2-GFP-pV has arrived in the cytosol. We suggest that this early loss of GFP-pV coincides with structural changes of the capsid, such as the loss of fibers and pentons, or capsid-stabilizing proteins IIIa and VIII (Fabry, et al., 2005; Greber, et al., 1993; Nakano, et al., 2000; Saban, et al., 2006). These disassembly steps occur in most of the entry-competent virions (Greber, et al., 1993), and are manifested also by the exposure of pVI epitopes on viral particles early in infection (Wodrich, et al., 2010). Biochemical experiments and crosslinking studies have suggested that pV attaches the viral DNA to the capsid possibly via pVI (Chatterjee, et al., 1985; Matthews & Russell, 1998). pVI has recently been assigned to hexon cavities inside the capsid (Perez-Berna, et al., 2009; Silvestry, et al., 2009), but it remains unknown, precisely how the 360 copies of pVI are arranged within the capsid. Intriguingly, unassigned structures around the 5-fold symmetry of the vertices projecting towards the DNA-core have been detected in cryo-EM studies, and these structures have been tentatively assigned to pVI (Fabry, et al., 2005; Stewart, et al., 1993). Since dimers of pVI bind pV in biochemical assays, it is possible that pV acts as a DNA-organizer near the vertices. pV could be released when penton base or fibers detach from the capsid, either together or separately from pVI and penton base.

The second novel step for adenovirus uncoating identified here was that about 30% of GFP-pV dissociates from the cytoplasmic particles and this was inhibited by LMB. LMB blocks the attachment of incoming Ad2/5 to the nuclear pore complex and inhibits capsid disintegration (Strunze, et al., 2005), consistent with a key role of the nuclear pore complex in the final step of capsid disassembly (Trotman, et al., 2001). This suggests that, in addition to linking the viral DNA to the capsid, pV functions in core assembly and organisation, in close contact with the virion DNA, as supported by UV-crosslinking and fractionation studies (Brown, Westphal, Burlingham, Winterhoff, & Doerfler, 1975; Chatterjee, Vayda, & Flint, 1986c; Everitt, Sundquist, Pettersson, & Philipson, 1973).

Remarkably, the pVII-positive DNA-cores inside the nucleus do not contain GFP-pV or wild type pV (Hindley, Lawrence, & Matthews, 2007; Le, et al., 2006). The absence of pV or GFP-pV on these cores has been underlined by earlier studies, showing that the viral DNA and pVII alone can be a template for replication and transcription without pV (Chatterjee, Vayda, & Flint, 1986a; Haruki, Okuwaki, Miyagishi, Taira, & Nagata, 2006; Xue, et al., 2005). Possibly, post-translational modifications of the viral core proteins pV and pVII, including ADP-ribosylation, phosphorylation or acetylation facilitate a relaxation of the core, and thereby aid the detachment of DNA from the capsid (Dery, et al., 1986; Fedor & Daniell, 1980; Weber & Khittoo, 1983). In summary, Ad2-GFP-pV provides evidence for a role of virus clusters in aqueous transmission of virus infections, and may in the future give insights into viral spreading dynamics in organisms in disease and therapy.

Experimental procedures

Construction of Ad2-GFP-pV

Ad2_BAC53 is derived from Ad2 reference strain "adenoid 6" (Imelli, et al., 2009). The Ad2-GFP-pV insertion mutant was obtained using exposon mutagenesis as described (Ruzsics, et al., 2006). Briefly, in the first step a mini-Tn cassette (transprimer-1) was amplified from pGPS1.1 and inserted by ET recombination into BAC53 containing the full length wild type genome of Ad2 (Imelli, et al., 2009). Synthetic oligonucleotide primers for insertion of Transprimer-1 contained at their 5' end homologies to position 16491-16538 (upstream) and 16539-16586 (downstream) relative to the adenoviral genome. The priming sequences for the transprimer-1 cassette of pGPS1.1 were as published (Ruzsics, et al., 2006). Successful insertion of transprimer-1 was examined by restriction analysis and partial sequencing of the insertion sites. To replace the transprimer-1 element with eGFP coding sequences recombinant BAC-DNA was amplified from two independent clones and transprimer-1 sequences were excised in vitro using TnsABC* (New England Biolabs) in the presence of the acceptor plasmid pST76T. The insertion fragment containing the ORF of eGFP was obtained as follows. The eGFP gene including a small linker portion was PCR amplified from pEGFP-C1 (Clontech). Priming regions were designed such that the fragment contained position 613-1380 of the plasmid. The 5' extensions contain the recognition site for SapI, one random base plus 3 bases identical to the upstream or downstream region of the insertion site. Primer sequences were as follows: upstream primer (5'-GTC AGC TCT TCC GCT ATG GTG AGC AAG GGC GAG-3'), downstream primer (5'-CAA GGC TCT TCT CAT GGT ACC GTC GAC TGC AGA ATT C-3'). The SapI excised insertion fragment was ligated into the TnsABC* linearised BAC and the recombinants were recovered by transformation into competent bacteria. Successful replacement was confirmed by restriction analysis and partial sequencing of the insertion sites. Four independent colonies were chosen and amplified for reconstitution of virus by

calcium phosphate transfection of 80% confluent HER-911 cells in a 10 cm cell culture dish with 10 µg SnaBI linearised BAC DNA. 48 h post-transfection cells were split 1 to 4, and viruses harvested from cells and supernatant at onset of cytopathic effects (passage 1, p1), serially passaged in four 10 cm dishes of A549 cells (p2), and then in twenty 10 cm dishes (p3), followed by virus purification from cells. The supernatants were used for further amplification rounds until p7. Viruses from passages lower than 8 had normal DNA patterns of restriction enzyme digests.

Supplemental data describe the details of cell culture, transfections, antibodies, Western blots and protein determinations, virus purifications and quantifications, one step growth curves, preparation of pyridine cores, thermostability assays. Similarly, single particle fluorescence analyses, live-cell microscopy, kinetics of GFP-pV release from Atto-647-Ad2 and EM analyses are described in supplemental data.

References

Bergelson, J. M., Cunningham, J. A., Droguett, G., Kurt-Jones, E. A., Krithivas, A., Hong, J. S., et al. (1997). Isolation of a common receptor for Coxsackie B viruses and adenoviruses 2 and 5. *Science, 275*, 1320-1323.

Berk, A. J. (2007). Adenoviridae: the viruses and their replication. In D. M. Knipe & P. M. Howley (Eds.), *Fields Virology* (5 ed., Vol. 2, pp. 2355-2436). Philadelphia, PA, USA: Lippincott Williams & Wilkins.

Black, B. C., & Center, M. S. (1979). DNA-binding properties of the major core protein of adenovirus 2. *Nucleic Acids Res, 6*(6), 2339-2353.

Boulo, S., Akarsu, H., Ruigrok, R. W., & Baudin, F. (2007). Nuclear traffic of influenza virus proteins and ribonucleoprotein complexes. *Virus Res, 124*(1-2), 12-21.

Brandenburg, B., & Zhuang, X. (2007). Virus trafficking - learning from single-virus tracking. *Nat Rev Microbiol, 5*(3), 197-208.

Brown, D. T., Westphal, M., Burlingham, B. T., Winterhoff, U., & Doerfler, W. (1975). Structure and composition of the adenovirus type 2 core. *J Virol, 16*(2), 366-387.

Burckhardt, C. J., & Greber, U. F. (2009). Virus movements on the plasma membrane support infection and transmission between cells. *PLoS Pathog, 5*(11), e1000621.

Chatterjee, P. K., Vayda, M. E., & Flint, S. J. (1985). Interactions among the three adenovirus core proteins. *J Virol, 55*(2), 379-386.

Chatterjee, P. K., Vayda, M. E., & Flint, S. J. (1986a). Adenoviral protein VII packages intracellular viral DNA throughout the early phase of infection. *Embo J, 5*(7), 1633-1644.

Chatterjee, P. K., Vayda, M. E., & Flint, S. J. (1986b). Identification of proteins and protein domains that contact DNA within adenovirus nucleoprotein cores by ultraviolet light crosslinking of oligonucleotides 32P-labelled in vivo. *J Mol Biol, 188*(1), 23-37.

Chatterjee, P. K., Vayda, M. E., & Flint, S. J. (1986c). Identification of proteins and protein domains that contact DNA within adenovirus nucleoprotein cores by ultraviolet light crosslinking of oligonucleotides 32P-labelled in vivo. *Journal of Molecular Biology, 188*(1), 23-37.

Chen, J., Morral, N., & Engel, D. A. (2007). Transcription releases protein VII from adenovirus chromatin. *Virology, 369*(2), 411-422.

Chiou, S. K., & White, E. (1998). Inhibition of ICE-like proteases inhibits apoptosis and increases virus production during adenovirus infection. *Virology, 244*(1), 108-118.

Corden, J., Engelking, H. M., & Pearson, G. D. (1976). Chromatin-like organization of the adenovirus chromosome. *Proc Natl Acad Sci U S A, 73*(2), 401-404.

Cullen, B. R. (2003). Nuclear mRNA export: insights from virology. *Trends Biochem Sci, 28*(8), 419-424.

Dery, C. V., de Murcia, G., Lamarre, D., Morin, N., Poirier, G. G., & Weber, J. (1986). Possible role of ADP-ribosylation of adenovirus core proteins in virus infection. *Virus Res, 4*(4), 313-329.

Dultz, E., Zanin, E., Wurzenberger, C., Braun, M., Rabut, G., Sironi, L., et al. (2008). Systematic kinetic analysis of mitotic dis- and reassembly of the nuclear pore in living cells. *J Cell Biol, 180*(5), 857-865.

Engelsma, D., Valle, N., Fish, A., Salome, N., Almendral, J. M., & Fornerod, M. (2008). A supraphysiological nuclear export signal is required for parvovirus nuclear export. *Mol Biol Cell, 19*(6), 2544-2552.

Everitt, E., Sundquist, B., Pettersson, U., & Philipson, L. (1973). Structural proteins of adenoviruses. X. Isolation and topography of low molecular weight antigens from the virion of adenovirus type 2. *Virology, 52*, 130-147.

Fabry, C. M., Rosa-Calatrava, M., Conway, J. F., Zubieta, C., Cusack, S., Ruigrok, R. W., et al. (2005). A quasi-atomic model of human adenovirus type 5 capsid. *Embo J, 24*(9), 1645-1654.

Fedor, M. J., & Daniell, E. (1980). Acetylation of histone-like proteins of adenovirus type 5. *J Virol, 35*(3), 637-643.

Franqueville, L., Henning, P., Magnusson, M., Vigne, E., Schoehn, G., Blair-Zajdel, M. E., et al. (2008). Protein crystals in Adenovirus type 5-infected cells: requirements for intranuclear crystallogenesis, structural and functional analysis. *PLoS ONE, 3*(8), e2894.

Gastaldelli, M., Imelli, N., Boucke, K., Amstutz, B., Meier, O., & Greber, U. F. (2008). Infectious adenovirus type 2 transport through early but not late endosomes. *Traffic, 9*(12), 2265-2278.

Greber, U. F. (1998). Virus assembly and disassembly: the adenovirus cysteine protease as a trigger factor. *Rev. Med. Virol., 8*, 213-222.

Greber, U. F., Singh, I., & Helenius, A. (1994). Mechanisms of virus uncoating. *Trends Microbiol, 2*(2), 52-56.

Greber, U. F., Suomalainen, M., Stidwill, R. P., Boucke, K., Ebersold, M., & Helenius, A. (1997). The role of the nuclear pore complex in adenovirus DNA entry. *EMBO J., 16*, 5998-6007.

Greber, U. F., & Way, M. (2006). A super highway to virus infection. [review]. *Cell, 124(4)*, 741-754.

Greber, U. F., Webster, P., Weber, J., & Helenius, A. (1996). The role of the adenovirus protease on virus entry into cells. *Embo J, 15*(8), 1766-1777.

Greber, U. F., Willetts, M., Webster, P., & Helenius, A. (1993). Stepwise dismantling of adenovirus 2 during entry into cells. *Cell, 75*(3), 477-486.

Haruki, H., Okuwaki, M., Miyagishi, M., Taira, K., & Nagata, K. (2006). Involvement of template-activating factor I/SET in transcription of adenovirus early genes as a positive-acting factor. *J Virol, 80*(2), 794-801.

Hindley, C. E., Lawrence, F. J., & Matthews, D. A. (2007). A role for transportin in the nuclear import of adenovirus core proteins and DNA. *Traffic, 8*(10), 1313-1322.

Hochstein, N., Muiznieks, I., Mangel, L., Brondke, H., & Doerfler, W. (2007). Epigenetic status of an adenovirus type 12 transgenome upon long-term cultivation in hamster cells. *J Virol, 81*(10), 5349-5361.

Imelli, N., Ruzsics, Z., Puntener, D., Gastaldelli, M., & Greber, U. F. (2009). Genetic reconstitution of the human adenovirus type 2 temperature-sensitive 1 mutant defective in endosomal escape. *Virol J, 6*, 174.

Janicki, S. M., & Spector, D. L. (2003). Nuclear choreography: interpretations from living cells. *Curr Opin Cell Biol, 15*(2), 149-157.

Kanda, T., Sullivan, K. F., & Wahl, G. M. (1998). Histone-GFP fusion protein enables sensitive analysis of chromosome dynamics in living mammalian cells. *Curr Biol, 8*(7), 377-385.

Le, L. P., Le, H. N., Nelson, A. R., Matthews, D. A., Yamamoto, M., & Curiel, D. T. (2006). Core labeling of adenovirus with EGFP. *Virology, 351*(2), 291-302.

Lehmberg, E., Traina, J. A., Chakel, J. A., Chang, R. J., Parkman, M., McCaman, M. T., et al. (1999). Reversed-phase high-performance liquid chromatographic assay for the adenovirus type 5 proteome. *J Chromatogr B Biomed Sci Appl, 732*(2), 411-423.

Lieberman, P. M. (2008). Chromatin organization and virus gene expression. *J Cell Physiol, 216*(2), 295-302.

Lindert, S., Silvestry, M., Mullen, T. M., Nemerow, G. R., & Stewart, P. L. (2009). Cryo-electron microscopy structure of an adenovirus-integrin complex indicates conformational changes in both penton base and integrin. *J Virol, 83*(22), 11491-11501.

Luger, K., & Richmond, T. J. (1998). DNA binding within the nucleosome core. *Curr Opin Struct Biol, 8*(1), 33-40.

Malkin, A., & McPherson, A. (1993). Crystallization of satellite tobacco mosaic virus II. Postnucleation events. *Journal of Crystal Growth, 126*(4), 555-564.

Mangel, W. F., Baniecki, M. L., & McGrath, W. J. (2003). Specific interactions of the adenovirus proteinase with the viral DNA, an 11-amino-acid viral peptide, and the cellular protein actin. *Cell Mol Life Sci, 60*(11), 2347-2355.

Matthews, D. A., & Russell, W. C. (1998). Adenovirus core protein V is delivered by the invading virus to the nucleus of the infected cell and later in infection is associated with nucleoli. *J Gen Virol, 79 (Pt 7)*, 1671-1675.

Meier, O., Boucke, K., Hammer, S. V., Keller, S., Stidwill, R. P., Hemmi, S., et al. (2002). Adenovirus triggers macropinocytosis and endosomal leakage together with its clathrin-mediated uptake. *J Cell Biol, 158*(6), 1119-1131.

Meier, O., & Greber, U. F. (2003). Adenovirus endocytosis. *J Gene Med, 5*(6), 451-462.

Mettenleiter, T. C., Klupp, B. G., & Granzow, H. (2009). Herpesvirus assembly: an update. *Virus Res, 143*(2), 222-234.

Meulenbroek, R. A., Sargent, K. L., Lunde, J., Jasmin, B. J., & Parks, R. J. (2004). Use of adenovirus protein IX (pIX) to display large polypeptides on the virion--generation of fluorescent virus through the incorporation of pIX-GFP. *Mol Ther, 9*(4), 617-624.

Mirza, M. A., & Weber, J. (1982). Structure of adenovirus chromatin. *Biochim Biophys Acta, 696*(1), 76-86.

Mothes, W., Sherer, N. M., Jin, J., & Zhong, P. (2010). Virus cell-to-cell transmission. *J Virol*.

Nakano, M. Y., Boucke, K., Suomalainen, M., Stidwill, R. P., & Greber, U. F. (2000). The first step of adenovirus type 2 disassembly occurs at the cell surface, independently of endocytosis and escape to the cytosol. *J Virol, 74*(15), 7085-7095.

Nguyen, E. K., Nemerow, G. R., & Smith, J. G. (2010). Direct evidence from single-cell analysis that human alpha-defensins block adenovirus uncoating to neutralize infection. *J Virol*.

Paulus, C., Nitzsche, A., & Nevels, M. (2010). Chromatinisation of herpesvirus genomes. *Rev Med Virol, 20*(1), 34-50.

Perez-Berna, A. J., Marabini, R., Scheres, S. H., Menendez-Conejero, R., Dmitriev, I. P., Curiel, D. T., et al. (2009). Structure and uncoating of immature adenovirus. *J Mol Biol, 392*(2), 547-557.

Puntener, D., & Greber, U. F. (2009). DNA-tumor virus entry - from plasma membrane to the nucleus. *Sem Cell Dev Biol, 20*, 631-642.

Russell, W. C. (2009). Adenoviruses: update on structure and function. *J Gen Virol, 90*(Pt 1), 1-20.

Ruzsics, Z., Wagner, M., Osterlehner, A., Cook, J., Koszinowski, U., & Burgert, H. G. (2006). Transposon-assisted cloning and traceless mutagenesis of adenoviruses: Development of a novel vector based on species D. *J Virol, 80*(16), 8100-8113.

Saban, S. D., Silvestry, M., Nemerow, G. R., & Stewart, P. L. (2006). Visualization of alpha-helices in a 6-angstrom resolution cryoelectron microscopy structure of adenovirus allows refinement of capsid protein assignments. *J Virol, 80*(24), 12049-12059.

San Martin, C., & Burnett, R. M. (2003). Structural studies on adenoviruses. *Curr Top Microbiol Immunol, 272*, 57-94.

Silvestry, M., Lindert, S., Smith, J. G., Maier, O., Wiethoff, C. M., Nemerow, G. R., et al. (2009). Cryo-electron microscopy structure of adenovirus type 2 temperature-sensitive mutant 1 reveals insight into the cell entry defect. *J Virol, 83*(15), 7375-7383.

Stewart, P. L., Fuller, S. D., & Burnett, R. M. (1993). Difference imaging of adenovirus: bridging the resolution gap between X-ray crystallography and electron microscopy. *EMBO J., 12*, 2589-2599.

Strunze, S., Trotman, L. C., Boucke, K., & Greber, U. F. (2005). Nuclear targeting of adenovirus type 2 requires CRM1-mediated nuclear export. *Mol Biol Cell, 16*(6), 2999-3009.

Sung, M. T., Cao, T. M., Coleman, R. T., & Budelier, K. A. (1983). Gene and protein sequences of adenovirus protein VII, a hybrid basic chromosomal protein. *Proc Natl Acad Sci U S A, 80*(10), 2902-2906.

Suomalainen, M., Nakano, M. Y., Boucke, K., Keller, S., Stidwill, R. P., & Greber, U. F. (1999). Microtubule-dependent minus and plus end-directed motilities are competing processes for nuclear targeting of adenovirus. *J. Cell Biol., 144*, 657-672.

Tal, M., Silberstein, A., & Nusser, E. (1985). Why does Coomassie Brilliant Blue R interact differently with different proteins? A partial answer. *J Biol Chem, 260*(18), 9976-9980.

Talbert, P. B., & Henikoff, S. (2010). Histone variants--ancient wrap artists of the epigenome. *Nat Rev Mol Cell Biol, 11*(4), 264-275.

Trotman, L. C., Mosberger, N., Fornerod, M., Stidwill, R. P., & Greber, U. F. (2001). Import of adenovirus DNA involves the nuclear pore complex receptor CAN/Nup214 and histone H1. *Nature Cell Biology, 3*, 1092-1100.

Ugai, H., Borovjagin, A. V., Le, L. P., Wang, M., & Curiel, D. T. (2007). Thermostability/infectivity defect caused by deletion of the core protein V gene in human adenovirus type 5 is rescued by thermo-selectable mutations in the core protein X precursor. *J Mol Biol, 366*(4), 1142-1160.

Ugai, H., Wang, M., Le, L. P., Matthews, D. A., Yamamoto, M., & Curiel, D. T. (2010). In vitro dynamic visualization analysis of fluorescently labeled minor capsid protein IX and core protein V by simultaneous detection. *J Mol Biol, 395*(1), 55-78.

van Oostrum, J., & Burnett, R. M. (1985). Molecular composition of the adenovirus type 2 virion. *J. Virol., 56*, 439-448.

Vayda, M. E., Rogers, A. E., & Flint, S. J. (1983). The structure of nucleoprotein cores released from adenovirions. *Nucleic Acids Res, 11*(2), 441-460.

Voorhees, P. (1992). Ostwald ripening of two-phase mixtures. *Annual Review of Materials Science, 22*, 197-215.

Walkiewicz, M. P., Morral, N., & Engel, D. A. (2009). Accurate single-day titration of adenovirus vectors based on equivalence of protein VII nuclear dots and infectious particles. *J Virol Methods, 159*(2), 251-258.

Weber, J. M., & Khittoo, G. (1983). The role of phosphorylation and core protein V in adenovirus assembly. *J Gen Virol, 64 (Pt 9)*, 2063-2068.

Wickham, T. J., Mathias, P., Cheresh, D. A., & Nemerow, G. R. (1993). Integrin alpha v beta 3 and integrin alpha v beta 5 promote adenovirus internalization but not virus attachment. *Cell, 73*, 309-319.

Wodrich, H., Henaff, D., Jammart, B., Segura-Morales, C., Seelmeir, S., Coux, O., et al. (2010). A capsid-encoded PPxY-motif facilitates adenovirus entry. *PLoS Pathog, 6*(3), e1000808.

Wold, W. S., Tollefson, A. E., & Hermiston, T. W. (1995). E3 transcription unit of adenovirus. *Curr Top Microbiol Immunol, 199*(Pt 1), 237-274.

Xue, Y., Johnson, J. S., Ornelles, D. A., Lieberman, J., & Engel, D. A. (2005). Adenovirus protein VII functions throughout early phase and interacts with cellular proteins SET and pp32. *J Virol, 79*(4), 2474-2483.

Acknowledgements

We thank Dr. Silvio Hemmi and the members of the Greber lab for helpful discussions, Dr. Maarit Suomalainen for comments to the manuscript and the Swiss National Science Foundation for grant support to UFG.

Figure Legends

Fig. 1: Construction of Ad2-GFP-pV

A. Schematic overview of the pV and pVII loci of Ad2 (left) and Ad2-GFP-pV (right) with boxed open reading frames for pVII and pV, and nucleotide numbers of the starting and terminating nucleotides.

B. XhoI restriction enzyme analysis of genomic DNA isolated from purified Ad2 and Ad2 GFP-pV with an *in silico* predicted restriction pattern (right) and molecular weight markers (M) in kbp.

C. DNA sequence analysis and derived amino acid sequence at the GFP-pV junction from Ad2-GFP-pV virion DNA with nucleotide numbers.

Fig. 2: Biochemical characterization of Ad2-GFP-pV

A. 12% SDS-PAGE stained with Coomassie brilliant blue, including protein marker (M) with relative mass in kDa. Roman numbers denote viral structural proteins.

B. Anti-pV (left panel) or anti-GFP (right panel) stained Western blot of purified Ad2 and Ad2-GFP-pV, including recombinant GFP with a nuclear export sequence (NES).

C. Estimation of copy numbers of viral structural proteins by densitometric analysis of Coomassie blue stained SDS-PAGE. The table shows calculated molecular weight (MW in Dalton) values for indicated proteins, the isoelectric point (pI), the copy numbers based on the virus structure (Zubieta, Schoehn, Chroboczek, & Cusack, 2005), the copy numbers estimated by metabolic labeling (van Oostrum & Burnett, 1985), the measured optical density (OD), the amount of protein based on the BSA standard curve (panel D, linear regression value R^2 0.9924) and the estimated copy numbers.

E, F. Sucrose density gradient-fractionated pyridine-extracted Ad2 or Ad2-GFP-pV, including a pellet (loaded as pellet plus fractions fr 13+14), molecular weight markers (M) and input sample. Gels were stained with Coomassie blue (left), or Western blotted against pV (right). Note that both intact and partially degraded pV and GFP-pV fractionate with the core protein pVII.

G. Purified Ad2 (open bars) and Ad2-GFP-pV (black bars) were heated in the presence of the DNA-intercalating dye TOTO-3 and fluorescence of the DNA-bound dye analyzed by the Tecan SAFIRE II microplate reader at 642 ± 8 nm excitation and 660 ± 9 nm emission. One from three typical independent experiments is shown.

Fig. 3: Capsid labeled Ad2-GFP-pV particles contain GFP-pV

A. Fluorogram of Atto647-Ad2-GFP-pV separated by 12% SDS-PAGE and excited by by 633 nm light. Positions of pII (hexon), pIII and pVI are indicated.

B. Transmission-EM analysis of negatively stained Ad2 (left) and Ad2-GFP-pV show monodispersed intact particles.

C. Fluorescence analysis of Atto647-Ad2-GFP-pV at 96-well clear bottom imaging plates by ImageXpress Micro microscope using 600-640 nm (Atto647 channel, top left) and 450-480 nm excitation (GFP channel, top right), including merged pseudo-colored images (lower left). The particles scored by Matlab routine are shown in green and the size-threshold rejected background puncta in red. Arrows indicate examples of double labeled particles, and arrow heads single labeled Atto647-particles.

D. Frequency profiles of Ad2-GFP-pV fluorescence showing Atto647 (top), GFP (middle) and merged ratiometric colors (bottom), including background thresholds (blue lines).

Fig. 4: Growth of Ad2-GFP-pV

A. Quantitative EM analysis of Ad2 and Ad2-GFP-pV entry into HeLa-ATCC cells, scoring virus particles at the plasma membrane (left), endosomes (middle) and the cytosol (right). Green: Ad2-GFP-pV, light brown: Ad2. Note that 15-20% of the Ad2-GFP-pV particles are not internalized. Data points show the means of indicated cells, including SEM.

B. E1A expression analyses by immunofluorescence of Ad2 or Ad2-GFP-pV infected A549 cells using dilutions of 1 µg virus. Each point represents the mean of three independent measurements including SEM.

C. Multi-round growth curves of Ad2 and Ad2-GFP-pV in A549 cells infected with 5 fluorescent focus forming units (fffu) per cell and fffu titers of cell-associated or supernatant virus shown at indicated time points as the mean of three experiments with corresponding SEM.

D. End point titers of Ad2 and Ad2-GFP-pV measured as tissue culture infectious dose 50 (TCID50) units or fffu in HER-911 cells with SEM from four independent experiments.

E. Transmission EM images of ultrathin 80 nm sections from epon embedded HER-911 cells 37 h pi. The images show clustered and solitary Ad2 (left) or Ad2-GFP-pV particles (right) in the nucleus (n) and the cytoplasm (c), and also crystalline inclusions (incl) of viral proteins (Franqueville, et al., 2008). Note that the virus particles have different shades of grey depending on whether they are partly (grey) or completely (dark) included in the section.

Fig. 5: Live cell analyses of GFP-pV dynamics and lytic egress of Ad2-GFP-pV from HeLa cells

A. Live cell confocal fluorescence microscopy of H2B-mCherry cells infected with Ad2-GFP-pV at moi 0.2 reveals dispersion of GFP-pV clusters from the nucleus to the cytoplasm at 35 to 37 h pi (time stamps min:s). Merged pseudo-colored maximum projections for GFP-pV (green) and H2B-mCherry (red), including black/white images for each channel at 37 h pi. The arrow indicates a

GFP-pV expressing H2B-mCherry positive nucleus, and arrow heads show GFP-pV positive clusters in the cytoplasm.

B. Lysis of Ad2-GFP-pV infected cell nuclei. Arrows point to GFP-pV positive nuclei. Note that both the GFP-pV and the H2B-mCherry signals of the two upper infected nuclei decreases close to the detection threshold.

C. Cell lysis events were scored by the disappearance of both GFP-pV and H2B-mCherry signals, quantified from eight different movies 24 to 45 h pi.

Fig. 6: Fluorescence microscopy of incoming Ad2-GFP-pV reveals progressive loss of GFP-pV from capsids before nuclear import of pVII.

A. Maximum projections of entire stacks from confocal fluorescence microscopy images of Atto647-Ad2-GFP-pV infected HER-911 cells depict progressive dissociation of GFP-pV from capsids highlighted in the fourth row with enlarged areas of quadruple merged channels and stippled outlines of the nuclei (n) and the cytoplasm (c). Yellow arrows indicate Atto647/GFP-pV double positive particles, red arrows Atto647-positive particles, green arrows GFP-pV particles and blue arrows Atto647/pVII double positive particles. Note that the arrows at 0 min pi denote Atto647 plus pV (yellow) and pVII (blue) signals outside of the cell. The green fluorescent background of the cell, the GFP-pV signal was thresholded (see materials and methods), which reduced its apparent intensity. The yellow frame in the second column indicates the enlarged area from the forth column.

B. Quantification of the total number of scored particles (light red) and the average Atto647 fluorescence per particle (dark red).

C. Average GFP fluorescence per scored particle (green) and ratio of average GFP/Atto647 fluorescence. The ratio of GFP/Atto647 average fluorescence is shown in the inset.

D. Quantification of pVII positive Atto647-particles (blue), and average fluorescence intensity of pVII in Atto647-particles (magenta).

E. Average GFP-pV fluorescence of pVII-positive Atto647-particles.

Fig. 7: LMB blocks the late dissociation of incoming GFP-pV from capsids

A. HER-911 cells on 96-well plates were infected with Atto647-Ad2-GFP-pV and analysed by fluorescence imaging for GFP-pV, Atto647-fluorescence and the merged pseudocolored images, including the periphery of the nuclei (n) determined by DAPI staining and the cytoplasm (c) (white lines, and not shown).

B. GFP-pV quantification of the scored Atto647-particles, including total numbers of analyzed viral particles, cells and numbers of experiments (exps), error bars with SEM and number of experiments (n), and P-values from two tailed T-tests.

References to Figure Legends

Franqueville, L., Henning, P., Magnusson, M., Vigne, E., Schoehn, G., Blair-Zajdel, M. E., et al. (2008). Protein crystals in Adenovirus type 5-infected cells: requirements for intranuclear crystallogenesis, structural and functional analysis. *PLoS ONE, 3*(8), e2894.

van Oostrum, J., & Burnett, R. M. (1985). Molecular composition of the adenovirus type 2 virion. *J. Virol., 56*, 439-448.

Zubieta, C., Schoehn, G., Chroboczek, J., & Cusack, S. (2005). The structure of the human adenovirus 2 penton. *Mol Cell, 17*(1), 121-135.

Figure 1

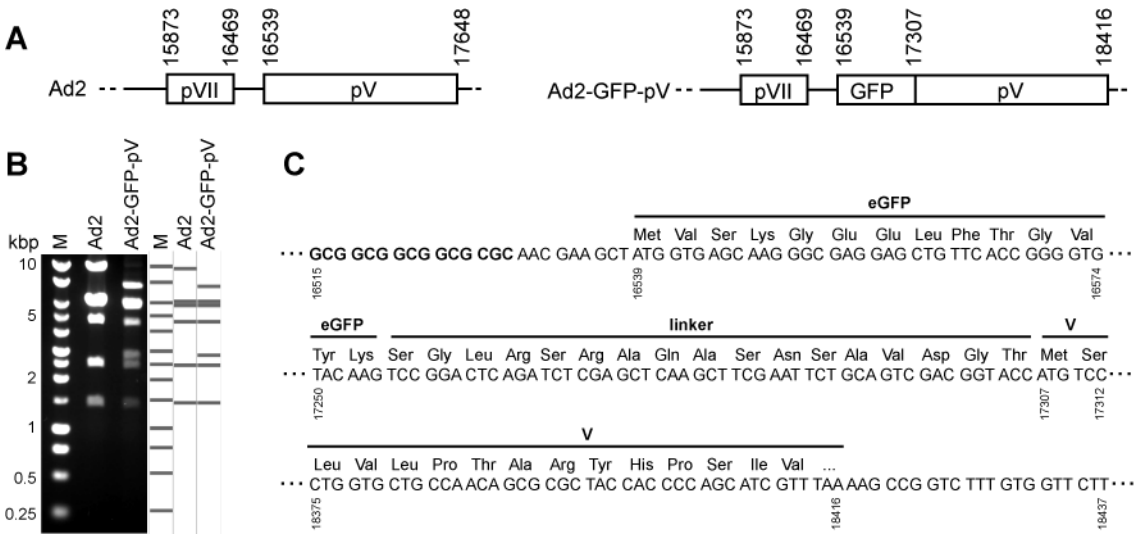
A
15873
16469
16539
17648
Ad2
pVII
pV
15873
16469
16539
17307
18416
Ad2-GFP-pV
pVII
GFP
pV
B
kbp
M
Ad2
Ad2-GFP-pV
M
Ad2
Ad2-GFP-pV
10
5
2
1
0.5
0.25
C
eGFP
Met Val Ser Lys Gly Glu Glu Leu Phe Thr Gly Val
GCG GCG GCG GCG CGC AAC GAA GCT ATG GTG AGC AAG GGC GAG GAG CTG TTC ACC GGG GTG
16515
16539
16574
eGFP
linker
V
Tyr Lys Ser Gly Leu Arg Ser Arg Ala Gln Ala Ser Asn Ser Ala Val Asp Gly Thr Met Ser
TAC AAG TCC GGA CTC AGA TCT CGA GCT CAA GCT TCG AAT TCT GCA GTC GAC GGT ACC ATG TCC
17250
17307
17312
V
Leu Val Leu Pro Thr Ala Arg Tyr His Pro Ser Ile Val ...
CTG GTG CTG CCA ACA GCG CGC TAC CAC CCC AGC ATC GTT TAA AAG CCG GTC TTT GTG GTT CTT
18375
18416
18437

Figure 2

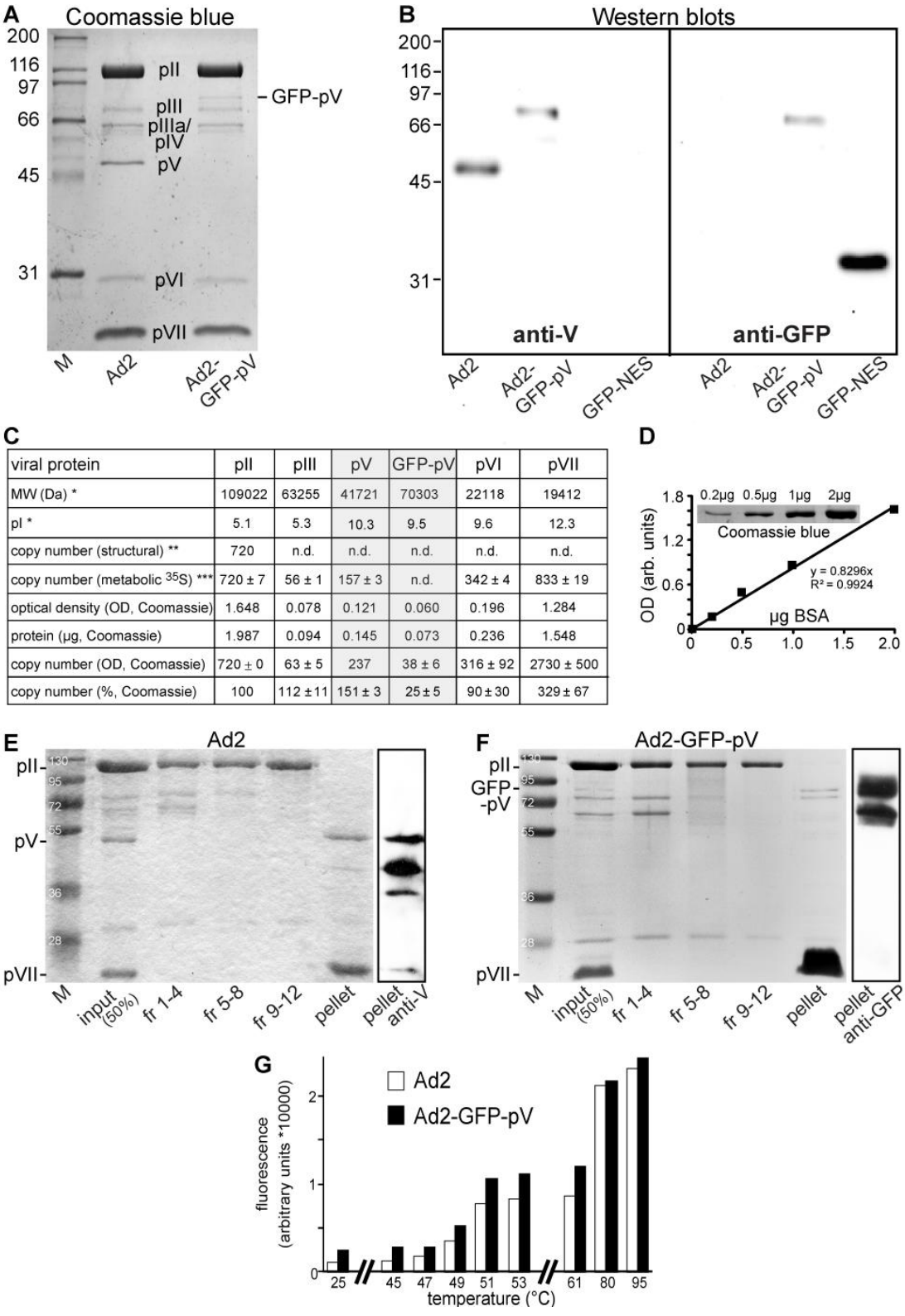

viral protein	pII	pIII	pV	GFP-pV	pVI	pVII
MW (Da) *	109022	63255	41721	70303	22118	19412
pI *	5.1	5.3	10.3	9.5	9.6	12.3
copy number (structural) **	720	n.d.	n.d.	n.d.	n.d.	n.d.
copy number (metabolic ^{35}S) ***	720 ± 7	56 ± 1	157 ± 3	n.d.	342 ± 4	833 ± 19
optical density (OD, Coomassie)	1.648	0.078	0.121	0.060	0.196	1.284
protein (µg, Coomassie)	1.987	0.094	0.145	0.073	0.236	1.548
copy number (OD, Coomassie)	720 ± 0	63 ± 5	237	38 ± 6	316 ± 92	2730 ± 500
copy number (%, Coomassie)	100	112 ± 11	151 ± 3	25 ± 5	90 ± 30	329 ± 67

Figure 3

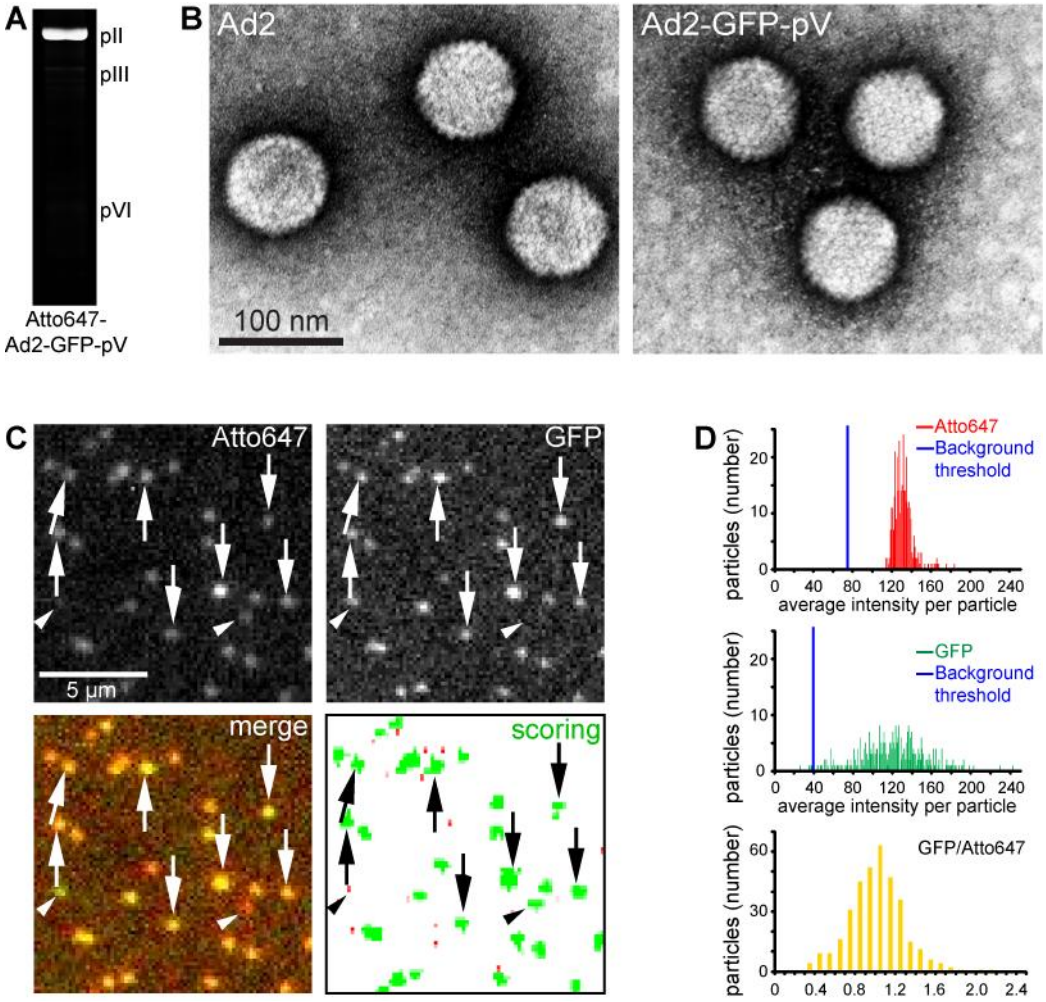
A
pII
pIII
pVI
Atto647-
Ad2-GFP-pV
B
Ad2
100 nm
Ad2-GFP-pV
C
Atto647
GFP
5 µm
merge
scoring
D
Atto647
Background
threshold
particles (number)
average intensity per particle
GFP
Background
threshold
GFP/Atto647

Figure 4

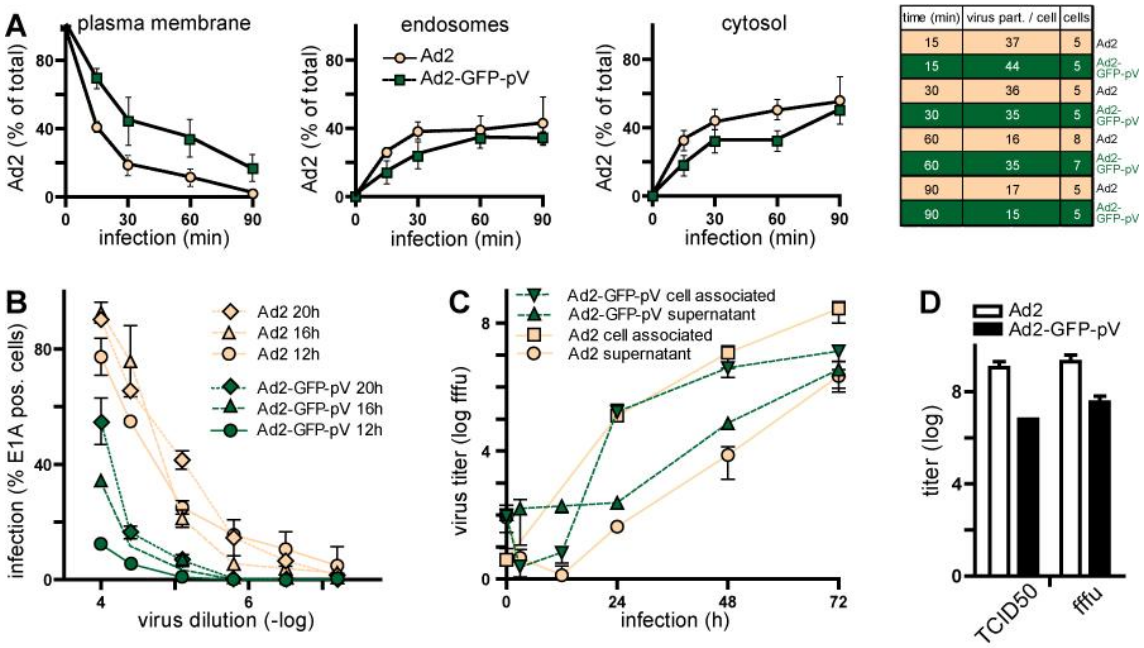

time (min)	virus part. / cell	cells	
15	37	5	Ad2
15	44	5	Ad2-GFP-pV
30	36	5	Ad2
30	35	5	Ad2-GFP-pV
60	16	8	Ad2
60	35	7	Ad2-GFP-pV
90	17	5	Ad2
90	15	5	Ad2-GFP-pV

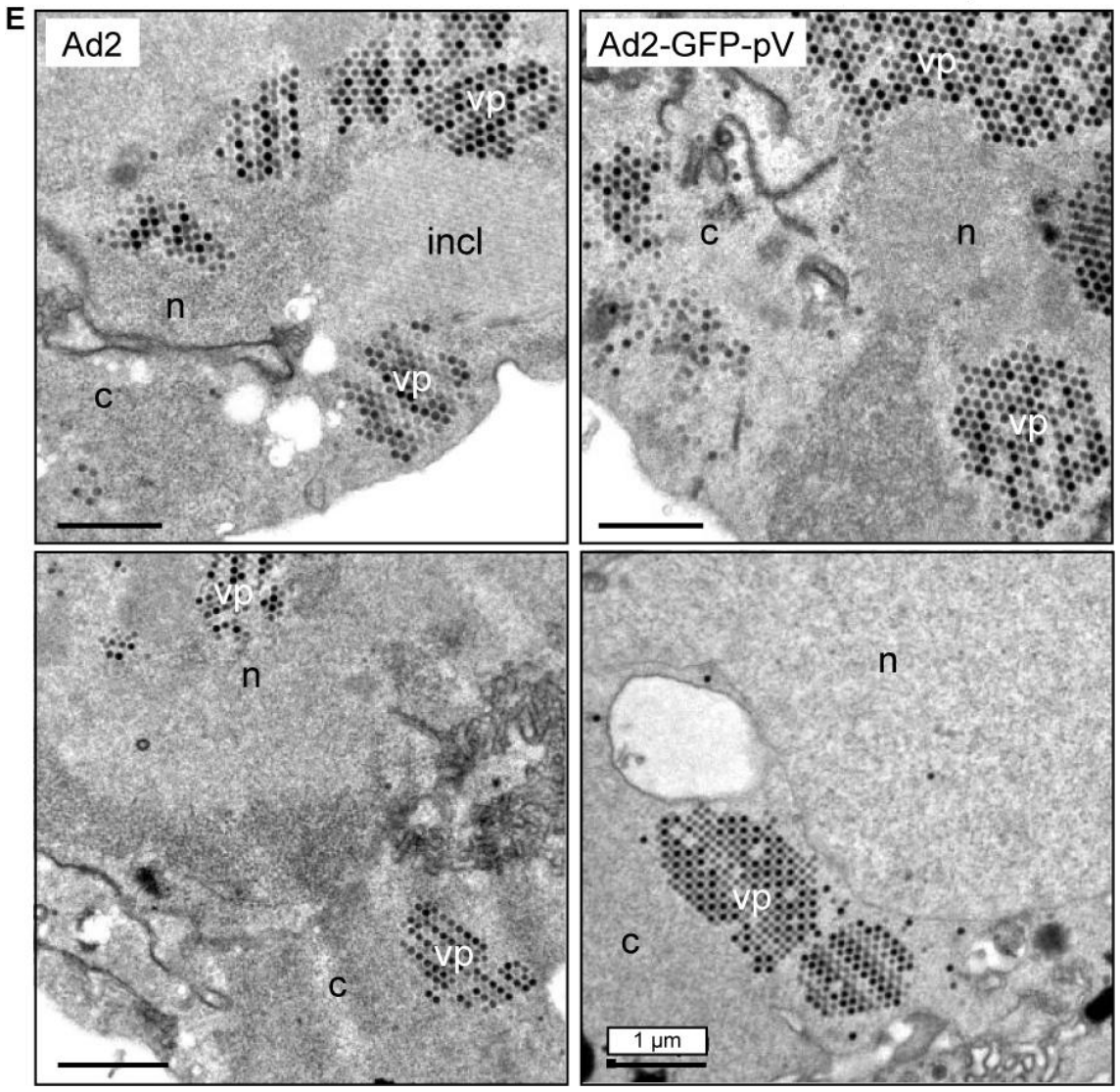

Figure 5

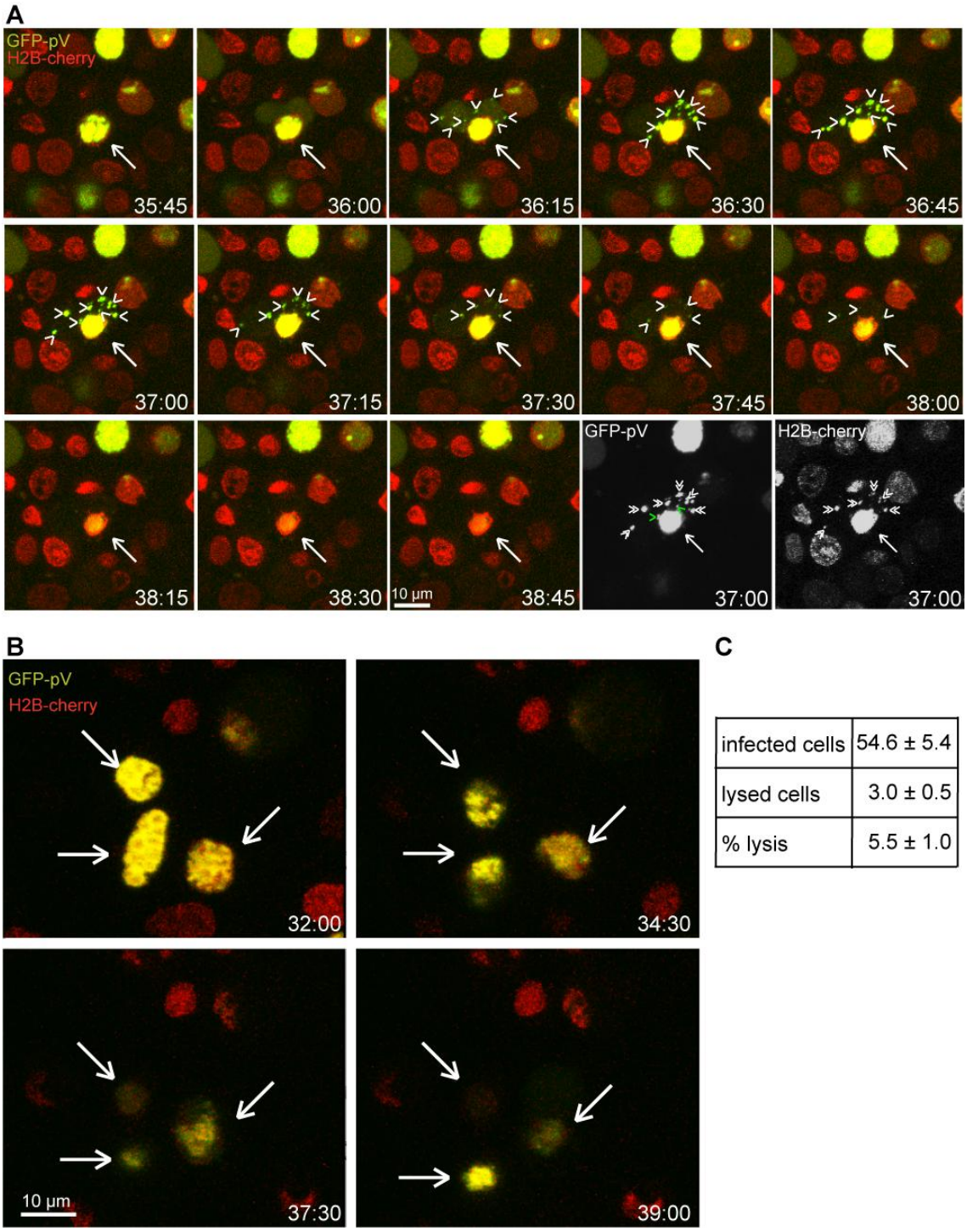

C

infected cells	54.6 ± 5.4
lysed cells	3.0 ± 0.5
% lysis	5.5 ± 1.0

Figure 6

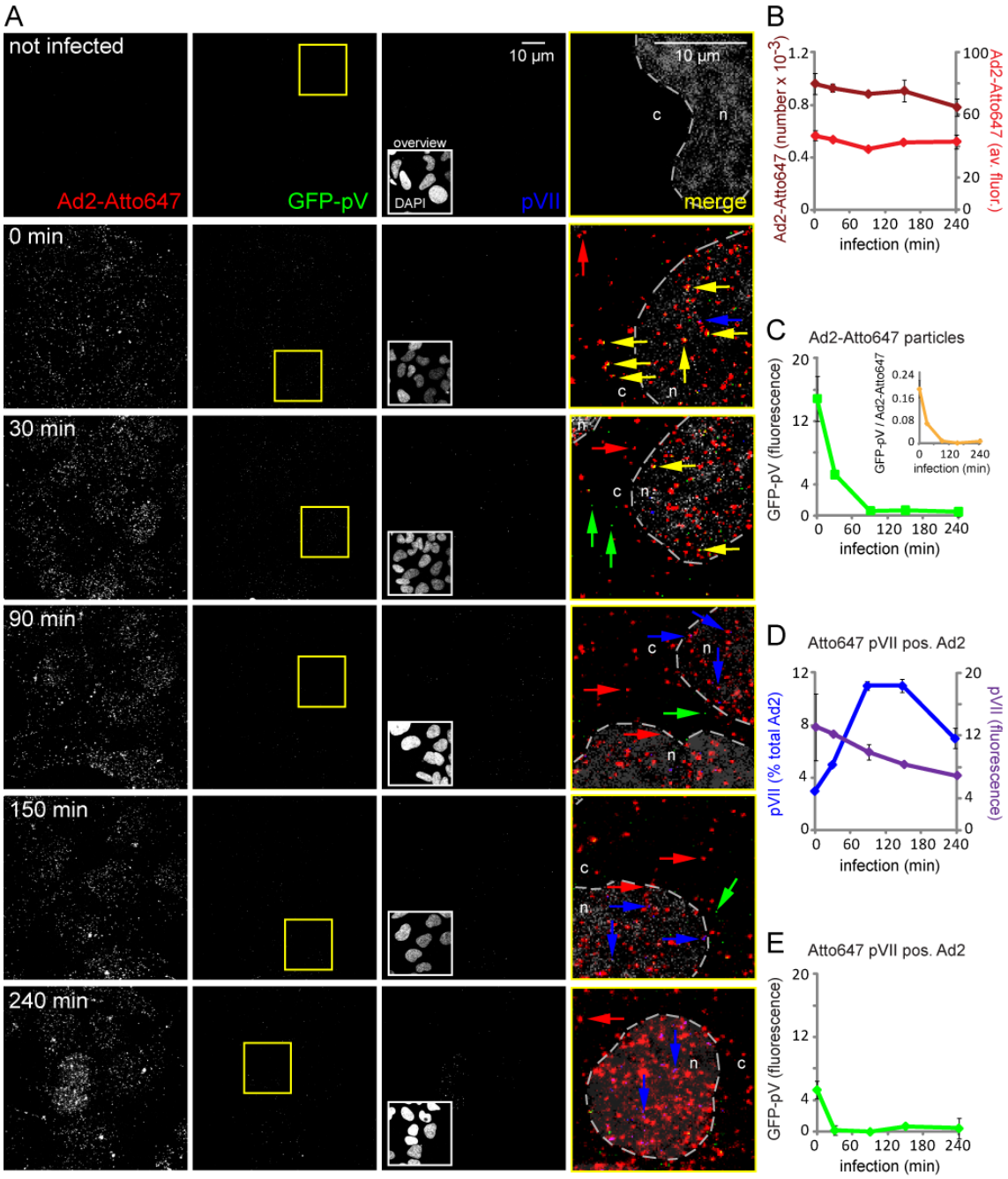
A
not infected
Ad2-Atto647
GFP-pV
10 µm
overview
DAPI
pVII
10 µm
c
n
merge
0 min
30 min
90 min
150 min
240 min
B
Ad2-Atto647 (number x 10-3)
Ad2-Atto647 (av. fluor.)
infection (min)
C
Ad2-Atto647 particles
GFP-pV (fluorescence)
GFP-pV / Ad2-Atto647
infection (min)
D
Atto647 pVII pos. Ad2
pVII (% total Ad2)
pVII (fluorescence)
infection (min)
E
Atto647 pVII pos. Ad2
GFP-pV (fluorescence)
infection (min)

Figure 7

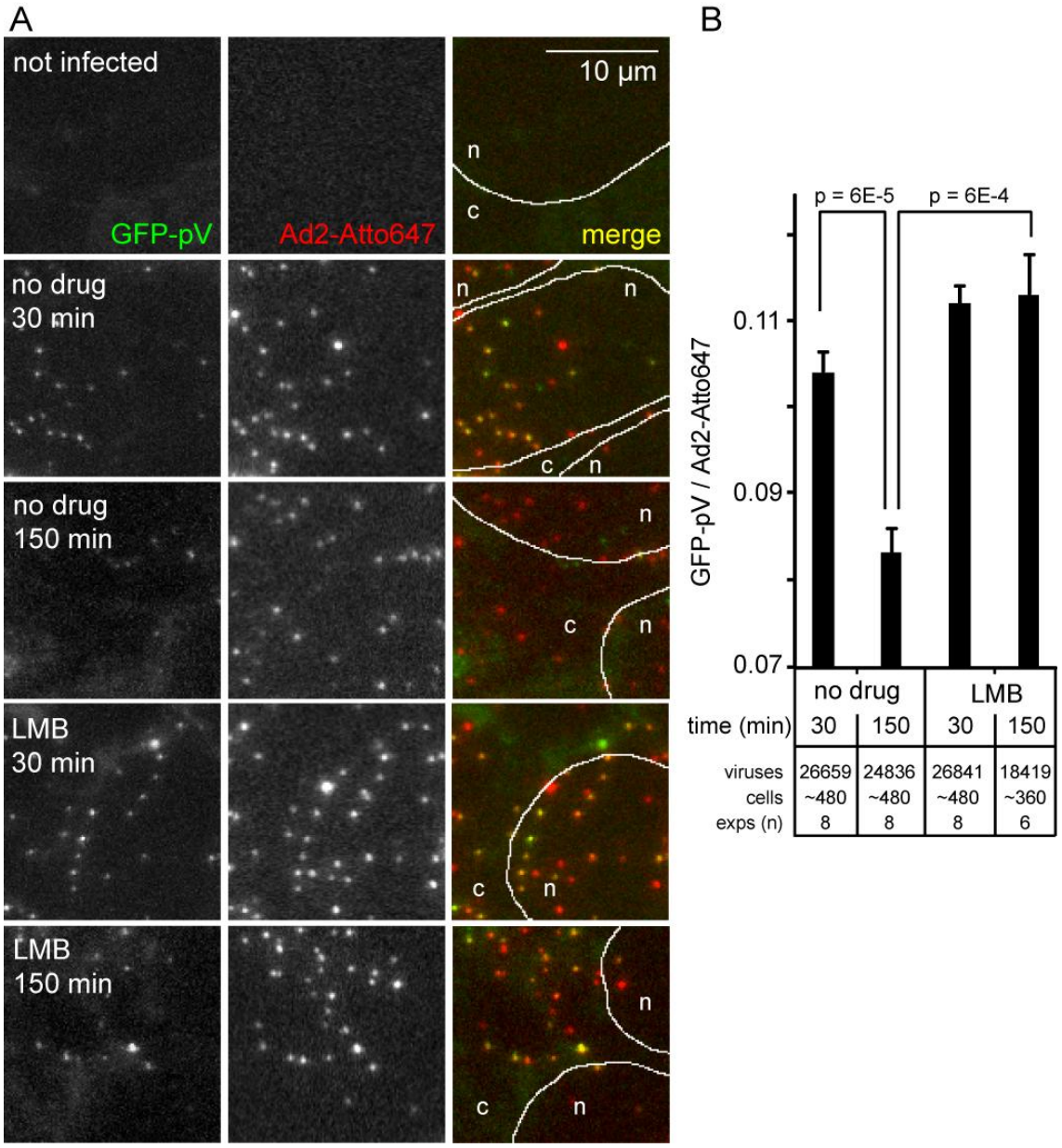
A
not infected
GFP-pV
Ad2-Atto647
10 µm
merge
n
c
no drug
30 min
no drug
150 min
LMB
30 min
LMB
150 min
B
p = 6E-5
p = 6E-4
GFP-pV / Ad2-Atto647
0.11
0.09
0.07
no drug
LMB
time (min)
30
150
30
150
viruses
26659
24836
26841
18419
cells
~480
~480
~480
~360
exps (n)
8
8
8
6

Legends to supplemental figures

Fig. S1: Imaging of single virus particles by spinning disc confocal fluorescence microscopy or MetaXpress automated microscopy

A. Ad2, Ad2-GFP-V, Atto565-Ad2 or Atto565-Ad2-GFP-pV were attached to coverslips, mounted and recorded by spinning disc confocal fluorescence microscopy in beamsplitter mode and identical illumination settings. Left column: fluorescence from the GFP channel, right column: fluorescence from the Atto565 channel. Note the absence of crosstalk between the channels.

B. Ad2, Atto647-Ad2, Ad2-GFP-pV or Atto647-Ad2-GFP-pV were bound to empty wells of a 96-well clear bottom plate and recorded with the MetaXpress-Micro automated microscope. Upper row shows GFP channel, lower row the Atto647 channel. Note the absence of crosstalk between the channels.

Fig. S2: Incoming Ad2-GFP-pV triggers fluid phase uptake similar to Ad2

A. HeLa-ATCC cells were cold-bound with Ad2 or Ad2-GFP-pV (5 µg/ml), washed and incubated at 37°C for 15 min in the presence of the fluid phase marker dextran-FITC (0.5 mg/ml), fixed and total cell-associated fluorescence was measured by flow cytometry as described (Meier, et al., 2002). Results are expressed as the ratio of fluorescence relative to noninfected cells. Note that the fluorescence of Ad2-GFP-pV was negligible compared to dextran-FITC.

B. Dextran release from endosomes in Ad2 or Ad2-GFP-pV infected cells (cold-bound with 5 µg/ml virus and washed) was assessed by measuring the dextran fluorescence over the nuclear area of fixed cells. Cells with significantly enhanced nuclear dextran were counted positive. For Ad2, n = 143 cells, and for Ad2-GFP-pV n = 157 cells were analysed.

Fig. S3: Newly synthesized GFP-pV from Ad2-GFP-pV has a similar subcellular localization as pV from Ad2

A. Hela-ATCC cells were infected or not infected with Ad2 or Ad2-GFP-pV at moi 2 for 20 h, fixed and stained for the viral DNA binding protein (DBP) and the nucleus (DAPI), or with an affinity-purified rabbit anti-pV antibody. Note that GFP-pV and pV are both excluded from DBP positive areas.

B. Purified Ad2 or Ad2-ts1 and cell lysates from Ad2 infected or not infected (not inf.) cells were fractionated by 12% SDS-PAGE, blotted and stained with affinity purified rabbit anti-pV antibody followed by goat anti-rabbit conjugated horse raddish peroxidase staining.

C. Hela-ATCC cells were infected with Ad2-GFP-pV for 20 h, stained with anti-pV antibody and Alexa594 goat anti-rabbit (rab594) or only with secondary Alexa 594 goat anti-rabbit antibody, and with DAPI. Note the extensive overlap of the GFP-pV signal with the anti-pV antibody stain.

Fig. S4: Ad2 isolated from H2B-mCherry expressing cells contains no detectable H2B-mCherry

HeLa cells stably expressing H2B-mCherry or human epithelial A431 cells were infected with Ad2 at moi 2 for 3 days. Virus was purified by CsCl gradient centrifugation, fractionated by 12% SDS-PAGE and stained with Coomassie blue (upper panel) or Western blotted and immunostained with an anti-mRFP antibody (Abcam, 1:1000, lower panel). Relative molecular weights are in kDa.

Fig. S5: Rapid cell binding of Atto565-Ad2-GFP-pV

A. Attachment of dual color Atto565-Ad2-GFP-pV (0.2 µg/ml) to HER-911 cells was monitored by live cell spinning disc confocal microscopy with a beamsplitter focusing on the lower parts of the cells. The left part of each picture shows the

GFP channel and the right part the Atto565 channel. Time stamps are in min and s.

B. The GFP image at 7 min 30 s was pseudo-colored in green and the Atto565 image in red. Processed images were merged, and the DIC image from the same time point are also shown. Arrows indicate a couple of dual color puncta.

Fig. S6: Schematic representation for the cell-based GFP-pV dissociation assay of incoming Ad2-GFP-pV

A. Image processing procedure. Image stacks from the GFP, Atto647 and DAPI channels were background subtracted, and based on the Atto647 channel also aberration corrected individually, merged using maximum intensity projection algorithm and analysed for GFP-pV and Atto647 colocalization.

B. Illustration of the aberration correction procedure. Multi fluorescent Tetraspec beads were bound to the bottom of a 96-well clear bottom plate and recorded with the MetaXpress Micro microscope in the GFP and Atto647 channels. The mismatch between the Atto647 channel and the GFP channel was corrected with a Matlab (MathWorks, Inc. Natick, MA,USA) routine post image acquisition, as shown with the GFP-pV/Atto647 merged original picture (upper left), and the shift-corrected image (upper right). Red arrows originate from the fixpoint used in the correction routine and define the direction of the correction displacement. The accuracy of the procedure is illustrated by the two lower images showing enlarged regions of the boxed areas in the two upper images.

C. Particle identification procedure in representative images taken with the MetaXpress Micro microscope of background and aberration corrected maximum projections from the Atto647, GFP and DAPI channels 30 min pi in the absence of drugs. The Matlab routine shown in the second panel identifies single particulate puncta in the Atto647 channel (green) and rejects nonhomogeneous signals (red) according to a size-threshold.

Fig. S7: Localisation of double positive Atto647-Ad2-GFP-pV near nuclear pore complexes

POM121-mCherry transfected HER-911 cells were infected with Atto647-Ad2-GFP-pV and live imaged with spinning disc confocal microscopy with focus near the bottom of the nucleus at 60 min pi. The left panel shows images recoded in the Atto647, GFP and cherry channels. A pseudo-colorized merged image is shown in the right panel where red represents Atto647 labeled Ad2, green GFP-pV and blue POM121-mCherry.

Movies S1 and S2: Live cell analyses of GFP-pV dynamics and lytic egress of Ad2-GFP-pV from HeLa cells

Hela cells stably expressing H2B-mCherry were infected with Ad2-GFP-pV at moi 0.2 and recorded by live cell confocal fluorescence microscopy from 24 to 45 h pi at 15 min per frame. Merged pseudo-colored maximum projections are shown with GFP-pV in green, and H2B-mCherry in red.

Movie S1: Dispersion of GFP-pV positive clusters from the nucleus into a confined cytoplasmic region around the nucleus (see cell in the center of the movie) 35:45 – 38:30 min pi. Note that the clusters as well nuclear GFP-pV signal disappear almost completely while GFP-pV of neighbouring cells remains visible.

Movie S2: Lysis of Ad2-GFP-pV infected cell nuclei. Note that both the GFP-pV and the H2B-mCherry signals of the two upper infected nuclei decrease to background levels.

Movie S3: Rapid cell binding of Atto565-Ad2-GFP-pV and dynamic colocalization of GFP-pV with Atto565 labeled capsids

HER-911 cells were infected with Atto565-Ad2-GFP-pV and live imaged by spinning disc confocal fluorescence microscopy in beam splitter mode, allowing simultaneous recordings of GFP-pV and Atto565 signals. Total recording time

was 15 min at 12 frames per min. Note that red and green signals were simultaneously detected in both channels at similar locations relative to the cell, indicating that at the time of cell binding, a large fraction of viral particles were double positive for Atto565 and GFP-pV.

Supplemental Experimental Procedures

Cells, transfection and antibodies

HeLa-ATCC and human lung carcinoma A549 cells were purchased from American Type Culture Collection, Rockville, MD. Ad5-E1 transfected human embryonic retinoblast 911 cells (Fallaux, et al., 1996) were obtained from Dr. S. Hemmi (University of Zurich, Switzerland). HeLa cells stably expressing H2B-mMCherry were obtained from Dr. Daniel Gerlich, ETH Zurich, prepared analogous to the HeLa clone stably expressing H2B-GFP (Kanda, Sullivan, & Wahl, 1998). A431 human epithelial carcinoma cell lysate was purchased from BD Transduction Laboratories (Lexington, KY, USA). Cells were grown as monolayers in Dulbecco's modified Eagle medium (DMEM) supplemented with 10% fetal bovine serum (GIBCO-BRL) on alcian blue-coated glass coverslips (Suomalainen, et al., 1999) or cell culture dishes. Plasmid POM121-mCherry (obtained from Dr. Daniel Gerlich, ETH Zurich) was transfected into 50% confluent cells using FuGENE 6 (Roche, Indianapolis, IN) according to the manufacture's protocol. Mouse anti-GFP was purchased from Roche (Roche Diagnostics (Schweiz) AG, Rotkreuz, Switzerland). Rabbit anti-protein V serum was obtained from W.C. Russell (University of St Andrews, UK, Matthews & Russell, 1998) and rabbit anti-protein VII antibody from L. Gerace (The Scripps Research Institute, La Jolla, USA). Guinea Pig anti-DBP (DNA Binding Protein) was from W. Deppert (University of Hamburg, Germany). Purified rabbit anti-pV C-term antibody was manufactured by immunizing rabbits with the synthetic peptide RRVAREGGRTLVLPTAR, position 347-363 of Ad2 pV. Serum was harvested and an enriched IgG fraction was affinity purified on immobilized peptide (Davids Biotechnologie, Regensburg, Germany).

SDS-PAGE, Western blots, fluorography and protein quantification

SDS-PAGE gels were run with a Hoefer minigel device according to the manufacturer's instructions, and stained with Coomassie Brilliant Blue. Pictures

were recorded either directly with the Syngene G:BOX gel documentation system (BIOLABO Scientific Instruments SA, Chatel-St-Denis, Switzerland) under white-light conditions or scanned after drying on filter paper. For Western Blots, SDS-PAGE gels were electro-transferred in semi-dry mode onto Millipore Immobilon-P^{SQ} 0.2 µm PVDF transfer membranes (Milian SA, Geneve, Switzerland), and developed with the Amersham ECL Plus Western Blotting Detection kit (GE Healthcare Life Sciences, Glattbrugg, Switzerland). Chemiluminescence was recorded either with the Kodak Digital Science Image Station 440CF or by exposing the membranes onto Amersham Hyperfilm ECL films (GE Healthcare Life Sciences, Glattbrugg, Switzerland). Fluorography of Atto647-Ad2-GFP-pV after 12% SDS-PAGE was recorded with the Amersham Typhoon 9400 gel scanner using the 633 nm Helium-Neon laser.

Protein bands from Ad2 and Ad2-GFP-pV (5 µg each) on Coomassie-stained SDS-gel were quantified with the MacBiophotonics ImageJ open source software (Rasband, W.S., ImageJ, U.S. National Institutes of Health, Bethesda, Maryland, USA, http://rsb.info.nih.gov/ij/, 1997-2010). Briefly, a region of interest (ROI) was drawn around the protein band of interest and the integrated density of the selection calculated. A background ROI with the same dimensions near the band was chosen and the integrated density subtracted from the protein band ROI. The protein amount was calculated relative to a BSA standard curve using the background subtracted total intensity of each bands. The number of molecules was determined by dividing the protein amount by the theoretical molecular mass of the protein. The copy number of an individual protein per virion was calculated relative to hexon (720 copies per virion). Calculated copy numbers were the mean of three independent experiments including SEM. Optical densities shown were derived from the same representative experiment. Molecular weights given in Dalton and the pI values were calculated with the “Compute pI/Mw tool” (http://www.expasy.ch/tools/pi_tool.html) from the Swiss Institute of Bioinformatics ExPASy Proteomics Server. Sequences used were from the

UniProtKB/Swiss-Prot database: P03277 (pII), P03276 (pIII), P03267 (pV), P03274 (pVI) and P68950 (pVII). In case of precursor proteins the mature form of the corresponding proteins was used for calculation. Values for copy numbers (structural) and copy numbers (^{35}S metabolic labeling) were obtained from the literature (van Oostrum & Burnett, 1985).

Amplification, purification and labeling of viruses

Ad2 and Ad2-GFP-pV were grown, isolated and labeled with Atto647 and Atto565 dyes (Atto-tec, Germany) as described (Greber, Webster, Weber, & Helenius, 1996; Nakano & Greber, 2000).

Virus quantification

Virus titers were determined using either tissue culture infective dose 50 ($TCID_{50}$) or a modified fluorescent focus assay (FFA). In both assays virus was titrated on HER 911 cells plated on 96-well plates. In case of $TCID_{50}$ infection was allowed to proceed for 6 days while in the FFA cells were fixed after 4 days. For the calculation of fluorescent focus forming units per ml (fffu/ml) cells were fixed, quenched, immunostained for expression of protein V and fluorescent focus units counted using a fluorescence microscope. A fluorescent focus was defined as 3 or more adjacent cells expressing protein V or GFP-pV. FFA titers were calculated using the formula of Spaerman and Kaerber. Protein concentrations of purified viruses were measured using the Micro BCA^{TM} Protein Assay Reagent Kit (Pierce, Thermo Fisher Scientific, Switzerland).

E1A measurement

50% confluent A549 cells in 96-well plates were infected with serial dilutions of 1 µg Ad2 or Ad2-GFP-pV in growth medium for 12, 16 or 20 h. Cells were fixed, immunostained with mouse anti-E1A (Harlow, Franza, & Schley, 1985) and goat anti-mouse Alexa 594 (1/500), DAPI stained and recorded with the ZEISS

Axiovert 40 CFL fluorescence microscope using suitable filters. The ratio between E1A expressing cells and DAPI positive nuclei was calculated and plotted against the virus dilution. Around 150 cells were counted per time point. The experiment was repeated 3 times with standard error of the mean (SEM).

One step growth curves

About 70% confluent A549 cells in 35 mm cell culture dishes were inoculated with 5 fffu of either Ad2 or Ad2-GFP-pV in a volume of 1 ml RPMI 0.2% BSA at 4°C on a shaker for 1 h. Cells were washed twice with PBS and incubated in 2 ml DMEM/10% FBS/NEA/PS (growth medium) at 37°C and 5% CO_2 for 0, 3, 12, 24, 48 or 72 h. Supernatant was collected in 2 ml tubes and frozen while cells were broken up in 1 ml medium by freeze-thaw 3 times, transferred to 2 ml tubes and supplemented with another ml of growth medium. Supernatants and cell lysates were centrifuged and viral titers determined on A549 cells.

Preparation of pyridine cores

Double CsCl gradient-purified Ad2 and Ad2-GFP-pV virions were dialyzed against 5 mM Tris pH 8.1, and 50 µg of each virus supplemented with 16 µl pyridine to 8% (v/v), similar to a previously described protocol (Everitt, Sundquist, Pettersson, & Philipson, 1973). Samples were incubated at 37°C for 2 h, followed by centrifugation on a 10-30% sucrose gradient at 111000 x g, 4°C for 2 h. 14 160 µl fractions were collected, TCA precipitated and dissolved in 20 µl sample buffer. Fractions 1-4, 5-8, 9-12 were combined as well as fraction 13 and 14 with the pellet (collectively the pellet fractions), and analyzed on a Coomassie stained 12% SDS-PAGE. From the pellet fractions of Ad2, a Western blot was prepared and immunostained with affinity-purified anti-pV antibody (1/200), and for Ad2-GFP-pV with anti-GFP antibody (1/1000).

Thermostability assay

Accessibility of viral DNA from double CsCl gradient purified Ad2 or Ad2-GFP-pV for the DNA intercalating fluorescent dye TOTO-3 iodide (1 mM solution in DMSO, Invitrogen) with 642/660nm excitation/emission was measured after heat-shock treatment at different temperatures. Specifically, samples containing 5 µg virus diluted in buffer containing 10 mM Tris pH 8.1, 150 mM NaCl, 1 mM MgCl and 1 µM TOTO-3 in a total volume of 50 µl were prepared in 1.5 ml Eppendorf tubes on ice, heated at indicated temperatures in a heating block for 3 min and rapidly chilled on ice. The samples were transferred to a 96-well plate and fluorescence was measured at 642±8 nm excitation and 660 ± 9 nm emission with the Tecan SAFIRE II microplate reader.

Single particle fluorescence analysis of Atto647-Ad2-GFP-pV

Atto647-Ad2-GFP-pV was adsorbed to the bottom of 96-well clear bottom plates at 20°C for 15 min, washed with PBS, and overlaid with 100 µl fresh PBS. Images were recorded with the automated ImageXpress^{MICRO} fluorescence microscope (Molecular Devices) using settings for Atto647 and GFP. Images were processed as described in supplemental methods. Briefly, images were corrected for background and aberration and single virus particles were scored. Average fluorescence intensities within the selected particle areas in the Atto647 and GFP channels were measured. For determination of background threshold 10 random ROIs which contained no virus particles were chosen using MacBiophotonics ImageJ and the average fluorescence intensity in the Atto647 or GFP channels calculated. The background thresholds are represented as blue lines in Fig. 5D. Population statistics were performed with Microsoft Office Excel software. The average intensity per particle (GFP and Atto647) and calculated ratios of average GFP/Atto647 intensities were plotted against the number of particles.

Live-cell microscopy

Live-cell confocal laser scanning fluorescence microscopy was conducted with an inverted Leica SP5 microscope (Leica Microsystems, Switzerland) equipped with a 63x (oil immersion, NA 1.4) objective, a diode laser (405 nm excitation), an argon laser (458/476/488/496/514 nm excitation), a helium laser (561/594/633 nm excitation) and a humidified chamber at 37°C and 5% CO_2. HeLa cells stably expressing H2B-mCherry were plated at 25% confluency onto 35 mm glass bottom microwell dishes, and cells were allowed to adhere overnight, followed by infection with Ad2-GFP-pV (0.8 µg) for 24 h. Image stacks were recorded every 15 minutes for 21.5 h and processed with ImageJ. From 8 movies cell lysis events were counted and plotted against total numbers of infected cells as judged by the expression of GFP-pV.

Kinetics of GFP-pV release and pVII epitope exposure of Atto647-Ad2-GFP-pV particles during infection

HER-911 cells were seeded to 60% confluency onto alician blue coated coverslips in 24-well cell culture dishes overnight. Growth medium was replaced by serum-free medium, and cells were starved overnight to reduce cell background. Cells were infected with 0.1 µg/ml Atto647-Ad2-GFP-pV at 37°C 5% CO_2 for 10 min, washed briefly and supplemented with 0.5 ml serum free medium. 0 min samples were immediately fixed with 3% PFA-PBS for 15 minutes, washed and quenched for 10 min with 25 mM NH_4Cl in PBS and permeabilized with 0.5% Triton X-100 in PBS for 10 min. Other samples were allowed to proceed for 30, 90, 150 or 240 min post-addition of virus. Cells were blocked with 20% goat serum and stained against pVII with preadsorbed anti-pVII/Alexa594 goat anti-rabbit and DAPI. Images were recorded on the same day with an inverted Leica SP5 single-point confocal microscope (Leica Microsystems, Switzerland) equipped with a 63x (oil immersion, NA 1.4) objective. Excitations were at 405 nm (DAPI), 488 nm (GFP), 594 nm (pVII) and 633 nm (Atto647). Individual stacks were recorded with 0.21 µm intervals using 10x accumulation and 4x averaging. Maximum projections were

generated with MacBiophotonics ImageJ. A Matlab-based routine (for details see supplementary information) was used to score individual viral particles and measure average fluorescence intensities in the particle areas from the Atto647 (capsid), GFP (GFP-pV) or Alexa594 (pVII) channels. Threshold values for fluorescence intensities were obtained by subtracting the average intensity of the entire image calculated using MacBiophotonics ImageJ from individual average intensities of single virus particles. Statistics were performed with Microsoft Office Excel. The total numbers of scored particles and average fluorescence intensities in the Atto647 channel (capsid) were plotted against time. Average GFP fluorescence intensities in scored (Atto647) particles were plotted against time as well as GFP/Atto647 average fluorescence ratios of single particles. The population of particles with pVII intensities over threshold (Atto647 and pVII positive Ad2) was determined and the ratio of this population relative to the total amount of scored (Atto647) particles plotted against time. From the same population average pVII fluorescence intensities were calculated and plotted against time, or average GFP fluorescence were calculated and plotted against time.

GFP-pV dissociation from Ad2

HER-911 cells were platted on 96-well clear bottom plates to 30% confluency in 75 µl DMEM/10% FBS/1% NEA/1% PS plus 25 µl Optimem and incubated for 3 days at 37°C and 5% CO_2. For background controls medium was added to wells containing no cells. Cells were supplemented with 10 µl LMB dissolved in DMEM/0.2% BSA/1% PS to a final concentration of 20 nM or were MOCK treated 1 h prior to infection. LMB was present during the whole experiment. Atto647-labelled Ad2-GFP-pV (0.125 µg, centrifuged for 10 min at 10000 rpm in an Eppendorf 5415 R centrifuge at 4°C prior use) was added in 10 µl DMEM/0.2% BSA/1% PS for 15 min. Medium was removed and fresh DMEM/0.2% BSA/1% PS was added. 30 or 150 min p.i. 25 µl 16% PFA in PBS was added for 10 min, cells were washed 2 times with PBS and quenched with 25 mM NH_4Cl in PBS for 10 minutes followed by another washing step and

treatment with 0.5% TX-100 in PBS containing 0.5 µg/ml DAPI for 10 min. Cells were then washed extensively and 100 µl PBS-N_3 was added prior to recording.

Fluorescence was recorded with the automated ImageXpress^{MICRO} fluorescence microscope (Molecular Devices) using a Nikon 40x air objective NA 0.95, Semrock BrightLine® filters (GFP-3035B-NTE-ZERO, Cy5-4040A-NTE-ZERO and DAPI-5060B-NTE-ZERO) and the Molecular Devices MetaXpress 2 software. 9 individual regions per well were recorded as stacks comprised of 9 sections with a z-distance of 1 µm and images were saved as 16 bit TIFFs. Illumination times were 6 seconds for GFP, 8 seconds for Atto647 and 5 ms for DAPI without binning. Images were processed as described in supplementary information. Briefly, images were corrected for background and aberration. Maximum projections were generated and single viral particles were scored in the Atto647 channel. Average fluorescence intensities in selected particle areas in the GFP and Atto647 channels were determined and GFP/Atto647 intensity ratios calculated for all scored particles individually. Average GFP/Atto647 intensities were plotted against time, and statistics performed with Microsoft Office Excel, including SEM calculated with n = 9.

Crosstalk control experiments

Ad2, Ad2-GFP-pV, Atto565-Ad2 or Atto565-Ad2-GFP-pV were attached to coverslips, mounted with DAKO and recorded by spinning disc confocal fluorescence microscopy in beamsplitter mode (GFP and Atto565) using identical illumination settings. Ad2, Atto647-Ad2, Ad2-GFP-pV or Atto647-Ad2-GFP-pV were adsorbed to the bottom of 96-well clear bottom plates at 20°C for 15 min. Wells were washed with PBS, medium removed and 100 µl fresh PBS was added. Virus particles were recorded with the MetaXpress-Micro automated microscope focusing on the bottom of the plate using identical illumination settings (GFP and Atto647) for all viruses.

Live cell SDCM microscopy

For live cell spinning disc confocal microscopy (SDCM), images were recorded with an N.A. 1.35 UplanApo 100x objective on an Olympus IX81 inverted microscope (Olympus Schweiz) equipped with a temperature controlled incubator box (Life imaging services), a Yokogawa scanning head QLC100 (VisiTech International) with a triple bandpass excitation filter (488 nm/565 nm/647 nm) (Chroma) and an Innova 70C mixed gas laser (Coherent). For simultaneous dual color imaging (GFP/Atto565) a Dualview MultiSpec-MicroImager (Optical Insights, USA) was used. Images were recorded onto a back-illuminated monochrome Cascade 512 EM-CCD camera (Photometrics) containing a 512x512 pixel chip. Microscope and camera were controlled with the Metamorph software package (Molecular Devices).

HER-911 cells were grown on cover slips, serum starved over night and maintained in DMEM with HEPES modification (SIGMA, D6171) containing 0.2% BSA during acquisition. Recording was started and Atto565-Ad2-GFP-pV was added to 0.2 µg/ml.

Image processing, particle scoring and quantification of GFP-pV from the Ad2 particles

Images were recorded with an automated ImageXpress^{MICRO} fluorescence microscope (Molecular Devices) controlled by the Molecular Devices MetaXpress 2 software as described earlier. Image stacks comprising 9 serial sections separated by a z-distance of 1 µm were recorded in the DAPI, GFP, and Atto647 channels and saved as 16 bit TIFF stacks. To correct for uneven illumination across the field of view, a well containing no cells was recorded using identical settings (background stack). From each slice in the sample stack the pixel intensity of the corresponding slice in the background stack was subtracted.

Lense aberrations caused a shift of the virus position in the GFP channel relative to its position in the Atto647 channel. This was corrected with a custom written Matlab script. A factor for the radial and linear increasing position shift was determined manually. The pixel intensity value associated with each element in the image matrix was distributed into elements of a new matrix relative to the calculated shift. This resulted in a new image matrix where intensity values were shifted to the corrected image locations.

A Matlab based algorithm was used for particle scoring. In brief, Otsu's method (Otsu, 1979) was used for thresholding of maximum intensity projections generated from background and aberration corrected images acquired in the Atto647 channel. A manually set area threshold was used to attribute contiguous pixel over the grey threshold to virus particles in an image mask. Particles that meet the area threshold were displayed in green whereas particle that did not fulfill the threshold criteria were depicted in red (Figure S6C). This image mask was subsequently employed to measure average fluorescent intensities over the particle areas in both average intensity projections from GFP channel images and Atto565 channel images. The following particle parameters were extracted and used for analysis: Particle size, average GFP fluorescence intensity, average Atto565 fluorescence intensity, and the ratio (GFP/Atto647) of the two aforementioned intensities. Statistical analysis was performed with Microsoft Office Excel. The source code of all Matlab routines is available from the authors upon request.

Live cell SDCM of POM121-mCherry transfected HER-911 cells

HER-911 cells were transfected with a POM121-mCherry expressing plasmid using FuGENE 6 (Roche) according to the manufacture’s instructions. Cells were serum starved overnight and warm infected with 0.2 µg/ml Atto647-Ad2-GFP-pV for 15 min, medium removed and incubated for another 45 min at 37°C

5% CO_2. Cells were recorded with the spinning disc confocal microscope without beamsplitter.

EM analyses

HeLa cells grown on alician blue coated coverslips at 70% confluency were incubated with 10 µg each Ad2 or Ad2-GFP-pV on ice for 1h, washed and incubated In DMEM-BSA at 37°C for 0, 30, 60 or 90 min. Cells were prepared for EM analyses as described and analyzed for subcellular localization of virus using ruthelium red as a plasma membrane marker post fixation (Gastaldelli, et al., 2008).

Fluid phase endocytosis and flow cytometry

Fluid phase uptake and dextran release assays were performed as described (Meier, et al., 2002). Briefly, HeLa-ATCC cells were cold-bound with 10 µg/ml Ad2 or Ad2-GFP-pV, washed and incubated at 37°C for 15 min in the presence of 1 mg/ml dextran-FITC and another 5 min in the absence of dextran-FITC. Cells were washed, acid stripped in 0.1 M sodium acetate, 0.05 M NaCl pH 5.5 and detached with trypsin. 10000 cells were analyzed by flow cytometry in an Epics XL cell sorter (Beckman Coulter, Miami, Fla). Dextran release from endosomes was assessed by measuring the dextran fluorescence over the nuclear area. Cells with significantly enhanced nuclear dextran stain were counted positive and plotted against total numbers of cells.

Localization of GFP-pV and pV relative to DBP and characterization of the anti-pV antibody

HeLa-ATCC cells were infected with Ad2 or Ad2-GFP-pV at moi 2 for 20 h or left non-infected. They were fixed, quenched, Triton X-100 treated and blocked for 1 h with 20% goat serum in PBS. DNA binding protein (DBP) was immunostained with a guinea pig anti-DBP antibody, pV with an affinity purified

rabbit anti-pV antibody and the cell nucleus with DAPI. Purified Ad2 or Ad2-ts1 and cell lysates from Ad2 infected cells (3, 18 and 30 h) or non-infected HeLa-ATCC cells grown on cell culture dishes were fractionated by 12% SDS-PAGE, blotted and stained with affinity purified rabbit anti-pV antibody followed by goat anti-rabbit conjugated horse raddish peroxidase staining.

Preparation of Ad2 from H2B-mCherry expressing HeLa cells

Ad2 was grown on HeLa cells stably expressing H2B-mCherry and purified. 5 µg of this virus was fractionated by 12% SDS-PAGE together with cell lysates from A431 human epithelial carcinoma cells (BD Transduction Laboratories, Lexington, KY, USA) and non-infected HeLa H2B-mCherry cells. A Western blot was prepared and stained for H2B-mCherry with a cross-reactive (mCherry) rabbit anti-mRFP antibody diluted 1:1000 (purchased from Abcam, ab62341) followed by goat anti-rabbit conjugated horse raddish peroxidase staining.

Supplemental references

Everitt, E., Sundquist, B., Pettersson, U., & Philipson, L. (1973). Structural proteins of adenoviruses. X. Isolation and topography of low molecular weight antigens from the virion of adenovirus type 2. *Virology, 52*, 130-147.

Fallaux, F. J., Kranenburg, O., Cramer, S. J., Houweling, A., Van Ormondt, H., Hoeben, R. C., et al. (1996). Characterization of 911: a new helper cell line for the titration and propagation of early region 1-deleted adenoviral vectors. *Hum Gene Ther, 7*(2), 215-222.

Gastaldelli, M., Imelli, N., Boucke, K., Amstutz, B., Meier, O., & Greber, U. F. (2008). Infectious adenovirus type 2 transport through early but not late endosomes. *Traffic, 9*(12), 2265-2278.

Greber, U. F., Webster, P., Weber, J., & Helenius, A. (1996). The role of the adenovirus protease on virus entry into cells. *Embo J, 15*(8), 1766-1777.

Harlow, E., Franza, B. R., Jr., & Schley, C. (1985). Monoclonal antibodies specific for adenovirus early region 1A proteins: extensive heterogeneity in early region 1A products. *J Virol, 55*, 533-546.

Kanda, T., Sullivan, K. F., & Wahl, G. M. (1998). Histone-GFP fusion protein enables sensitive analysis of chromosome dynamics in living mammalian cells. *Curr Biol, 8*(7), 377-385.

Matthews, D. A., & Russell, W. C. (1998). Adenovirus core protein V is delivered by the invading virus to the nucleus of the infected cell and later in infection is associated with nucleoli. *J Gen Virol, 79 (Pt 7)*, 1671-1675.

Meier, O., Boucke, K., Hammer, S. V., Keller, S., Stidwill, R. P., Hemmi, S., et al. (2002). Adenovirus triggers macropinocytosis and endosomal leakage together with its clathrin-mediated uptake. *J Cell Biol, 158*(6), 1119-1131.

Nakano, M. Y., & Greber, U. F. (2000). Quantitative microscopy of fluorescent adenovirus entry. *J. Struct. Biol., 129*, 57-68.

Otsu, N. (1979). A threshold selection method from gray-level histograms 9: 62–66. *IEEE Transactions on Systems, Man and Cybernetics, 9*(1), 62-66.

Suomalainen, M., Nakano, M. Y., Boucke, K., Keller, S., Stidwill, R. P., & Greber, U. F. (1999). Microtubule-dependent minus and plus end-directed motilities are competing processes for nuclear targeting of adenovirus. *J. Cell Biol., 144*, 657-672.

van Oostrum, J., & Burnett, R. M. (1985). Molecular composition of the adenovirus type 2 virion. *J. Virol., 56*, 439-448.

Figure S1

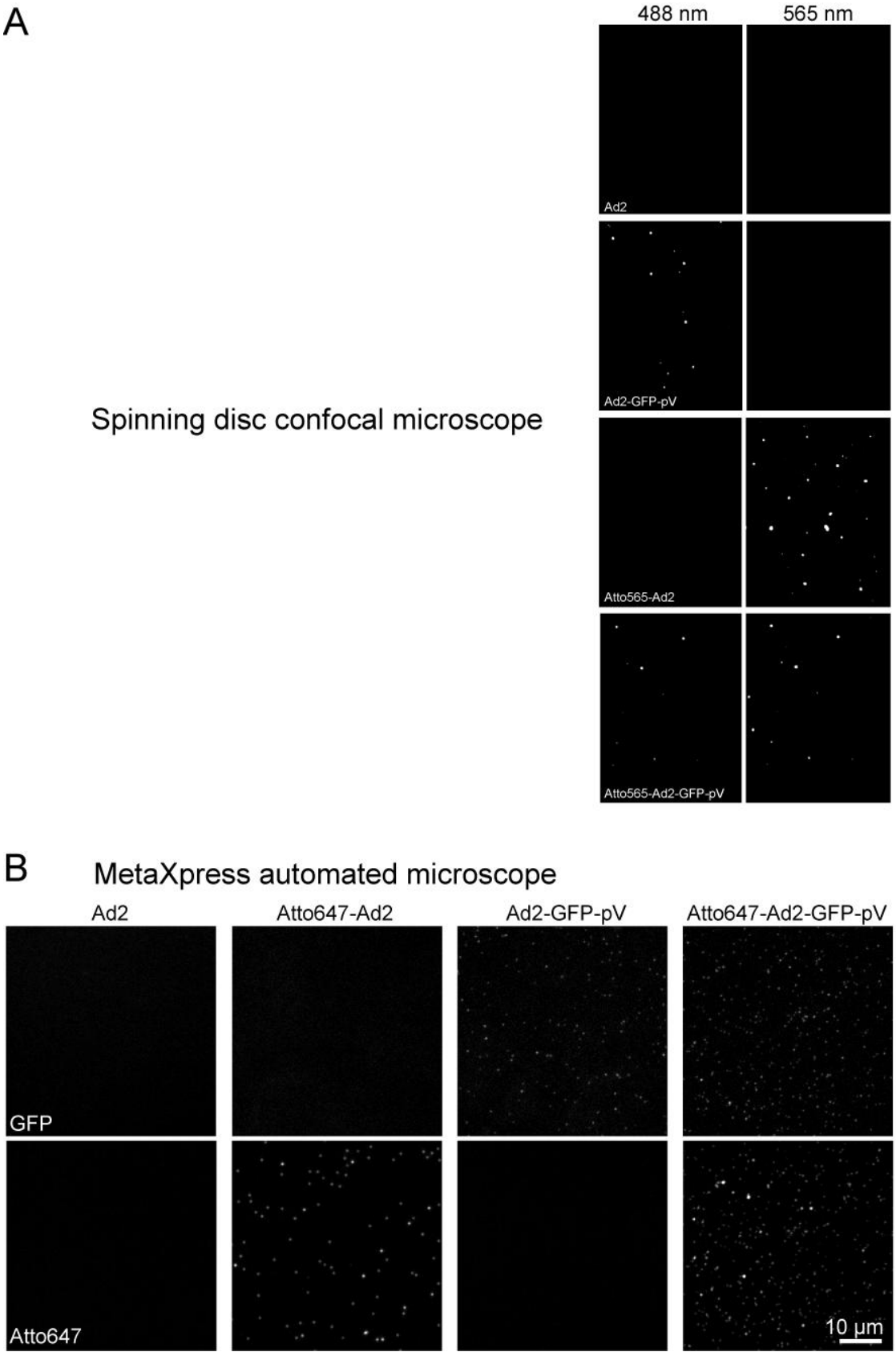
A
488 nm
565 nm
Ad2
Ad2-GFP-pV
Spinning disc confocal microscope
Atto565-Ad2
Atto565-Ad2-GFP-pV
B
MetaXpress automated microscope
Ad2
Atto647-Ad2
Ad2-GFP-pV
Atto647-Ad2-GFP-pV
GFP
Atto647
10 µm

Figure S2

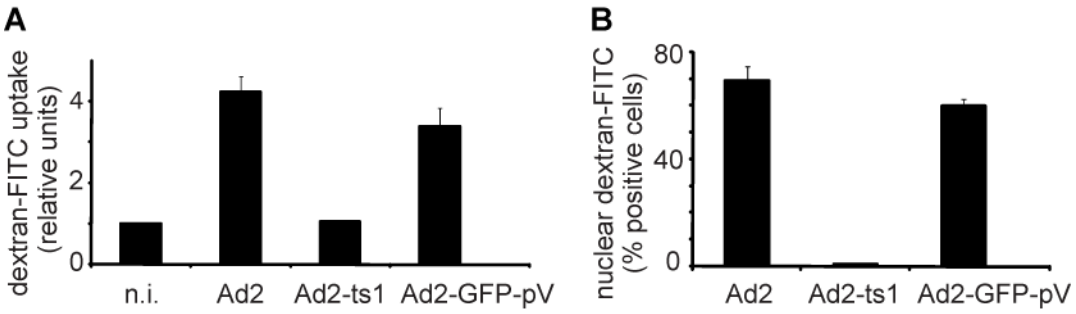
A
dextran-FITC uptake
(relative units)
0
2
4
n.i.
Ad2
Ad2-ts1
Ad2-GFP-pV
B
nuclear dextran-FITC
(% positive cells)
0
40
80
Ad2
Ad2-ts1
Ad2-GFP-pV

Figure S3

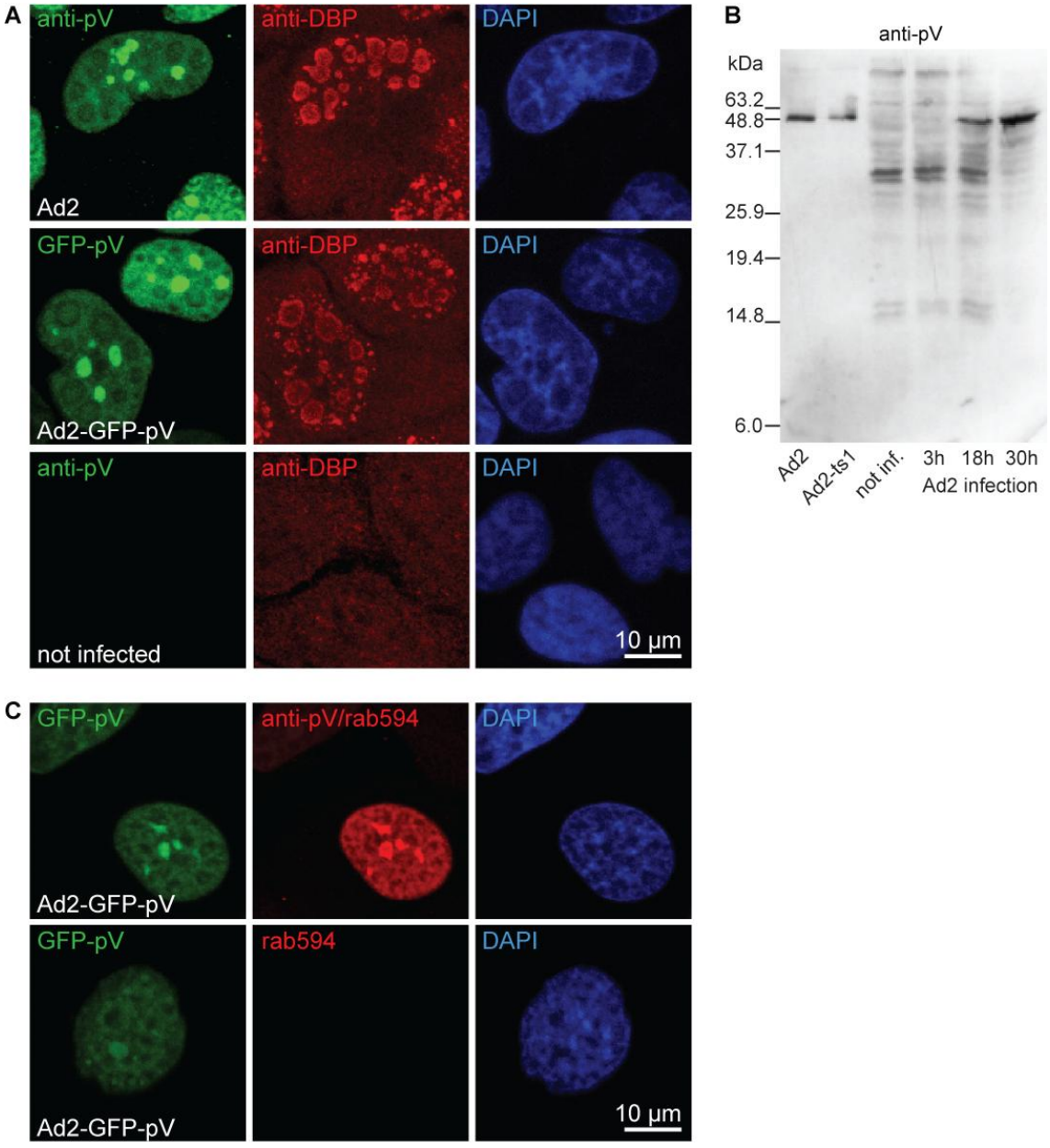
A
anti-pV
anti-DBP
DAPI
Ad2
GFP-pV
anti-DBP
DAPI
Ad2-GFP-pV
anti-pV
anti-DBP
DAPI
not infected
10 µm
B
anti-pV
kDa
63.2
48.8
37.1
25.9
19.4
14.8
6.0
Ad2
Ad2-ts1
not inf.
3h
18h
30h
Ad2 infection
C
GFP-pV
anti-pV/rab594
DAPI
Ad2-GFP-pV
GFP-pV
rab594
DAPI
Ad2-GFP-pV
10 µm

Figure S4

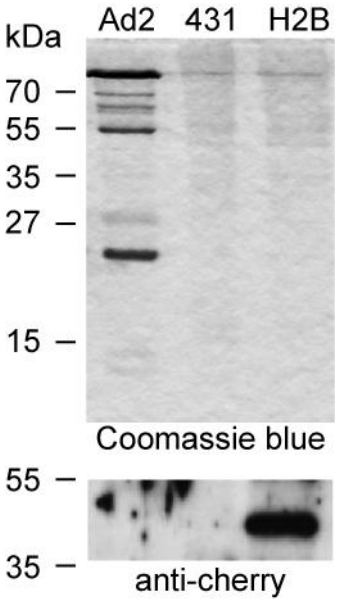

Figure S5

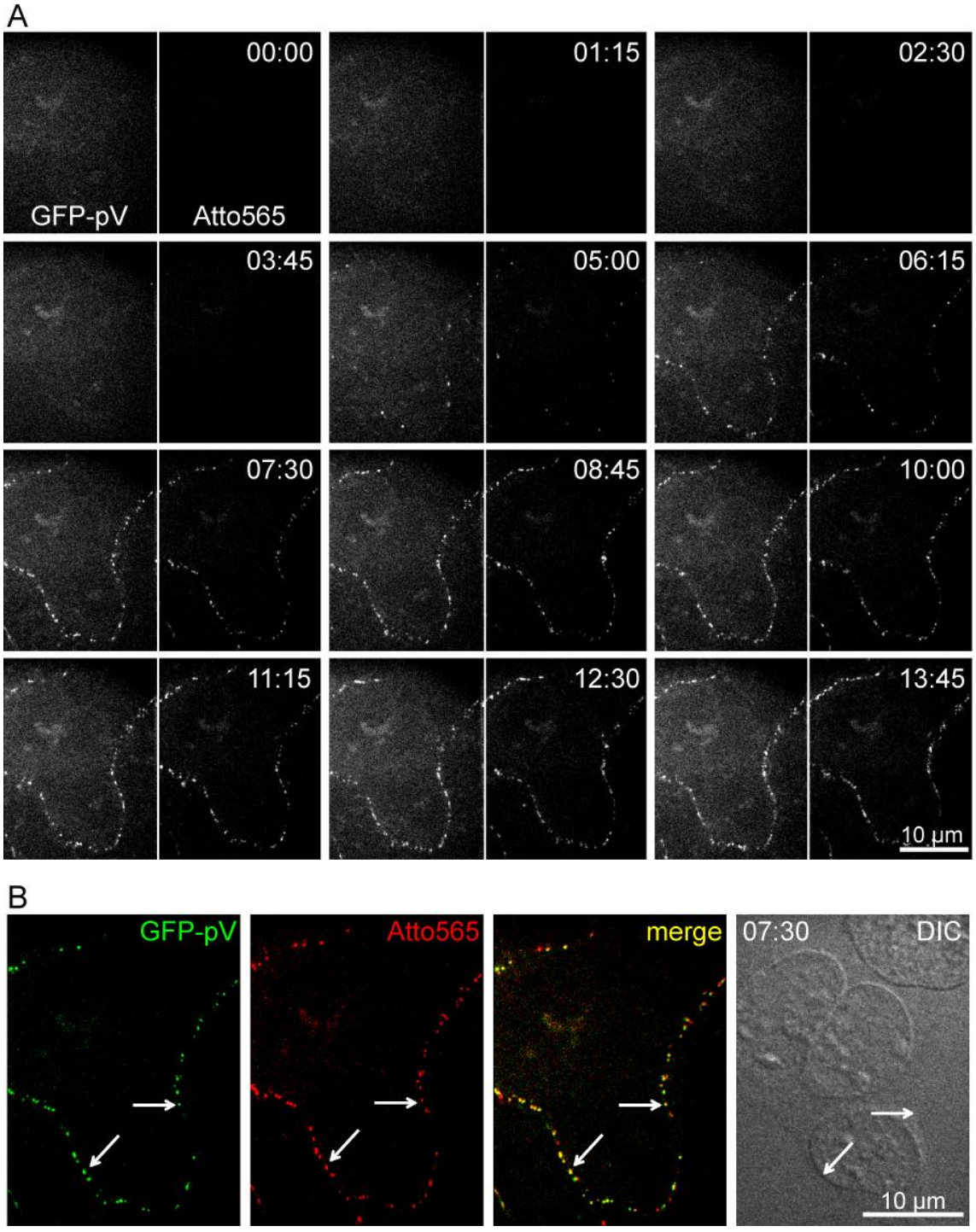
A
00:00
01:15
02:30
GFP-pV
Atto565
03:45
05:00
06:15
07:30
08:45
10:00
11:15
12:30
13:45
10 µm
B
GFP-pV
Atto565
merge
07:30
DIC
10 µm

Figure S6

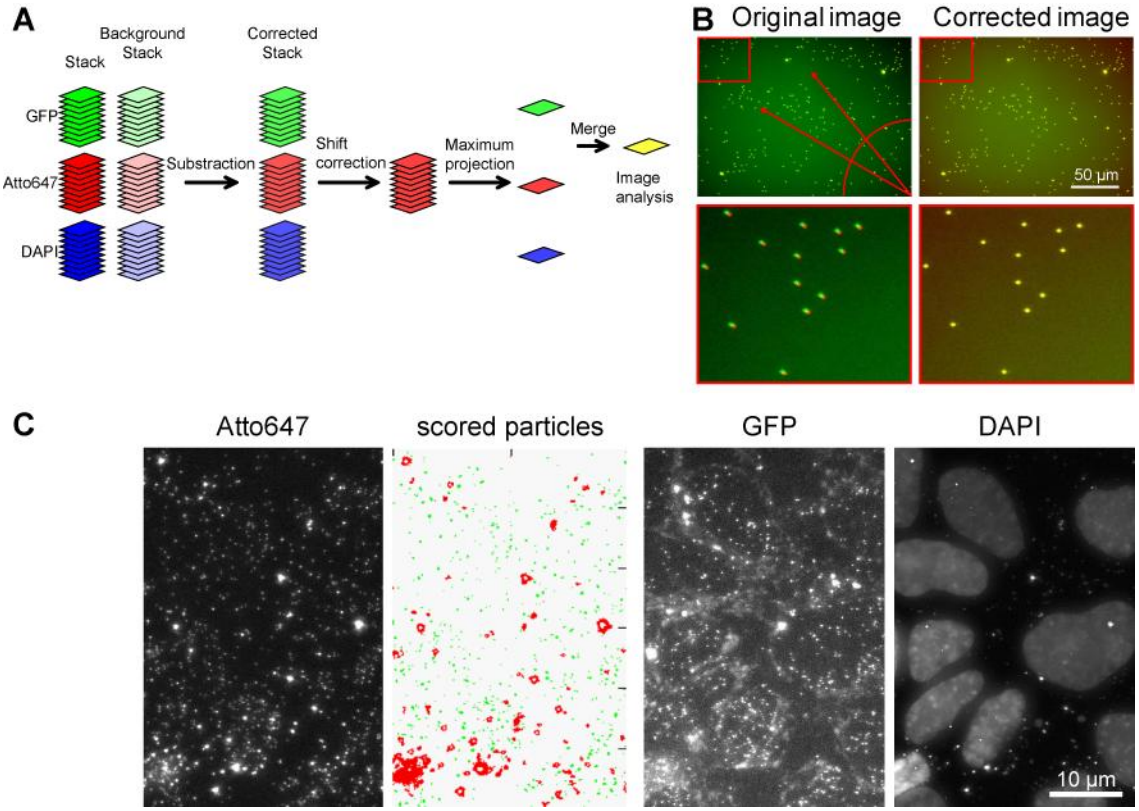
A
Stack
Background Stack
Corrected Stack
GFP
Atto647
DAPI
Substraction
Shift correction
Maximum projection
Merge
Image analysis
B
Original image
Corrected image
50 µm
C
Atto647
scored particles
GFP
DAPI
10 µm

Figure S7

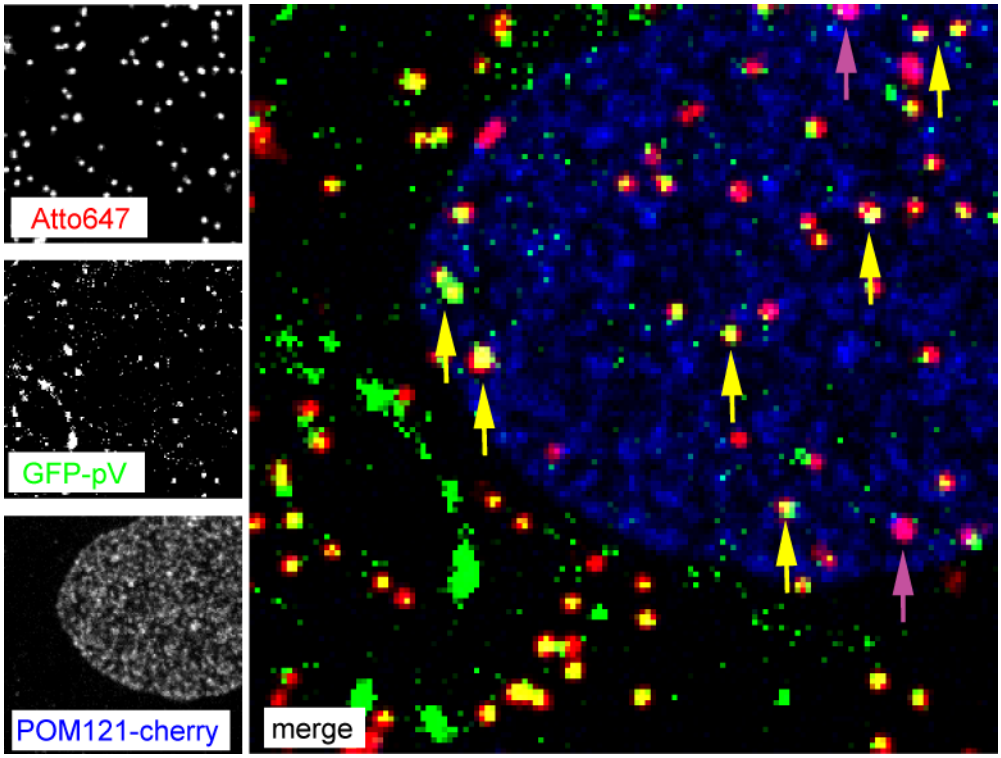

CONCLUSIONS AND FINAL REMARKS

Ever since humans were confronted with diseases, they aimed to counteract them. While resources to do so were rather limited in ancient times an increased understanding of the principles of life resulted in the development of effective treatments and therapies of current time. A big step forward in this direction was the description of the nature of DNA by James Watson and Francis Crick in 1953. This discovery preceded a revolution in biological sciences, which still continues today. The study of viruses and their interaction with the host cell contributed substantially to the increased understanding of basic biological mechanisms and revealed insights into key cellular events.

The rationale of this thesis was to shed some light on two basic steps in the life cycle of adenovirus in the context of its chromatin. First, we analyzed disassembly of adenovirus particles on its way to the nucleus and second we visualized egress of viral particles from infected cells through lysis. Therefore, we constructed a recombinant Ad2 where pV was replaced by GFP-pV. The resulting Ad2-GFP-pV possessed a fluorescent DNA core, successfully accomplished the whole replication cycle and could therefore be used for live cell imaging experiments. This virus is unique in that it is the first core-labeled genomically intact adenovirus available without any deletions or mutations beside the replacement of pV by GFP-pV.

Since the use of fluorescently-tagged viruses proved to be very successful in gaining new insights into adenovirus host interactions such as surface motions at the cell surface (Helmuth, Burckhardt, Koumoutsakos, Greber, & Sbalzarini, 2007), cell entry (Nakano, Boucke, Suomalainen, Stidwill, & Greber, 2000) and transport along microtubules (Suomalainen, Nakano, Boucke, Keller, & Greber, 2001; Suomalainen, et al., 1999), several fluorescent adenoviruses have been generated to date. One of the first available techniques was capsid labeling by chemical conjugation of synthetic fluorophores. More recently, GFP was fused to the minor capsid protein IX (Meulenbroek, Sargent, Lunde, Jasmin, & Parks, 2004). However, these labeling methods allow only visualization of the outer capsid structure, but not the inner core. In addition, the GFP-pIX labeled virus is

deleted in the E1 and E3 region and therefore is not capable to fully replicate in normal cells. The field of application of these viruses is therefore restricted to viral entry. As delivery of the viral genome into the nucleus as well as dynamics thereof is still not understood, many attempts were undertaken to generate recombinant viruses with fluorescently-tagged chromosomes. Glotzer et al. inserted tetO repeat sequences into the adenovirus genome, which was bound by the fusion protein tetR-GFP (Glotzer, Michou, Baker, Saltik, & Cotten, 2001). Although genome labeling could be demonstrated and exogenously provided tetR-GFP was incorporated into newly synthesized viral particles, usefulness proved to be limited as only around 20 copies of tetR-GFP were incorporated into the capsid and the signal therefore was very weak. In addition, this virus was devoid of regions E1 and E3 of the viral genome limiting use of the virus to cells that provide E1A *in trans* and to cell culture systems were no immune system is present. In addition, adenoviruses encoding pV-GFP or pre-pVII-GFP and a dual color Ad5 with pIX-RFP and pV-GFP were also reported (Le, et al., 2006; Ugai, et al., 2010). But again, all of those viruses suffered from a missing E3 region and in case of both pre-pVII-GFP- and pV-GFP -expressing viruses the recombinant proteins were under the control of an artificial promoter while endogenous pre-pVII and pV were also expressed, which resulted in low incorporation of recombinant proteins in virus particles. The pIX-RFP / pV-GFP labeled virions on the other hand were heterogeneous with respect to green and red fluorescence, and their cellular trafficking was difficult to elucidate (Ugai, et al., 2010).

How viral particles are released from infected cells at late stages of the replication cycle is poorly characterized. While there is an increasing amount of studies addressing this question in case of enveloped viruses such as herpesvirus (for a review see (Mettenleiter, 2002)), non-enveloped viruses such as adenoviruses are still lacking a detailed characterization. This can be explained in part by the lack of suitable tools to study this question.

Using a combination of live cell and quantitative fluorescence imaging, we now were able for the first time to visualize the dynamics of cellular disintegration events at late times of the adenovirus life cycle. We observed the release of GFP-pV positive clusters from the nucleus, which frequently remained

associated with the cytoplasm at late stages of infection and, later, a displacement of the clusters into the medium. Therefore we proposed that virus-induced cell lysis occurs in two morphologically defined steps. First, the nucleus is disintegrated and thereby releases its contents into the cytoplasm -and second, viruses are released into the extracellular space upon lysis of the plasma membrane. In support of this model, we identified viral clusters in the nucleus and the cytoplasm by EM analysis at similar time points, which is in agreement with published data from Puvion-Dutilleul that identified pre-lytic single viral particles in the cytoplasm (Puvion-Dutilleul, Besse, Pichard, & Cajean-Feroldi, 1998). Adenovirus death protein (ADP) was also identified to play a role in viral lysis (Tollefson, Ryerse, Scaria, Hermiston, & Wold, 1996). Intriguingly, an ADP deletion mutant produced smaller plaques and showed an enlarged nucleus upon infection, indicating that this protein has a role in nuclear membrane disruption (Tollefson, Scaria, et al., 1996). This fits well with our data as we observed an “explosion-like” nuclear disruption, which could be the result of an enhanced pressure onto the nuclear membrane from continuous import of viral proteins and subsequent accumulation of viral particles. The second step in our model, lysis of the plasma membrane, could be the consequence of release of the viral protease L3/p23, which is known to cleave cytokeratin, actin and microtubules (Mangel, Baniecki, & McGrath, 2003). Interestingly, actin is used as cofactor by the protease and therefore activates this enzyme. As actin is present in large quantities in the cytoplasm it is tempting to assume that once L3/p23 is released from the nucleus it is readily activated which subsequently induces disintegration of the cytoskeleton which makes the infected cell more susceptible to mechanical stress (Chen, Ornelles, & Shenk, 1993). Precisely how the plasma membrane is disrupted and the newly synthesized virions are released from the cell is, however, unknown. This can now be addressed with the help of the cell-lytic Ad2-GFP-pV particles.

In a second part, we analyzed viral chromatin during entry into cells. We could show that around 65% of GFP-pV was released within 30 minutes and the remaining 35% after 90 minutes pi. The release of the latter was inhibited upon treatment of cells with LMB. We therefore proposed that release of GFP-pV from Ad2-GFP-pV is a two step process. In a first rapid step, most of GFP-pV is

released from the viral particle while the remaining part is released upon capsid disassembly at the NPC. We speculate that the first step in GFP-pV release from the virions coincides with structural changes of the capsid, such as the loss of fibers and penton base proteins, or capsid-stabilizing proteins IIIa and VIII (Fabry, et al., 2005; Greber, Willetts, Webster, & Helenius, 1993; Nakano, et al., 2000). Interestingly, biochemical studies have suggested that pV attaches the viral DNA to the capsid via an interaction with pVI (Chatterjee, Vayda, & Flint, 1985; Matthews & Russell, 1998). In addition, thermal *in vitro* disassembly studies simulating disassembly in endosomes indicate that mature wild-type Ad virions release around 80% of penton base with around 25% of the hexons and around 80% of protein VI (Wiethoff, Wodrich, Gerace, & Nemerow, 2005) while 65% of pVI was found to be degraded upon infection of KB cells with Ad2 for 40 min in a degradation assay based on autoradiography (Greber, et al., 1993). In our own study, we observed, that 60-70% of GFP-pV signal is lost after 30 min endocytosis of Ad2-GFP-pV. This is in the range of the protein loss observed for pVI. We therefore speculate that GFP-pV is lost together with pVI. As a result, this could lead to a destabilization of the core preparing for the release of DNA into the nucleus. pV release might also support an early step in viral entry. However, the above mentioned data about pVI release are contradicting a model that suggests that pVI is associated with every capsomer (trimer of hexon) in the capsid (Silvestry, et al., 2009). As there are 240 capsomers present in each viral particle and around 360 copies of protein VI there are 120 copies of pVI that are not assigned. In addition it is somehow hard to explain how such a large fraction (80%) of pVI is lost from the capsid even if 25% hexon is lost (Wiethoff, et al., 2005) The remaining capsomers 180 in number should bind 180 copies of pVI which is not released. This corresponds to 50% of all pVI present in the capid. The authors therefore suggest a homotopic interaction among pVI proteins which then would lead to a higher loss of protein VI.

In summary, this thesis described the generation of a novel recombinant adenovirus with a fluorescently-tagged genome and characterization of it during specific stages of the adenovirus life cycle.

References

Chatterjee, P. K., Vayda, M. E., & Flint, S. J. (1985). Interactions among the three adenovirus core proteins. *J Virol, 55*(2), 379-386.

Chen, P. H., Ornelles, D. A., & Shenk, T. (1993). The adenovirus L3 23-kilodalton proteinase cleaves the amino-terminal head domain from cytokeratin 18 and disrupts the cytokeratin network of HeLa cells. *J Virol, 67*(6), 3507-3514.

Fabry, C. M., Rosa-Calatrava, M., Conway, J. F., Zubieta, C., Cusack, S., Ruigrok, R. W., et al. (2005). A quasi-atomic model of human adenovirus type 5 capsid. *Embo J, 24*(9), 1645-1654.

Glotzer, J. B., Michou, A. I., Baker, A., Saltik, M., & Cotten, M. (2001). Microtubule-independent motility and nuclear targeting of adenoviruses with fluorescently labeled genomes. *J Virol, 75*(5), 2421-2434.

Greber, U. F., Willetts, M., Webster, P., & Helenius, A. (1993). Stepwise dismantling of adenovirus 2 during entry into cells. *Cell, 75*(3), 477-486.

Helmuth, J. A., Burckhardt, C. J., Koumoutsakos, P., Greber, U. F., & Sbalzarini, I. F. (2007). A novel supervised trajectory segmentation algorithm identifies distinct types of human adenovirus motion in host cells. *J Struct Biol, 159*(3), 347-358.

Le, L. P., Le, H. N., Nelson, A. R., Matthews, D. A., Yamamoto, M., & Curiel, D. T. (2006). Core labeling of adenovirus with EGFP. *Virology, 351*(2), 291-302.

Mangel, W. F., Baniecki, M. L., & McGrath, W. J. (2003). Specific interactions of the adenovirus proteinase with the viral DNA, an 11-amino-acid viral peptide, and the cellular protein actin. *Cell Mol Life Sci, 60*(11), 2347-2355.

Matthews, D. A., & Russell, W. C. (1998). Adenovirus core protein V is delivered by the invading virus to the nucleus of the infected cell and later in infection is associated with nucleoli. *J Gen Virol, 79 (Pt 7)*, 1671-1675.

Mettenleiter, T. C. (2002). Herpesvirus assembly and egress. *J Virol, 76*(4), 1537-1547.

Meulenbroek, R. A., Sargent, K. L., Lunde, J., Jasmin, B. J., & Parks, R. J. (2004). Use of adenovirus protein IX (pIX) to display large polypeptides on the virion--generation of fluorescent virus through the incorporation of pIX-GFP. *Mol Ther, 9*(4), 617-624.

Nakano, M. Y., Boucke, K., Suomalainen, M., Stidwill, R. P., & Greber, U. F. (2000). The first step of adenovirus type 2 disassembly occurs at the cell surface, independently of endocytosis and escape to the cytosol. *J Virol, 74*(15), 7085-7095.

Puvion-Dutilleul, F., Besse, S., Pichard, E., & Cajean-Feroldi, C. (1998). Release of viruses and viral DNA from nucleus to cytoplasm of HeLa cells at late stages of productive adenovirus infection as revealed by electron microscope in situ hybridization. *Biol Cell, 90*(1), 5-38.

Silvestry, M., Lindert, S., Smith, J. G., Maier, O., Wiethoff, C. M., Nemerow, G. R., et al. (2009). Cryo-electron microscopy structure of adenovirus type 2 temperature-sensitive mutant 1 reveals insight into the cell entry defect. *J Virol, 83*(15), 7375-7383.

Suomalainen, M., Nakano, M. Y., Boucke, K., Keller, S., & Greber, U. F. (2001). Adenovirus-activated PKA and p38/MAPK pathways boost microtubule-mediated nuclear targeting of virus. *EMBO J, 20*(6), 1310-1319.

Suomalainen, M., Nakano, M. Y., Keller, S., Boucke, K., Stidwill, R. P., & Greber, U. F. (1999). Microtubule-dependent plus- and minus end-directed motilities are competing processes for nuclear targeting of adenovirus. *J Cell Biol, 144*(4), 657-672.

Tollefson, A. E., Ryerse, J. S., Scaria, A., Hermiston, T. W., & Wold, W. S. (1996). The E3-11.6-kDa adenovirus death protein (ADP) is required for efficient cell death: characterization of cells infected with adp mutants. *Virology, 220*(1), 152-162.

Tollefson, A. E., Scaria, A., Hermiston, T. W., Ryerse, J. S., Wold, L. J., & Wold, W. S. (1996). The adenovirus death protein (E3-11.6K) is required at very late stages of infection for efficient cell lysis and release of adenovirus from infected cells. *J Virol, 70*(4), 2296-2306.

Ugai, H., Wang, M., Le, L. P., Matthews, D. A., Yamamoto, M., & Curiel, D. T. (2010). In vitro dynamic visualization analysis of fluorescently labeled minor capsid protein IX and core protein V by simultaneous detection. *J Mol Biol, 395*(1), 55-78.

Wiethoff, C. M., Wodrich, H., Gerace, L., & Nemerow, G. R. (2005). Adenovirus protein VI mediates membrane disruption following capsid disassembly. *J Virol, 79*(4), 1992-2000.

ACKNOWLEDGEMENTS

I am grateful to Prof. Dr. Urs F. Greber for his ongoing support, scientific guidance and encouragement during the past years and for critical reading of this thesis.

I would like to thank the members of my thesis committee Prof. Dr. Michael O. Hottiger and Prof. Dr. Ulrike Kutay for their inspiring and critical contributions at the thesis committee meetings.

Many thanks to Dr. Maarit Suomalainen, Dr. Christian -and Deborah Lo Cascio Barton for critical reading this manuscript.

Thanks to Prof. Dr. Cornel Fraefel, PD Dr. Silvio Hemmi, Dr. Thomas Honegger and Dr. Zsolt Ruzsics for discussions and reagents.

I thank my bench mate Verena Lütschg for a very nice working environment and many pleasant hours.

Thanks to my master student Olmo Sonzogni, for a good time and well performed work.

Many thanks go to our technicians, former and current, Bettina Cardel, Corinne Wilhelm, Karin Boucke and Monika Straub for general and personal support in many aspects.

Special thanks go to my co-workers Andreas Jurgeit, Christoph Burckhardt, Markus Eisenhut, Martin Engelke, Nicola Imelli and Verena Lütschg for technical assistance.

I thank Hansjörg Baumann, Jacqueline Oberholzer, Marcel Freund, Michel Nakano, Raymond Grunder, Silvana Jacobo, Stephan Wüthrich, Tina Siegenthaler and Urs Ziegler for help with IT problems, microscopy, sequencing and administration support.

I would like to thank all people of the Greber Lab, former and current (alphabetical order): Andreas Jurgeit, Arthur Yakimovich, Beat Amstutz, Bettina

Cardel, Brigida Rusconi, Brigitte Kopf, Christine Neugebauer, Christoph Burckhardt, Corinne Wilhelm, Eliane Wandeler, Elisa Falke, Fabienne Di Gennaro, I-Hsuan Jessica Wang, Jack Daniels, Karin Boucke, Katharina Bengesser, Krishna Chaitanya, Maarit Suomalainen, Mark Lötzerich, Markus Eisenhut, Martin Engelke, Mattias Morf, Michele Gastaldelli, Monika Straub, Nicola Imelli, Nicole Liska, Nina Wolfrum, Olga Liska, Olmo Sonzogni, Pascal Roulin, Philipp Schönenberger, Ryo Koyanagi, Saskia Petrzilka, Sonja Kuttnig, Stefan Kälin, Sten Strunze, Susanne Keller and Verena Lütschg for the pleasant atmosphere and support in many aspects.

Thanks to Arthur, Christine, Corinne, Elisa, Jessica, Kathi, Martin, Nina, Stefan and Verena for having good times outside the lab.

I am most grateful to (alphabetical order): Christian, Christina, Deborah, Denise, Lea, Marianne, Markus, Nathalie, Nicole, Roger, Thomas, Sandra and my family for invaluable support and love during good and bad times.

ABBREVIATIONS

Ad	Human adenovirus
Ad2-GFP-pV	Adenovirus type 2 with pV replaced by GFP-pV
ADP	Adenovirus death protein
AIDS	Acquired immune deficiency syndrome
ATCC	American Type Cell Culture Collection
B23	Nucleophosmin
BAC	Bacterial artificial chromosome
BSA	Bovine serum albumin
C23	Nucleolin
CAR	Coxsackie B virus and adenovirus receptor
CLSM	Confocal laser scanning microscopy
CsCl	Cesium chloride
DAPI	4'-6'-diamidino-2-phenylindole
DBP	DNA binding protein
dHBV	Duck hepatitis virus
DIC	Differential interference contrast
DMEM	Dulbeccos's modified Eagle medium
DNA	Deoxyribonucleic acid
dsDNA	Double-stranded deoxyribonucleic acid
EBV	Epstein Barr virus
eGFP	Enhanced green fluorescent protein
EM	Electron microscopy
ER	Endoplasmic reticulum
FBS	Fetal bovine serum
FFA	Fluorescent focus assay
FFFU	Fluorescent focus forming unit
FG	Amino acid abbreviation for phenylalanine-glycine
FISH	Fluorescent *in situ* hybridization
FITC	Fluorescein isothiocyanate
GDP	Guanosine diphosphate
GFP	Green fluorescent protein
GON	Group-of-nine
GTP	Guanosine triphosphate
GTPase	Guanosine triphosphatase
HAd	Human adenovirus
HBV	Hepatitis B virus
HeLa	Cancer cell line named after deceased patient Henrietta Lacks
HEPES	4-(2-hydroxyethyl)-1-piperazineethanesulfonic acid
HHV	Human herpesvirus
HIV	Human immunodeficiency virus
HPV	Human papillomavirus
HSV	Herpes simplex virus
HTLV	Human T lymphotropic virus
INHAT	Inhibitor of acetyltransferase
INM	Inner nuclear membrane
Kbp	Kilo base pairs

kDa	Kilo Dalton
KSHV	Kaposi's sarcoma-associated herpesvirus
LMB	Leptomycin B
MAPK	Mitogen activated protein kinase
MCPyV	Merkel cell polyomavirus
MLP	Major late promotor
MOI	Multiplicity of infection
mRNA	Messenger ribonucleic acid
MTOC	Microtubule organizing center
NEA	Non-essential amino acid
NES	Nuclear export signal
NIH	National Institutes of Health
NLS	Nuclear localization signal
Nm	Nanometer
NPC	Nuclear pore complex
Nup	Nucleoporin
ONM	Outer nuclear membrane
PAGE	Polyacrylamide gel electrophoresis
PBS	Phosphate buffered saline
PFA	Paraformaldehyde
PKA	Protein kinase A
PM	Plasma membrane
PS	Penicillin/Streptomycin
Ran	Ras-related nuclear protein
RanGAP	Ran GTPase-activating protein
RanGEF	RanGDP/GTP exchange factor
RFP	Red fluorescent protein
RGD	Amino acid abbreviation for arginine-glycine-aspartate
RNA	Ribonucleic acid
ROI	Region of interest
SDCM	Spinning disc confocal microscope
SDS	Sodium dodecyl sulfate
SEM	Standard error of the mean
ssDNA	Single-stranded deoxyribonucleic acid
SV40	Simian virus 40
TAF	Template activating factor
TCA	Trichloroacetic acid
TCID50	Tissue culture infective dose 50
TEM	Transmission electron microscopy
VZV	Varizella zoster virus

CURRICULUM VITAE

PERSONAL DETAILS

Name: Daniel Püntener, Dipl. Natw. ETH
Address: Schaffhauserstrasse 286
CH-8057 Zürich
Switzerland

Date of birth: June 5, 1977
Nationality: Swiss
Marital status: Single

Phone: +41 78 749 92 68

Email: daniel.puentener@gmail.com

PROFESSIONAL EXPERIENCE

Since 02/2003 — University of Zürich, Zürich

Research assistant (Ph.D.), fulltime
Establishing of molecular biology based techniques for the generation of recombinant Adenoviruses.
In vivo and in vitro characterization of Adenovirus-based vector expressing GFP-tagged core protein.

Teaching and Leading
Supervision and guidance of students in cell biology/virology
Technical and scientific support of Ph.D. students and TAs.

2001-2003 — University Hospital Zürich, Zürich

Healthcare assistant, part time
Surveillance of critical patients

07/2000-10/2000 — Mettler-Toledo GmbH, Urdorf (ZH)

Lab technician in R&D, fulltime
Quality control

02/2000-05/2000 — University of Stockholm/Pharmacia Biotech AB, Uppsala, Sweden

Research collaboration project, protein purification

EDUCATION

Since 02/2003 — Ph.D. student at the Institute of Molecular Life Sciences, Cell Biology Laboratory directed by Prof. Dr. U.F. Greber, University of Zürich, Switzerland

10/2002 — Diploma (equal to Master degree) in Biochemistry and Molecular Biology at the ETH Zürich.

03/2001 - 09/2001	Diploma thesis with Prof. Dr. Ari Helenius, ETH Zürich; “The role of actin in caveolar endocytosis of Simian Virus 40”
10/2000-02/2001	15 weeks internship at the group of Prof. Dr. Ari Helenius, ETH Zurich, “Simian Virus 40 cell entry does not induce phosphorylation of caveolin-1 on tyrosine 14 in CV-1 cells”.
01/2000 - 06/2000	Erasmus exchange student at the University of Stockholm
09/1997 - 10/2002	Undergraduate student at the ETH Zürich, Biochemistry and Molecular Biology, Microbiology, Immunology and Biotechnology
1997	Matura at the Kantonsschule Zug, Zug

PUBLICATIONS

Fluorescent DNA-core dynamics in entry and egress reveal nonisotropic hatching of viruses from infected cell nuclei. **Daniel Puntener**, Martin F. Engelke, Nicola Imelli, Zsolt Ruzsics, Karin Boucke, Corinne Wilhelm and Urs F. Greber. Manuscript submitted to **PLoS Pathogens**.

DNA-tumor virus entry – from plasma membrane to the nucleus. **Puntener, D**. & U.F. Greber. **Seminars in Cell & Developmental Biology** 2009 20: 631-642

Genetic reconstitution of the human adenovirus type 2 temperature-sensitive 1 mutant defective in endosomal escape. Imelli, N., Ruzsics, Z., **Puntener, D.,** Gastaldelli, M., Greber, U.F. **Virology Journal** 2009 6:174.

Local actin polymerization and dynamin recruitment in SV40-induced internalization of caveolae. Pelkmans, L., **Puntener, D**., Helenius, A. **Science** 2002 Apr 19;296(85567):535-9.

Kinesin-1 gates nuclear import of viral DNA by disrupting capsids and nuclear pore complexes. Sten Strunze, Martin Engelke, Karin Boucke, **Daniel Puntener**, Sibylle Schleich, Michael Way, Philipp Schoenenberger, Christoph J. Burckhardt & Urs F. Greber. Manuscript in preparation.

SCHOLARSHIPS

Member of the elite promotional program of the Swiss Study Foundation 1998 – 2008. www.studienstiftung.ch

International Chemistry Olympiad in Moscow 1996. www.icho.ch

International Chemistry Olympiad in Beijing 1995. www.icho.ch

“The fourth international summer chemical school for youth” at the N.D. Zelinsky Institute of organic chemistry, Moscow, 1994

“Schweizer Jugend Forscht” project: The color of organic substances, 1994

LANGUAGE AND COMPUTER SKILLS

German mother tongue

English advanced (oral and written)

French good (oral and written)

Swedish basic (oral and written)

Operating systems: Microsoft Windows, Macintosh OSX

Software: MS Office; Adobe Photoshop, Illustrator, Dreamweaver, Flash and Lightroom; Thomson ISI ResearchSoft Endnote; Invitrogen Vector NTI Advance; Molecular Devices Metamorph; NIH ImageJ; Bitplane Imaris.

ACTIVITIES

Body Combat, Photography

REFERENCES

On request